Energy Storage Systems for Traction and Renewable Energy Applications

Hamad Abdullah Aldawsari
Marquette University

ENERGY STORAGE SYSTEMS FOR TRACTION AND RENEWABLE ENERGY APPLICATIONS

By

Hamad A. Aldawsari

A Thesis Submitted to the Faculty of the Graduate School,
Marquette University,
in Partial Fulfillment of the Requirements for
the Degree of Master of Science

(Electrical and Computer Engineering)

Milwaukee, Wisconsin

May 2020

ABSTRACT
ENERGY STORAGE SYSTEMS FOR TRACTION AND
RENEWABLE ENERGY APPLICATIONS

Hamad A. Aldawsari

Marquette University, 2020

Energy storage systems are the set of technologies used to store various forms of energy, and by necessity, can be discharged. Energy storage technologies have a wide range of characteristics and specifications. Like any other technology, each type of energy storage has its pros and cons. Depending on the application, it is crucial to perform a tradeoff study between the various energy storage options to choose the optimal solution based on the key performance objectives and various aspects of those technologies. The purpose of this thesis is to present a thorough literature review of the various energy storage options highlighting the key tradeoffs involved. This thesis focuses on evaluating energy storage options for traction and renewable energy applications

Hybrid Electric Vehicles (HEVs) is one key application space driving breakthroughs in energy storage technologies. The focus though has been typically on using one type of energy storage systems. This thesis investigates the impact of combining several types of batteries with ultracapacitor. A case study of integrating two energy storage systems in a series-parallel hybrid electric vehicle is simulated by using MATLAB-*SIMULINK* software.

The other key application space is renewable energy especially wind and solar. Due to the intermittent nature of renewable energy sources, energy storage is a must to achieve the required power quality. Therefore, this thesis aims to investigate different cases of combining different types of energy storage with wind and solar. Hybrid Optimization Model for Electric Renewables (HOMER) software is utilized to study the economic and sizing aspects in each case.

ACKNOWLEDGMENTS

Hamad A. Aldawsari

Table of Contents

LIST OF TABLES

LIST OF FIGURES

ACRONYMS AND ABBREVIATIONS

Acronyms and Abbreviations			
$	US. Dollars	**LF**	Load Following
$/L	US. Dollars per Liter	**Li-ion**	Lithium-ion
1MWh-Li	one Mega watt-hour lithium-ion battery	**mm**	milli meter
4hr-Li-battery	Lithium-ion battery with 4 hours storage duration	**MPG**	Miles-per-gallon
AC	Alternating Current	**msec**	milli-seconds
AGM	Absorbed Glass Mat	**MW**	Mega Watts
Ah	Amper-hour	**MWh**	Mega Watt-hour
ARES	Advanced Rail Energy Storage	**Na-beta**	Sodium Beta
BES	Batteries Energy Storage	**Na-MeCl$_2$**	sodium-metal halide
CA	California	**Na-S**	sodium-sulfur
CAES	Compressed Air Energy Storage	**Ni-Cd**	Nickel-Cadmium
CC	cycle charging	**Ni-MH**	Nickel Metal Hydride
COE	Levelized Cost of Energy	**NPC**	net present cost
CV	conventional vehicles	**NREL**	National Renewable Energy Laboratory
DC	Direct Current	**O&M**	Operating and Maintenance
DoD	depth of discharge	**OCV**	Open-circuit voltage
e.g.	exempli gratia (for example)	**Pb-A**	Lead-Acid
EDLC	electric double-layer capacitors	**PEV**	plug-in electric vehicle
EIA	Energy Information Administration	**PHES**	Pumped Hydroelectric Energy Storage
EPA	Environmental Protection Agency	**PI**	proportional-integral
EPR	equivalent parallel resistance	**PMSM**	permanent magnet synchronous motors
ESR	equivalent series resistance	**PV**	Photovoltaic
ESS	Energy Storage System	**rpm**	Revolutions per minute
etc	Et cetera	**SC**	Supercapacitor
EV	Electric Vehicle	**SCES**	Super Capacitors Energy Storage
FES	Flywheels Energy Storage	**sec**	Seconds
Fig	Figure	**SMES**	Superconducting Magnetic Energy Storage
FL	Florida	**SoC**	State of Charge
ft	Feet	**SoH**	state of health
GBES	Ground-Breaking Energy Storage	**TES**	Thermal Energy Storage
GW	Gega Watts	**UC**	ultra-capacitor
GWh	Gega Watt-hour	**V-47**	Vestas wind turbine (V47-660 kW)
HESS	Hybrid Energy Storage System	**V-82**	Vestas wind turbine (V82-1.65 MW)
HEV	Hybrid Electric Vehicle	**VLA**	vented lead-acid
HFB	Hybrid flow batteries	**VRFB**	Vanadium redox flow batteries
HFC	Hydrogen Fuel Cells	**VRLA**	valve regulated lead-acid
HOMER	Hybrid Optimization Model for Electric Renewables	**W/kg**	Watts per Kilogram
HPEV	Hybrid Plug-in Electric Vehicle	**Wh/kg**	Watt-hour per Kilogram
hr	Hour	**WI**	Wisconsin
i.e.	id est (in other words)	**ZEBRA**	zero-emission battery research activity
IC engine	internal combustion engine	**Zn-Air**	zinc-air
IEA	International Energy Agency	**Zn-Br**	zinc-bromine
IM	Induction Motors	**η**	efficiency
kg	kilogram	CO_2	Carbon dioxide
kW	Kilo Watts	**°F**	Fehrenhite
kW/m^3	Kilo Watt per cubic meter	**°C**	Celsius
kWh	Kilo Watt-hour	K^o	Kelvin
kWh/m^3	Kilo Watt-hour per cubic meter	R_s	equivalent series resistance
LA	Lead-Acid	R_p	parallel resistance
LAES	Liquid Air Energy Storage	C_p	parallel capacitor
LCOE	Levelized Cost of Energy	V_{oc}	Open-circuit voltage
LCOS	Levelized Cost of Storage	V_{batt}	battery terminal voltage

Chapter 1: Introduction and Literature Review

1.1 Introduction

Since the discovery of electricity, in a bid to improve the power generation systems to meet the rapidly growing demand for electricity, mankind has been deploying a considerable effort and a substantial amount of resources. During the industrial revolution, human activities such as burning fossil fuels (oil, coal, or natural gas) have been increasing dramatically. Burning those fossil fuels produces energy which can be used in power plants, cars, and industrial facilities. In response to an accelerated increase in energy consumption in the last century, building new combustion power plants, which also burn fossil fuels, has been considered as a promising solution to meet these demands on electricity due to their economic feasibility. However, burning these fossil fuels was and still is the major contributor to increasing global greenhouse emissions (mainly water vapor, carbon dioxide (CO_2) and methane). According to the United States Environmental Protection Agency (EPA), burning fossil fuels for heat, electricity, and transportation is the largest source of greenhouse gas emissions in the United States [1].

With the passing decades, there was a consensus on the necessity to find alternative technologies that are environmentally friendly and not dependent on limited energy sources. Therefore, there was an agreement on the advantages of producing electricity by using renewable energy sources (e.g., wind, solar, water, etc.) and utilizing electric vehicles (EVs) in the transportation sector, which would reduce these greenhouse emissions.

Unfortunately, the effectiveness of renewable energy sources is reduced by their intermittency. Also, energy storage systems are considered the main part of electric vehicles. Thus, this has led to finding efficient and proper ways to store the produced energy for later use when the sun does not shine, and the wind does not blow. In recent years, the technologies used to store energy have evolved and adapted to modern energy requirements and availabilities [2].

There is a vast spectrum of energy storage options available today for many applications. Many criteria categorize these energy storage technologies; for example, the response time (energy storage or power storage), suitable storage duration (short-term, medium-term, long-term), scale (small-scale, medium-scale, large-scale) [3]. Moreover, Energy storage systems have been further categorized based on the form in which they are stored in the following nine categories which are also shown in Figure (1.1).

- Gravitational Energy Storage Systems

- Electrical Energy Storage Systems

- Mechanical Energy Storage Systems

- Thermo-Mechanical Energy Storage Systems

- Thermal Energy Storage Systems

- Chemical Energy Storage Systems

- Thermochemical Energy Storage Systems

- Electromechanical Energy Storage Systems

- Hybrid Energy Storage Systems
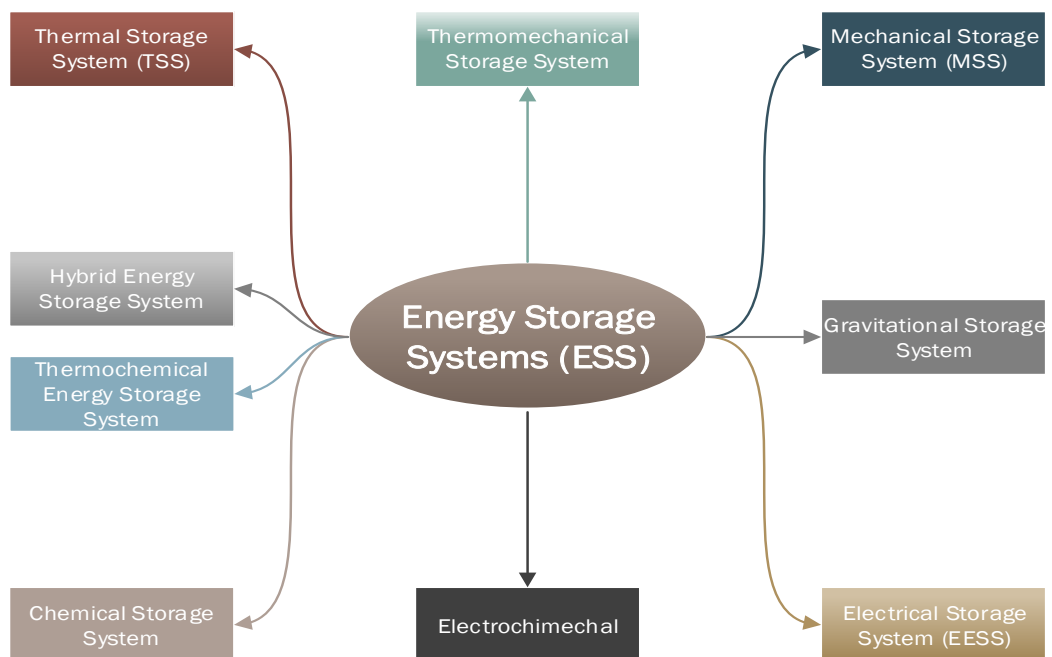
Figure (1.1) ESS classification

To better understand the extent of these technologies, Figure (1.2) presents a detailed classification of ESS based on the storing form.
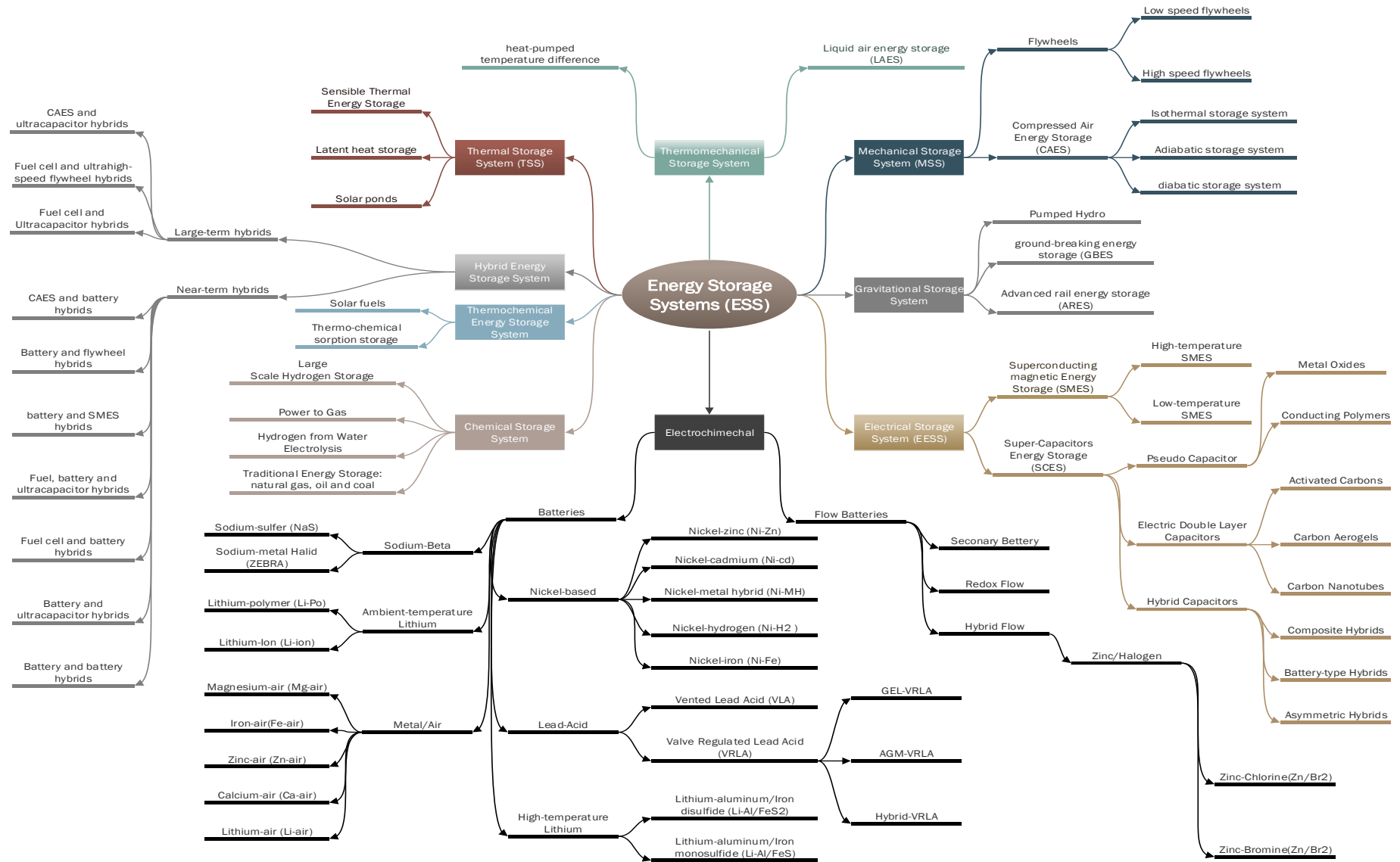
Figure (1.2) Detailed classification of energy storage systems

Moreover, Table (1.1) compares different types of energy storage systems based on the response time, suitable storage duration, scale, stored energy form, and efficiency [3,4].

Table (1.1) Comparison of Energy Storage Systems [3,4]

Comparison of Energy Storage Systems					
Technology	Response time	Storage duration	Scale	Stored Energy form	Round-trip efficiency (%)
1 **Pumped Hydroelectric Energy Storage (PHES)**	3-5 mins	Hours-months	Small-large	Gravitational potential energy.	70-85
2 **Compressed Air Energy Storage (CAES)**	mins	Hours-months	Small-large	Pressurized gas	30
3 **Flywheels Energy Storage (FES)**	msec-sec	secs-mins	Medium-large	Kinetic Energy	55-80
4 **Super Capacitors Energy Storage (SCES)**	msec	secs-hours	Small-medium	Electrical energy	85-95
5 **Superconducting Magnetic Energy Storage (SMES)**	msec	Hours-days	small-medium	Electrical energy	95
6 **Lithium-ion (Li-ion) batteries**	msec	mins-days	All scales	Electrochemical energy	85-95

From Table (1.1), it can be observed that energy storage technologies have a wide range of characteristics; thus, energy storage technologies that have been investigated and published in the literature will be reviewed, and more comparison criteria will be presented, in which also this table will be reviewed with a better understanding of these technologies and their characteristics, to be able to compare them and select the best option for different applications.

1.1.1   Research problem statement:

Energy storage has been gaining attention over the past three decades. Energy storage is considered to be the key enabler of many applications including traction, aerospace and renewable energy applications. There has been a wide range of energy storage technologies developed over the past few decades. Like any other technology, each type of energy storage has its pros and cons. Depending on the application, it is crucial to perform a tradeoff study between the various energy storage options to choose the optimal solution based on the key performance objectives. This thesis will present a thorough literature review of the various energy storage options highlighting the key tradeoffs involved. This thesis will focus on evaluating energy storage options for traction and renewable energy applications.

1.1.2   Research objectives and document organization:

There has been a large body of work presented in the literature that covers various aspects of energy storage technologies. Hybrid Electric Vehicles (HEVs) have been one key application space driving breakthroughs in energy storage technologies. The focus though has been typically on using one type of energy storage systems. This thesis will investigate the impact of combining different types of batteries. The other key application space is renewable energy especially wind and solar. Due to the intermittent nature of such renewable energy sources, energy storage is a "must" to achieve the required power quality. This thesis will investigate different cases of combining different types of energy storage with wind and solar.

Moreover, the goal of this research is to provide the reader with the appropriate knowledge to judge the integration of hybrid energy storage systems for different applications. Thus, in Chapter 1, various energy storage technologies will be explained, compared, and summarized. Chapter 2 will be mainly focusing on electric vehicles (EVs) and hybrid electric vehicles (HEVs) and their energy storage technologies, then, a case study of a series-parallel hybrid electric vehicle will be simulated. Subsequently, a MATLAB-*SIMULINK* software, which was developed by Mathworks Inc., will be used to model, simulate and show the results of integrating two energy storage systems in a series-parallel hybrid electric vehicle. Chapter 3

will be focusing on energy storage systems for residential, commercial, and utility-scale in microgrids and renewable energy applications. Also, three cases for three different states will be simulated by a software called Hybrid Optimization Model for Electric Renewables (HOMER) to study the economic and sizing aspects in each state.

1.2 Types of Energy Storage Systems (ESS):

1.2.1   Gravitational energy storage systems

The name gravitational energy storage system describes the essential factor for the operation of such systems, which is gravity. The fundamental concept of this method is very much similar to the hydraulic lift of massive bodies. The basic principle of operation of the gravitational energy storage system is very identical to the hydraulic lift of the heavy objects (e.g. rocks). With the help of the electrical water pumps, water moves under a heavy moveable piston. With the help of this liquid, heavy objects can be lifted upwards and gain a considerable amount of hydraulic/gravitational potential energy. When the demand for electricity is high, this heavy object is released by displacing the water under the piston which is directed to the turbines. Hence using the basic hydro station methodology, this potential energy ultimately gets converted into electrical power [5].

Although these systems can store a large amount of energy, their basic design inherits engineering limitations. These systems must be installed on ground levels with no elevation differences. External conditions must be suitable, and the presence of the multi-layered rocks is favorable. But it is also necessary to seal the piston against the surrounding area to keep the flow of water without any hindrance caused by these rocks. Also, a proper survey has to be done beforehand, which makes this costly procedure even more expensive [5].

1.2.1.1 Ground-breaking energy storage (GBES)

Ground-breaking energy storage is one of the main derivatives of the gravitational energy storage system. In this type of ESS, the working principle and the layout of the main structure is still the same as in gravitational energy storage systems. However, this technology

still has limitations, including location, operating pressure, and the need for massive working mass to be able to store a considerable amount of energy. According to Letcher, in order to store 1 MW over one day, the working mass might be as big as the Empire State Building (400,000 t). Also, the construction cost will be too expensive to build such a system. Slight modifications can be made in the layout of the structure to get different storage capacities; The ground-breaking energy storage system can be constructed as shown in Figure (1.3) [5].
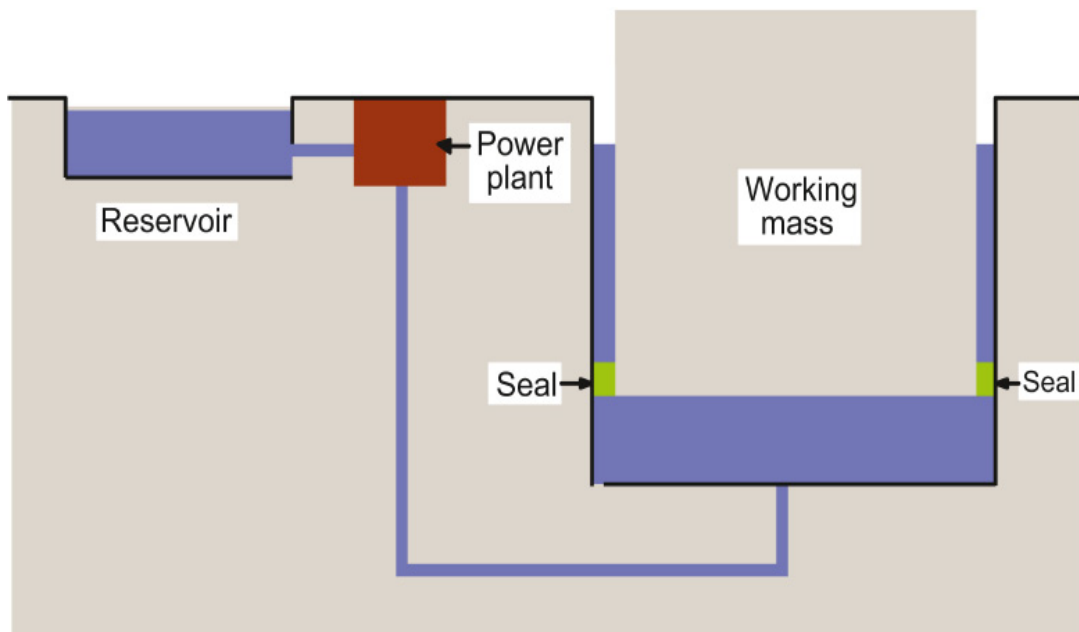
Figure (1.3) Piston-in-cylinder GBES system [5]

1.2.1.2 Advanced rail energy storage (ARES)

The basic principle of operation of advanced rail energy storage involves the movement of massive mass towards the top of some elevated area by using cars, railroad shuttles, or other heavy vehicles and then letting such bodies travel downwards, Figure (1.4). Similar to ground-breaking energy, the potential energy can be converted into electrical power with the help of generators. Figure (1.4) shows a picture of the first commercial ARES project in Tehachapi, California [5,6].

Figure (1.4) ARES Tehachapi Project [5]

1.2.1.3 Pumped Hydro Energy Storage (PHES)

Similar to advanced rail energy storage systems, the potential energy is converted into electrical energy, but the significant difference in the PHES system, as shown in Figure (1.5), is the working mass involved. In this type, the moving object is water. Water is pumped upwards to the high elevated area (upper reservoir) then allowed to flow with gravity toward the lower reservoir, so that the hydro-turbines can spin; hence the potential energy stored by the water is converted into mechanical energy by rotating the turbines' rotor/runner and which in turn rotate the generators thus energy is then converted into electrical power. [5].
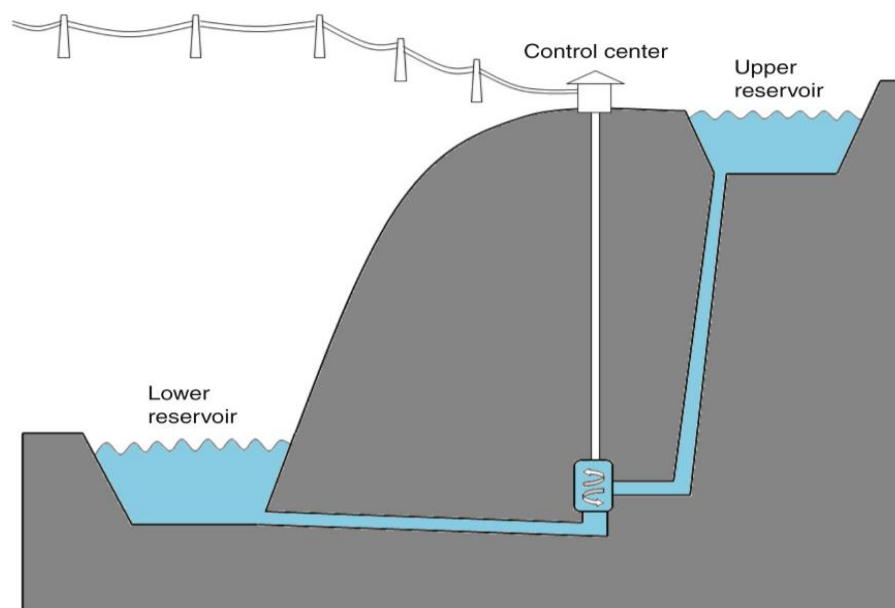
Figure (1.5) Basic design of PHES system [5]

Nowadays, PHES technology is considered the most developed, mature, and widespread energy storage technology worldwide. Like any other energy storage technology, PHES has many advantages, such as high power capacity, long lifetime and lifecycles, and low self-discharge rate. Moreover, PHES can be used in existing hydropower stations, but it has some limitations such as high capital cost, geographical limitation, and environmental impacts. PHES also has relatively low energy density and slow charge-discharge duration (once per day). There is some novel pumped hydroelectric energy storage technologies that would overcome the conventional PHES's drawbacks (e.g. seawater PHES, underground PHES, compressed air PHES, undersea PHES, etc.).

Additional information about this technology is summarized in the Table (1.2). However, before going any further, some technical specifications should be defined for more clarity. First, energy and power are different quantities at a specific rate of discharge; power is the instantaneous rate of energy being released and is measured by watts, while energy is measured by watt-hours. Second, energy density measures the maximum amount of stored energy per unit volume, while specific energy measures the maximum amount of stored energy per unit weight. Third, the maximum stored power per unit volume is power density. Next, round-trip efficiency is the efficiency of the whole system (output energy over input energy). Another specification is the depth of discharge (DoD), which is the percentage of power capacity that can be discharged, and it is also the converse of the state of charge (SoC). Lifecycle is the estimation of the full charge and discharge cycles of the system. Lifetime is the period of the useful life of the plant or device. Besides, the daily self-discharge rate is the rate of reduction of the stored energy without any connection to the load; in other words, it is the percentage of energy loss in the device. Moreover, the response time is the time that a storage system needs to ramp up supply. The storage duration is the period of time that a storage system can store energy. Discharge duration is the period of time that a storage system can discharge at its rated power without being recharged. Finally, maturity means how much-developed such a technology is.

Table (1.2) PHES system technical specifications [3,4]

	PUMPED HYDROELECTRIC ENERGY STORAGE				
1	Energy rating (MWh)	200-500	10	Daily self-discharge rate	0
2	Power range (MW)	10-5000	11	Storage duration	Hours-Months
3	Energy Density (kWh/m^3)	0.5-1.33	12	Discharge duration	1- 24+ hrs
4	Power Density (kW/m^3)	0.01-0.12	13	Response time	3-5 mins
5	Specific Energy (Wh/kg)	0.5-1.5	14	Typical size	Large
6	Round-Trip Efficiency (%)	70-85	15	Maturity	Mature technology.
7	DoD (%)	95	16	Energy Capital Cost ($/kWh)	5-100
8	Technology Lifetime (years)	30-60	17	Power Capital Cost ($/kW)	500-2000
9	Lifecycle (cycles) %	10000-30000	18	Operating and Maintenance (O&M) Costs ($/kW-year)	3

1.2.2 Mechanical energy storage systems

Mechanical energy storage systems are the oldest type of energy storage systems. These systems convert mechanical energy, which is usually stored in the forms of potential energy, kinetic energy, pressurized gas, or forced spring, into electrical power. The most common types used either use the conversion of the kinetic energy of moving bodies into electrical power, such as kinetic energy in flywheels, or pressurized gas such as compressed air into electrical energy.

The major drawback of such a system is the heat losses and the amount of wasted energy during the conversion process [5,7]. The two significant derivatives of mechanical

energy storage technologies are flywheels energy storage (FES) systems and compressed air energy storage (CAES) systems.

1.2.2.1 Flywheels Energy Storage (FES)

Flywheels generally are comprised of the rotor, bearings, electrical machine (motor/generator), power converters, and supporting media such as a vacuum chamber and vacuum pump, as shown in Figure (1.6) [8].
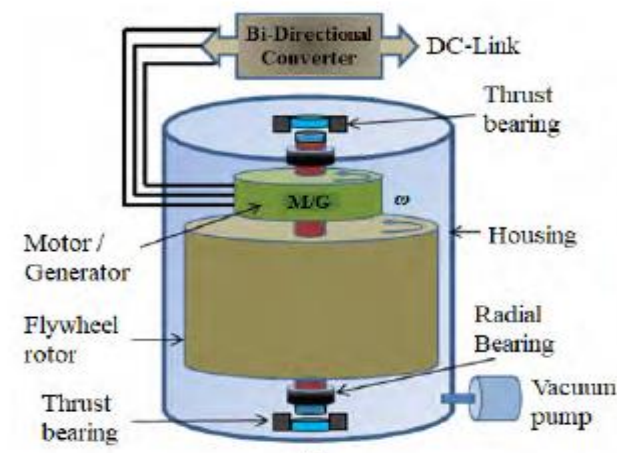
Figure (1.6) FES system [8]

In FES systems, kinetic energy is stored in a significant central axis rotating body (rotor). This rotor gets accelerated with the help of motors, shafts, and gears which are attached to the central axis. As long as there is a need to store energy, the motor keeps on rotating but in the hours of need, the same motor acts as a generator and converts the kinetic energy back into electrical power [7]. The stored kinetic energy in such FES systems depends on speed and inertia. The major drawback of this system is its high discharge rate. However, it is suitable for short discharge time applications [8].

Depending upon the speed of rotation, flywheel systems are of two types; low-speed flywheels: in this type, the rotation speed is less than 10,000 revolutions per minute. Such systems are capable of storing an adequate amount of energy. Also, such systems are efficient as they encounter fewer amounts of friction and heat losses as compared to the high-speed flywheels. The second type is the high-speed flywheels, where the rotation speed can reach up to 100,000 revolutions per minute. Because of such high rotational speed, they encounter more losses of friction and heat. Their speed gives them the edge to store vast amounts of energy [4,8].

1.2.2.2 Compressed Air Energy Storage (CAES)

The compressed air energy storage system works based on the compression of gasses (usually air) and stores this produced energy in the form of pressurized air in an underground cavern or overground reservoir based on the application. During high power demand, this compressed energy can then be expanded to start rotating turbines that are connected to electric generators to produce electricity. Depending upon the gas injecting and storing method, compressed air storage systems are further categorized into three types: diabetic, adiabatic, and Isothermal storage systems [5].

1.2.3 Electrochemical energy storage systems

Electrochemical energy storage systems use both electric and chemical media to store energy. A DC power is stored in the reversible chemical reaction through an electrolyte, and it gets discharged when it is needed. The basic examples of these systems are rechargeable batteries and flow batteries. The major drawback of batteries is the life span and maintenance cost.

1.2.3.1 Batteries Energy Storage (BES) systems

In the past few decades, batteries have been serving either as the primary or secondary power sources for many applications ranging from residential to industrial use; nowadays, they are serving in almost every electrical field ranging from powering up the basic electric circuits to advanced electric vehicles and grid stations.

Batteries are made of groups of cells connected in parallel or series. Those cells, which are small electrochemical units, produce voltage depending upon the chemistry and the materials used inside them. Every cell consists of positive and negative electrodes, electrolyte, and separator. As for illustration, a lithium-ion (Li-ion) cell is shown in Figure (1.7) [9].
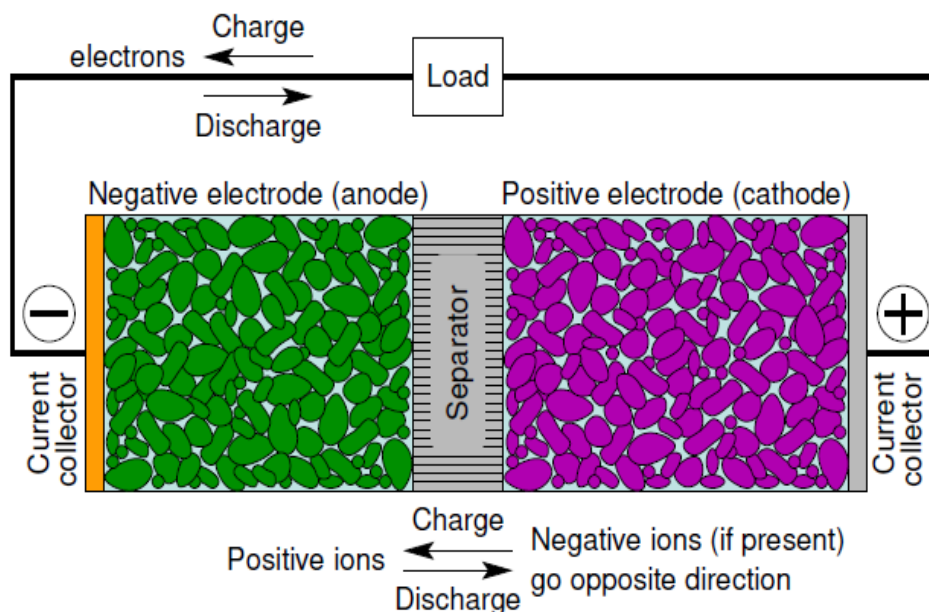
Figure (1.7) Li-ion Battery [9]

During the discharging mode, the cell delivers the stored electrochemical energy to the load as electrons that are moving from the negative electrode through the external circuit to the positive electrode. During charging, that process will be in the opposite direction, and the negative electrode now is accepting electrons. The electrolyte in lithium-ion (Li-ion) cells is mostly a lithium salt (e.g. Lithium hexafluorophosphate). The separator is a porous membrane separating anode and cathode spatially and electrically [9,10].

In this illustration of Figure (1.7), the lithium-ion cell was picked as an example, but the basic principle of operation can apply for all other types of cells. However, depending upon the chemistry and production techniques, batteries are of several types. And some of these types will be described extensively in the following subsections.

1.2.3.1.1   Lead-Acid (Pb-A) Batteries

Lead-acid batteries are the oldest rechargeable batteries, which were invented by French physicist Gaston Planté in 1859 [4]. The chemical materials of these batteries are very mature as compared to other available types. The primary issue in lead-acid batteries is the lifetime of the cells that mainly depends on the current rates and the number of charging and discharging times.

Lead-acid batteries are categorized into two types which are: valve regulated (sealed) lead-acid batteries (VRLA) and vented lead-acid batteries (VLA). The valve-regulated lead-acid batteries (VLRA) have significantly improved and overcame the major drawback of vented lead-acid battery (VLA), which demand for their operation periodically water replenishment, by arranging and preserving the oxygen pressure inside the cell. During the charging phase in VRLA, some hydrogen and oxygen molecules are produced which can be recombined to form water during the discharge phase [3]. In other words, the valve regulating process compensates for frequent water replacement in VLA; therefore, VRLA batteries are known as dry batteries or maintenance-free batteries. Two types of VRLA technologies are used in the present time, which are AGM and GEL VRLA. In the AGM or Absorbed Glass Mat VRLA, the battery is sealed by a glass of fiber to reduce evaporation. In the GEL-VRLA type, silica gel is introduced in the electrolyte to form a gelled electrolyte structure to improve the efficiency of the battery. Also, a new hybridization of both AGM and GEL VRLA batteries, which is called Hybrid-VRLA, has advanced and improved design features and gained the advantages of both technologies [11].

1.2.3.1.2   Sodium Beta (Na-beta) Batteries

Sodium Beta batteries use sodium ions as the main components in their chemistry. In Na-beta batteries, sodium is set as the anode of the cell, while the beta alumina is used as an electrolyte. Sodium-beta batteries are mainly categorized based on the cathode material into two types which are sodium-sulfur (Na-S) batteries and sodium-metal halide (Na-MeCl_2) cells, which are also called (ZEBRA) cells referred to zero-emission battery research activity.

Sodium-sulfur (Na-S) batteries have been proven as among the most promising batteries. In sodium-sulfur cells, the anode is made of sodium, while sulfur is set as the cathode of the cell, and the beta alumina ceramics are used as an electrolyte and separator, as shown in Figure (1.8) [8]. High power can be generated in these systems with the active reaction of sodium and the sulfurin which forms the sodium-poly-sulfide while discharging. During the charging mode, this reaction is reversed with the decomposition of sodium-poly-sulfide into

sodium and sulfur. Moreover, these batteries have a high power density, long lifetime, and their power produced is cheap because of the abundant raw materials in nature, which makes Na-S batteries suitable for grid applications [3,12]. The operating temperature of the system is between 300-350 Celsius; however, Abu Dhabi Department of Energy has opened the world's largest virtual sodium-sulfur battery plant with a capacity of 108 MW/648 MWh distributed across the emirate [13,14]. Furthermore, the applications that require high energy density and long life cycles such as EVs or hybrid EVs, sodium-metal halide batteries (ZEBRA batteries) are a suitable option for them. This technology has been
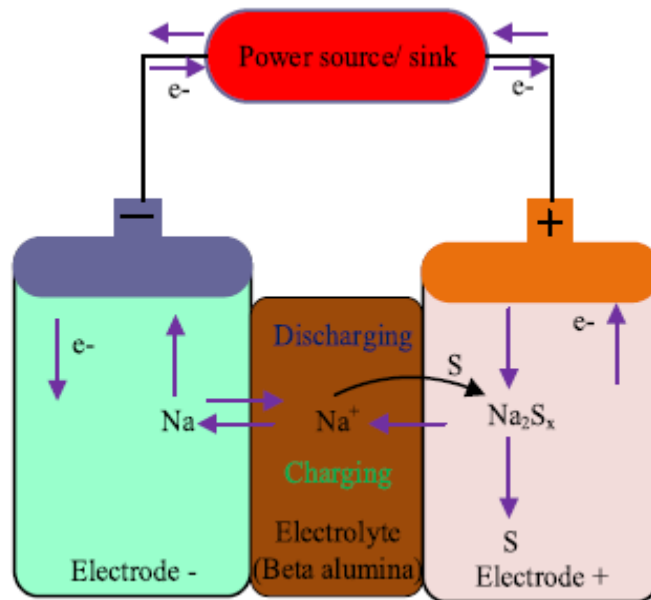
Figure (1.8) schematic diagram of Na-S battery [8]

improved to serve heavy-duty vehicles and to provide overcharging/discharging tolerance. Their production rate and lifetime exceed by far the lead-acid batteries. The cells of the sodium halide batteries consist of solid sodium metal which serves as the anode, and a semisolid porous active chloride ($MeCl_2$) cathode. In between the cathode and anode, liquefied sodium that is used as an electrolyte and for separation. The operating temperature of the system is about 300 Celsius [15].

1.2.3.1.3   Lithium Batteries

Lithium batteries are generally divided into two categories high-temperature lithium batteries and low-temperature (ambient temperature) lithium batteries based on their temperature resilience [16]. In both, lithium ions move from cathode to anode following the traditional current direction during charging periods, and the setup is totally reversed

discharging mode [8]. Lithium-ion battery is a suitable option for applications in which the high response time, smaller sizes, lightweight installations and long lifetimes are required Moreover, TESLA has built the world's largest lithium-ion battery plant in South Australia with a capacity of 100MW/129MWh, and it is connected to Neoen Hornsdale wind farm [17, 18].

1.2.3.1.4   Metal-Air Batteries

In metal-air batteries, energy is stored when electrochemical reactions occur between the metal's anode (usually lithium Aluminum, Iron, Sodium, or Zinc) and the air negative cathode. Both liquefied and solid electrolytes can be used in these batteries. The metal itself occupies most of the density of the battery's cell, and hence they have a sufficiently large energy density. The primary issue of this type of battery is its high self-discharge rate. Zinc-Air batteries have been serving in various industrial applications for many years, but these batteries are used as a secondary option after the other advanced batteries [19].

1.2.3.1.5   Nickel-based Batteries

This type is one of the oldest technologies in the field of electrochemical batteries. Of all kinds of nickel-based cells, the anode is usually of nickel material, whereas the cathode can be cadmium, metal hydride, iron, zinc or hydrogen. Potassium hydroxide often serves as the electrolyte material to carry out the charging and discharging reactions. Nickel Metal Hydride (Ni-MH) and Nickel-Cadmium (Ni-Cd) batteries are commonly used as compared to other nickel-based cells since they are more reliable and have long lifecycles [3].

1.2.3.2 Flow Batteries

In flow batteries, the chemical energy converted into electrical energy and vice versa because they have two separate tanks Vanadium Redox flow batteries (VRFB) and hybrid flow batteries (HFB) are the most common types of this technology. In VRFB, the reactions of oxidation and reduction occur between the vanadium redox couples of the anolyte and catholyte, as shown in Figure (1.9) [3]. These types of reactions are entirely reversible, and so the original elements can be restored completely.
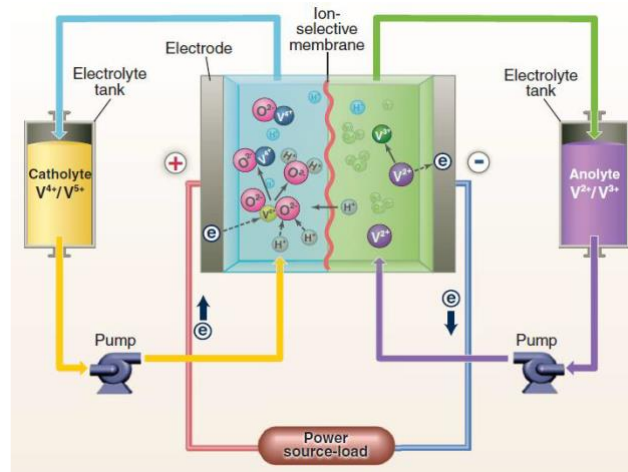
Figure (1.9) Vanadium redox flow battery [3]

Moreover, the halogen redox flow battery, which is known as a hybrid flow battery, is a combination of flow and secondary batteries. Also, it has two types, known as zinc chlorine and zinc-bromine flow batteries [3,18,20].

To summarize, batteries are attracting more and more researchers and manufacturing groups because of their wide range of specifications. It is worth noting that most of these technologies are sharing the same characteristics as fast response time (milliseconds); in contrast, they are different in other criteria like weight and size. However, Figure (1.10) and Table (1.3) show a brief comparison of electrochemical energy storage technologies, including batteries and flow batteries.
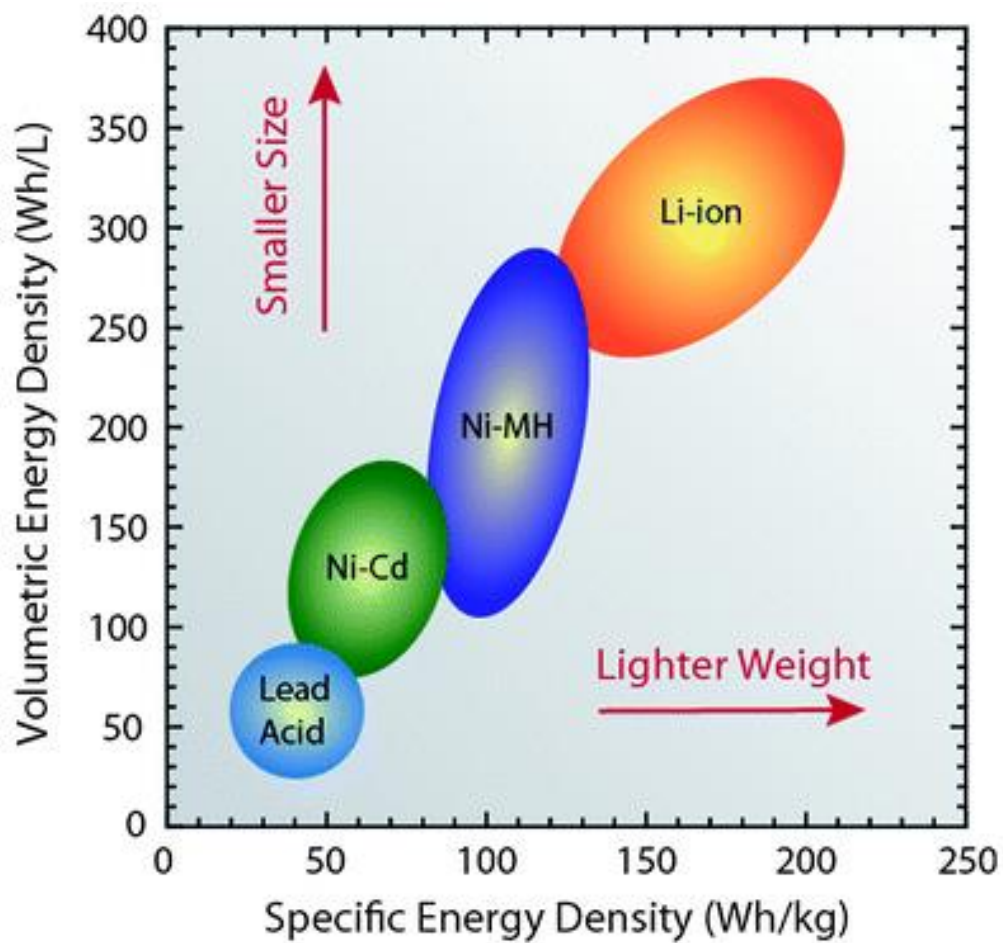
Figure (1.10) Energy density comparison of weight and size [21]

Table (1.3) Comparison of several types of batteries [3,4,5]

Electrochemical Energy Storage Technologies								
Technology	Storage duration	Power rating (MW)	Energy rating (MWh)	Round-trip efficiency (%)	Daily self-discharge (%)	Lifetime (years)	Operating temperature (°C)	Maturity
(Pb-A) Batteries	mins-days	0-20	18-100	70-90	0.1-0.4	5-15	−30-50	Mature
(Na-S) Batteries	secs-hours	10-34	245	75-90	0.05-20	10-15	300-350	Commercial
(ZEBRA) Batteries	secs-hours	0.005-1	0.12-5	70-85	20, 15	5-15	270-350	Commercial
(Li-ion) Batteries	mins-days	0.05-100	0.25-25	85-95	0.03	20-25	−20-60, 10-60	Commercial
(Zn-Air) Batteries	hours-months	0-1	0.06-0.15	50-65	~ 0	0.17-30	0-50	Developing
(Ni-MH) Batteries	-	0.01-3	0.00001-0.5	70-80	5-20	5-10	20-45	Mature
(Ni-Cd) Batteries	mins-days	0-40	6.75	60-90	0.1-0.2	10-20	45-60	Mature
(VRFB) Batteries	hours-months	0.01-10	4-40	60-75	~ 0	10-20	−10-40	Commercializing
(HFB) Batteries	hours-months	2-10	0.05-0.5	60-80	~ 0	5-10	−20-30	Demonstration

1.2.4   Thermal Energy Storage (TES) Systems

In the thermal energy storage systems, power is stored in the form of latent heat or latent freeze during the conversion of heat to electrical energy and vice versa. The power is released when the demand is high. With advances in this type of technology, many grid stations have been using this form of storage as secondary banks. The direct derivates of this technology are the solar ponds, latent heat energy, and the sensible thermal energy storage systems [8]. In solar ponds TES, the thermal energy coming from the sun are collected and stored as heat through the surfaces of water ponds or lakes [5]. Solar ponds TES can be categorized based on the formulation factors of the insulation zone between the hot water in the bottom layer and cold water in the top layer into: first, convecting or non-convecting solar ponds, which means that the solar ponds use the salinity gradient as an insulator to prevent the heat exchange form the lower and upper zones. Second partitioned or nonpartitioned solar ponds. Third, gelled or non-gelled solar ponds, where the gelled solar pond uses a solar gel, such as a polymer gel to reduce the heat losses by minimizing evaporation losses from the surface of the upper layer. Forth, in-pond storage or separate collector and storage [5].

In sensible TES, the energy storage capacity can be determined by the mass and temperature of the working material. Water is rated as one of the best sensible heat storage materials since it has high heat capacity [5]. Different forms of solids, liquids, and gasses can be used as a working material. The materials must be thermally conductive because this feature is essential for storing energy. High energy density is the distinguishing feature of this technology. The major and most commonly used application of this technology is the storage of ice in the reservoirs and then releases the energy and is converted back to water [5,8].

1.2.5   Thermomechanical Energy Storage Systems

In developed countries, the difference in supply and demand of the electric power is resolved by installing thermo-mechanical energy systems in the grid and power plants to obtain bulk energies. Usually, the two most common strategies used in this system are the heat pump

temperature difference systems and the cryogenic storage systems, which are sometimes called Liquid Air Energy Storage (LAES) systems.

1.2.5.1 Liquid Air Energy Storage (LAES) systems

In the cryogenic energy system, which is illustrated in Figure (1.11), the air is compressed in the charging phase to produce liquefied air. This liquefied air can be stored for long times. When power is required, air can be pumped to high altitudes to absorb heat and get converted back to the gaseous form. This gaseous air is then directed towards turbine blades to turn a generator on [22].
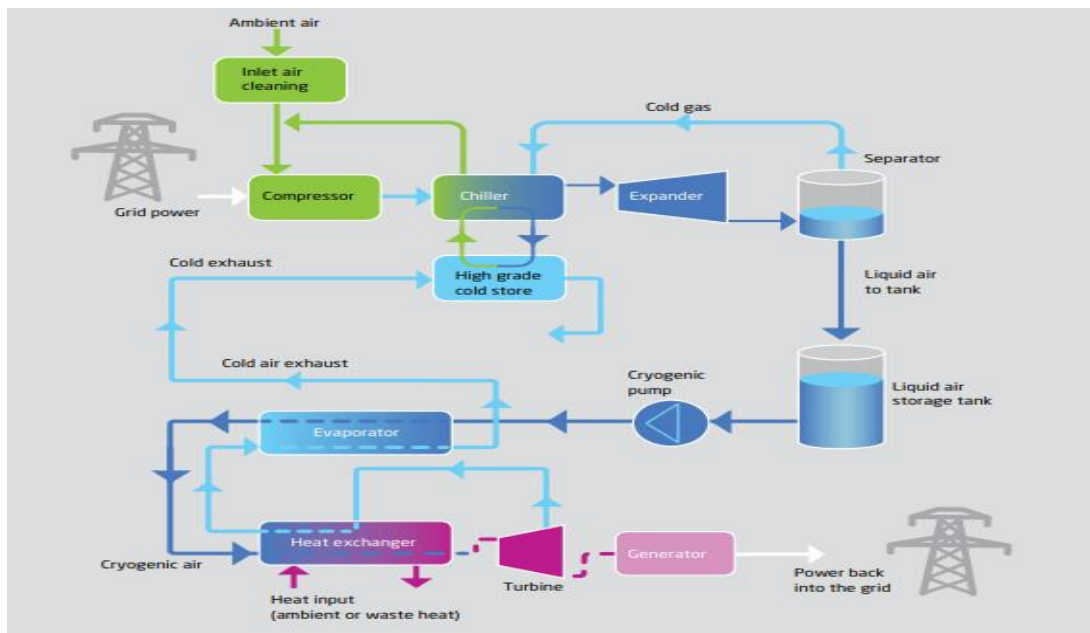
Figure (1.11) LAES system [22]

1.2.6 Thermochemical Energy Storage System

The thermochemical energy storage system stores thermal energy that is produced by a chain of chemical reactions. It must be able to store the heat generated during reactions in reactor tanks so that it can be used to ignite the irreversible reactions. Thermochemical systems are categorized into solar fuels and thermal sorption energy technologies. Both systems can operate at higher temperatures, and that is their key feature of them [18].

1.2.7 Electrical Energy Storage Systems

Electrical energy storage systems store electrical charges during an energy/power surplus time and supply them to the load when needed. Energy can be stored in the system with the help of supercapacitors or superconducting magnetic systems, which are the two major derivatives of the electrical energy storage systems [8].

1.2.7.1 Supercapacitor Energy Storage (SCES) systems

Supercapacitor energy storage (SCES) systems are also known either as ultra-capacitor (UC) energy storage systems or electric double-layer capacitors (EDLC). The major feature of such systems is the storage of electrical energy between two metal conducting electrodes of different polarities, separated by an electrolyte that only permits ions (not electrons) to pass through, as shown in Figure (1.12) [3, 4].
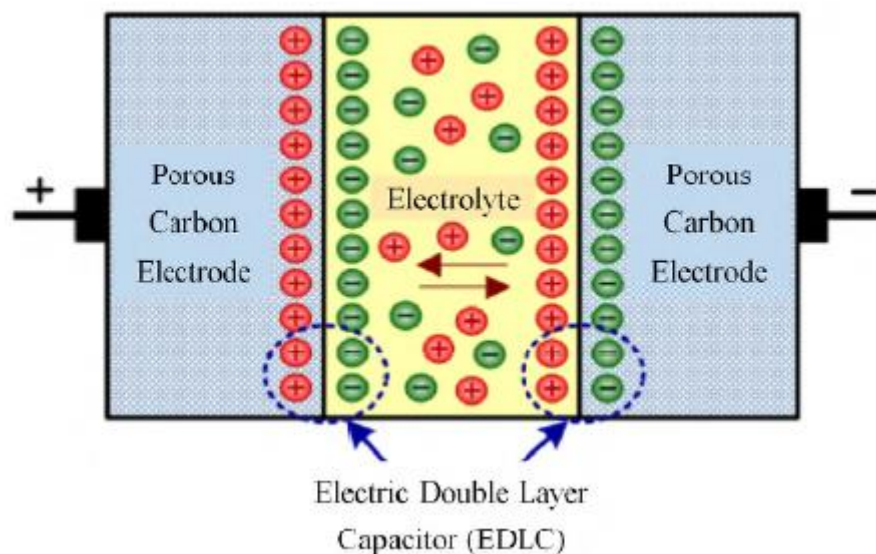
Figure (1.12) schematic diagram of EDLC [8]

Regardless of the mutual configuration between EDLC and batteries, no electrochemical reactions are involved in ELDC. These systems exhibit the properties of high peak power and power density. In comparison with the batteries, UCs can be charged and discharged up to millions of times as they possess a long service life. They have a fast response time. Supercapacitors are of three types: pseudo-capacitors, double-layered capacitors, and

hybrid capacitors. The wide range of characteristics of supercapacitors can help the energy storage field to perform many tasks, such as load balancing and power quality improvement. The drawbacks of supercapacitors are low specific energy, low energy density, high capital cost, and high self-discharge rate [8]. More technical specifications are tabulated in Table (1.4).

Table (1.4) SCES system technical specifications. [3,4]

SUPERCAPACITORS ENERGY STORAGE (SCES)					
1	Stored Energy form	Electrical energy	12	Round-Trip Efficiency (%)	85-98
2	Energy rating (MWh)	10^{-6}- 5×10^{-3}	13	DoD (%)	100
3	Power range (MW)	0-0.3, 0.01-0.3	14	Technology Lifetime (years)	10-12, 25-30
4	Energy Density (kWh/m^3)	1-35	15	Lifecycle (cycles) %	106, 100k-500k
5	Power Density (kW/m^3)	15-4,500	16	Maturity	Developing
6	Specific Energy (Wh/kg)	2.5-15, 0.05-15	17	Operating Temperature (℃)	-40 – 85
7	Specific Power (W/kg)	500-5,000, 10-1,000,000	18	Energy Capital Cost ($/kWh)	300-2,000
8	Suitable Storage duration	Secs-hours	19	Power Capital Cost ($/kW)	100-300
9	Discharge duration	msec-min	20	Operating and Maintenance (O&M) Costs ($/kW-year)	6
10	Response time	msec	21	Impacts	Chemical disposal issues
11	Daily self-discharge rate (%)	20-40, 10-40	22	Applications	Short term storage applications. Applications required many charge-discharge cycles.

1.2.7.2 Superconducting Magnetic Energy Storage (SMES) systems

During a charging mode in SMES, with the help of AC-DC power converters, energy is stored in the form of magnetic fields energy when current is circulating through a coil of superconducting material. In a discharging mode, DC to AC power converter is used to release the energy stored in the magnetic fields. However, heat losses (Ohmic) are the main disadvantage in such devices. These heat losses can be minimized if the temperature is maintained below a specific temperature threshold of a conducting material; therefore, a refrigeration (cooling) system, including liquid coolant (e.g. liquid helium, liquid nitrogen) is utilized in SMES such a system is presented in Figure (1.13).
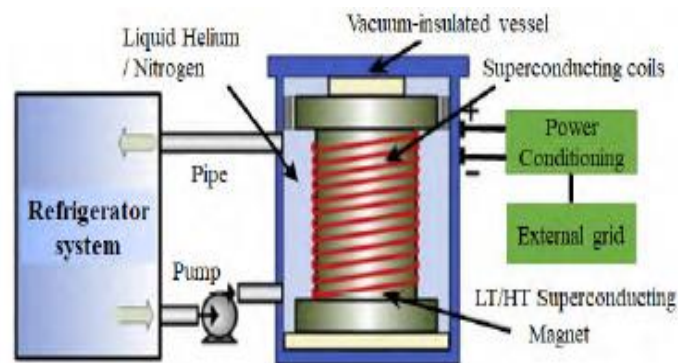
Figure (1.13) SMES system [8]

In addition, SMES systems can be categorized based on the system's operating temperature into a high-temperature system which operates at 70K ($-203.15°C$), and low-temperature system which operates at approximately 7K ($-266.15°C$). These systems have storage duration that can last for years, but they require high capital costs [8]. Moreover, additional technical specifications are tabulated in Table (1.5).

Table (1.5) SMES system technical specifications [3,4,23,24,25]

SUPERCONDUCTING MAGNETIC ENERGY STORAGE (SMES)					
1	Stored Energy form	Magnetic field	12	Round-Trip Efficiency (%)	95, 90-97

2	Energy rating (MWh)	0.015, 15-100	13	DoD (%)	100
3	Power range (MW)	0.1-10, 0.01-10	14	Technology Lifetime (years)	20-30
4	Energy Density (kWh/m^3)	0.2-13.8, 0.2-2.5	15	Lifecycle (cycles) %	$\sim \infty$, 20,000-100,000
5	Power Density ((kW/m^3)	300-4,000	16	Maturity	Commercializing
6	Specific Energy (Wh/kg)	0.5-5, 40-60	17	Operating Temperature (℃)	162-253
7	Specific Power (W/kg)	500-2000	18	Energy Capital Cost ($/kWh)	1,000-10,000
8	Suitable Storage duration	Hours-days	19	Power Capital Cost ($/kW)	200-350
9	Discharge duration	msec-sec	20	Operating and Maintenance (O&M) Costs ($/kW-year)	18.5
10	Response time	msec	21	Impacts	Light environmental impact
11	Daily self-discharge rate (%)	10-15	22	Applications	Suitable for applications that required a fast discharge rate, and short term energy storage applications.

1.2.8   Chemical Energy Storage Systems

In chemical energy storage systems, energy can be stored in the form of chemical bonds of molecular compounds. In comparison with other power storage systems, the energy density in the chemical system is much higher. The most promising chemical storage technology is the hydrogen system which uses hydrogen fuel to store energy [8]. Hydrogen can be obtained by

performing electrolysis on the water to store it in tanks. After that, it can be used to produce power just by reversing the process [26].

1.2.8.1 Hydrogen Fuel Cells (HFC)

Hydrogen fuel cells have the ability to store a significant amounts of energy, which makes this technology a promising solution for the automobile industry. Hydrogen fuel only releases water vapor into the environment, and that makes it convenient for emissions-free applications. On the other hand, the complicated procedure to store hydrogen, low conversion efficiency, and the high cost of hydrogen refueling are the main drawbacks of HFC. However, due to the compactness and movability of the chemicals, a considerable amount of research is being done, and the future is bright for this technology since researchers came up with a thermochemical method, known as a "solar hydrogen approach", to extract the hydrogen directly from solar power [3].
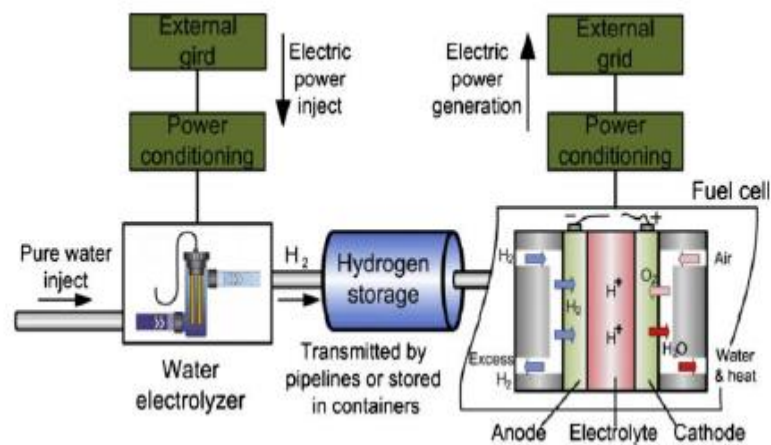
Figure (1.14) HFC system [3]

1.3 Comparison:

According to the proposed use of the energy storage systems, there are miscellaneous technical and operational performance characteristics to be taken into consideration, such as power and energy density, storage duration, response time, self-discharge rate, lifetime, life cycle, round-trip efficiency, etc. Therefore, Table (1.6) presents an extensive comparison

between 19 energy storage technologies based on 20 technical and operational criteria [3,4,23,24,25]. Moreover, in order to design a hybrid energy storage system, someone needs a comprehensive and effective assessment, and an in-depth comparison between these technical and operational features to evaluate the feasibility of a system.

Table (1.6) Technical and Operational characteristics of ESSs [3,4,23,24,25]

	Technology	Stored Energy	Storage duration	Power rating	Energy rating	Power Density	Energy Density	Specific Power	Specific Energy	Response Time	Discharge duration
					Energy Storage Technologies						
1	GBES	potential	30-300	2000-25000	-	-	-	-	-	-	-
2	ARES	potential	2-24 hours	100-3000	-	-	-	-	-	5-25 sec	34 sec
3	PHES	potential	Hours-months	10-5,000	200-500	0.01-0.12	0.5-1.33	0.01-0.12	0.5-1.5	3-5 mins	1-24+ hrs
4	CAES	Pressurized gas	Hours-months	5-300	200-2,000	0.04-10	0.4-20	2.2-24	10-30	mins	1-24+ hrs
5	FES	Kinetic	secs-mins	0.01-0.25	0.025-5	40-2,000	0.25-424	1,000	5-80	msec-sec	secs-15 mins
6	SCES	Electrical	secs-hours	0.01-0.3	< 0.005	15-4,500	1-35	500-5,000	2.5-15	msec	msec-min
7	SMES	Electrical	Hours-days	0.01-10	0.01-0.03	300-4,000	0.2-2.5	500-2,000	40-60	msec	msec-sec
8	TES	thermal	mins-days	0.1-300	-	-	-	10-30	80-200	NOT rapid	1-24+ hrs
9	LAES	Liquefied Air	hours	10-200	2.5	-	80-120	-	214	mins	-
10	HFC	chemical	hours-months	0.3-50	< 200	1-300	25-770	5-50	200-1200	secs	sec-24 hrs
11	(Pb-A) Batteries	Electrochemical Reaction	mins-days	0-20	18-100	10-400	25-90	180	30-50	msec	sec-5 hrs
12	(Na-S) Batteries	Electrochemical Reaction	secs-hours	10-34	245	1.3-50	150-345	150-240	120	msec	6-7.2 hrs
13	(ZEBRA) Batteries	Electrochemical Reaction	secs-hours	0.005-1	0.12-5	54-300	108-190	174	120	msec	sec-hr
14	(Li-ion) Batteries	Electrochemical Reaction	mins-days	0.05-100	0.25-25	56-800	94-500	500-2,000	100-200	msec	min-1 hr
15	(Zn-Air) Batteries	Electrochemical Reaction	hours-months	0-1	0.06-0.15	10-208	22-1673	60-225	450-650	msec	10-15 hrs
16	(Ni-MH) Batteries	Electrochemical Reaction	-	0.01-3	0.00001-0.5	8-588	39-300	220	50-75	msec	hrs
17	(Ni-Cd) Batteries	Electrochemical Reaction	mins-days	0-40	6.75	38-141	15-150	140-180	35-60	msec	1-8 hrs
18	(VRFB) Batteries	Electrochemical Reaction	hours-months	0.01-10	4-40	2.5-33.4	10-33	80-150	30-50	msec	5-10 hrs
19	(HFB) Zn Br Batteries	Electrochemical Reaction	hours-months	2-10	0.05-0.5	3-8.5	5.2-70	100	75-85	msec	8-10 hrs

Energy Storage Technologies									
Technology	DoD(%)	Round-trip	Daily self-discharge	Lifetime (years)	Lifecycle (cyclec)	Operating temperatu	Power capital	Energy capital	Operating &	Maturity
1 GBES	100	-	-	35-40	-	-	-	-	-	Developing
2 ARES	100	78-80	~ 0	40	-	-	1350	168	-	Developing
3 PHES	95	70-85	~ 0	30-60	10,000-30,000	Ambient	500-2,000	5-100	3	Mature
4 CAES	100	41-75	~ 0	20-40	8,000-13,000	Ambient	500-1,800	50-400	19-25	Developed
5 FES	100	90-95	55-100	15-20	20,000-100,000	20-50+	100-300	1,000-5,000	20	Commercial
6 SCES	100	85-95	20-40	25-30	100,000-500,000	−40-85	100-300	300-2,000	6	Developing
7 SMES	100	95	10-15	20+	20,000-100,000	−162-253	200-350	1,000-10,000	18.5	Demonstration
8 TES	-	~30-60	0.05-1	10-20	-	-	200-300	20-60	-	Demonstration
9 LAES	100	55-80	~ 0	25+	-	-	900-1,900	260-530	-	Developing
10 HFC	90	30-50	~ 0	5-15	20,000	50-100	400-2,000	1-15	0.002-0.2	Developing
11 (Pb-A) Batteries	80	70-90	0.1-0.4	5-15	500-2,000	−30-50	175-600	150-400	50	Mature
12 (Na-S) Batteries	100	75-90	0.05-20	10-15	2,500-4,000	300-350	3,200-4,000	300-500	80	Commercial
13 (ZEBRA) Batteries	-	70-85	15-20	5-15	1,000-1,200	270-350	150-300	230-345	-	Commercial
14 (Li-ion) Batteries	80	85-95	0.03	20-25	1,000-10,000	−20-60, 10-60	1,200-4,000	400-2,500	-	Commercial
15 (Zn-Air) Batteries	-	50-65	~ 0	0.17-30	1,000-2,000	0-50	100-250	60-160	-	Developing
16 (Ni-MH) Batteries	50	70-80	5-20	5-10	800-3,000	20-45	600-1,800	720-2,880	-	Mature
17 (Ni-Cd) Batteries	100	60-90	0.1-0.2	10-20	800-2,500	45-60	500-1,500	600-2,400	20	Mature
18 (VRFB) Batteries	100	60-75	~ 0	10-20	>12,000	−10-40	1,400-3,700	500-800	70	Commercializing
19 (HFB) Zn Br Batteries	100	60-80	~ 0	5-10	2,000-3,500	−20-30	1,800-2,000	100-700	-	Demonstration

1.4 Hybrid Energy Storage System (HESS)

A hybrid energy storage system (HESS) possesses the properties of two or more ESSs, that are integrated together to achieve the unique characteristics of each technology and eliminate their limitations [8]. Usage type, energy density, power rating, charging/discharging characteristics, response time, operating temperature, environmental conditions, self-discharge rate, life cycle, efficiency, and cost determine the combinations of hybrid energy storage systems. Most often, the heterogeneous systems are organized in such a way that high power devices supply the short term power needs since they have high response time, and high energy devices supply the long term power needs due to the slow response time. Table (1.7) shows the ESS technologies that are recognized as high energy or high-power storage devices [3,4,8].

Table (1.7) Classification of high power and energy systems [3,4,8]

High power technologies	High energy technologies
Flywheels	PHES
SCES	CAES
SMES	HFC
Batteries	Batteries

Furthermore, as shown in Figure (1.15), HESSs are classified into near term hybrid systems and long-term hybrid systems. This classification is based on the system's response time and storage duration properties.
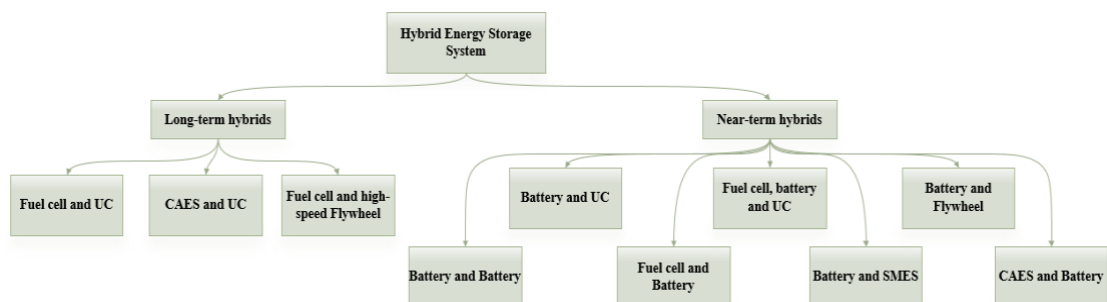
Figure (1.15) Classification of HESS

Near term hybrids represent the integration of the following independent technologies; battery and battery hybrid system, battery and ultra-capacitor hybrid system, battery and fuel cells hybrid system, battery and fuel cells and ultra-capacitor hybrid system, battery and flywheel hybrid system, and battery and CAES hybrid system. All these systems contain a battery as the mutual constituent as the battery has many types with a wide range of characteristics (e.g. high power and energy density) as compared to the other storage systems. Contrarily, long-term hybrid systems can be formed by the integration of the following systems; fuel cells and ultra-capacitor hybrid systems, fuel cells and the ultra-high-speed flywheel hybrid systems, and CAES and the ultra-capacitor hybrid system.

With the recent focus on HESS, most of these technologies became maturely developed (like batteries and supercapacitors) while others still require further development. However, due to the problems of sizing, safety, and cost-effectiveness with these hybrid systems, researchers around the globe are now focusing on eliminating their obstacles [3,8].

To summarize, different energy storage systems have been reviewed and a comprehensive comparison of these technologies was presented to illustrate their diversity. Consequently, this comparison can help select and decide the best energy storage system for any application.

Chapter 2: Energy Storage Systems for Traction Applications

2.1 Introduction

This chapter will be focusing on automotive applications and their energy storage technologies; therefore, it is crucial to understand the developments that have happened during the last century in the vehicle's production sector. For many decades, gasoline- and diesel-powered vehicles have dominated this industry, but since the early 1900s, electric vehicles have emerged as an ambitious competitor to gasoline-powered cars. However, the abilities of the first available electric vehicles of the early 1900s were significantly limited compared to gasoline-powered vehicles which have been improved due to the discovery of crude oil in the U.S. and around the world, which made gas cheap. As a result, electric vehicles disappeared by 1935, then entered a sort of dark ages with too slow advancement until the 1990s, when new government policies and regulations, especially in California, begun to change [2, 27].

These changes in the transportation emissions regulations have profoundly helped make automakers reconsider electric vehicles as an interesting option again. Following these regulations, automakers began investing more money in research and development to improve electric vehicles until around the end of the 20_{th} century and the beginning of the 21_{st} century, when Toyota Prius hybrid and Honda Insight hybrid became commercially viable. Later in 2006, Tesla Motors announced entering the market of electric vehicles, and then in 2010, the U.S. Department of Energy lent Tesla \$465 million to build and develop the infrastructure for electric vehicles. Tesla's announcement was the real notification of the beginning of a new era in the electric vehicles industry [27, 28].

Over the next few years, other companies, such as BMW, Chevrolet, Nissan, etc. started producing and selling new versions of electrified vehicles ranging from small-sized to luxury vehicles in the U.S. market. According to a global EVs outlook report published by the International Energy Agency (IEA), in 2018, the global electric cars exceeded 5.1 million, and more than 2 million cars were sold in this year which is almost doubling the number of new

electric car registrations from the previous year [1]. Figure (2.1) shows the annual EV sales in major markets from 2010 to 2018 [29].
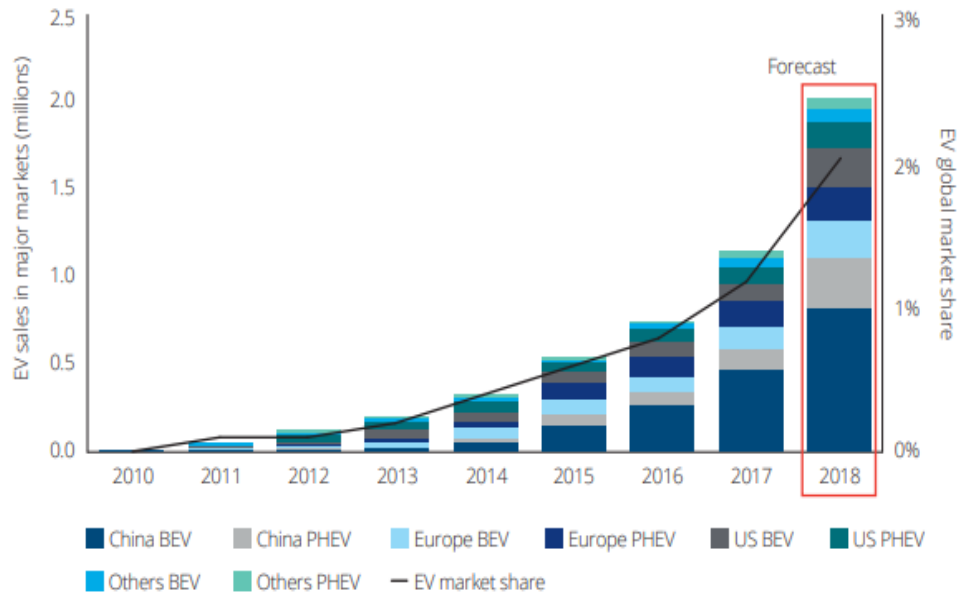
Figure (2.1) Electric vehicles annual sales in major regions [29]

China is the world's largest electric car market, followed by Europe and the United States. In response to the high demand for electric vehicles and the new city's policies and regulations, the growth in the electric car market will be at a rapid pace. Figure (2.2) shows the expected market demand for electric vehicles versus industry supply [29].
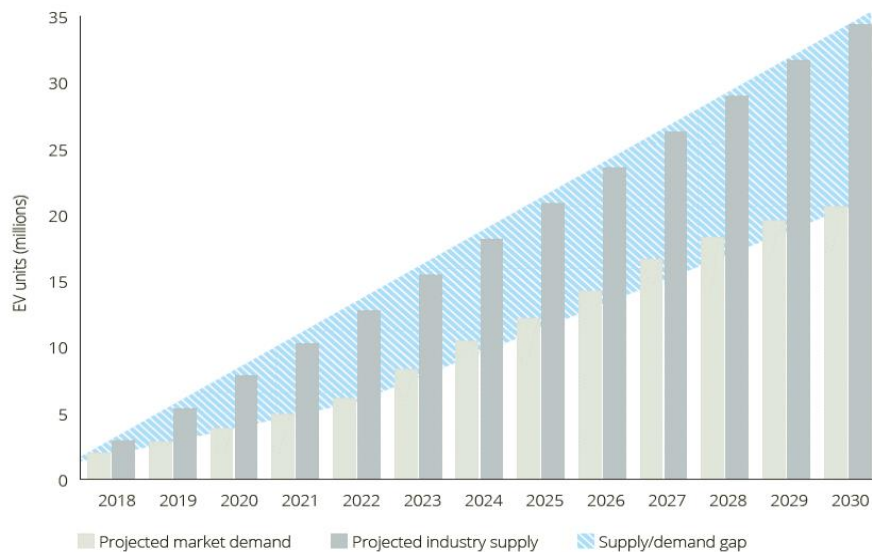
Figure (2.2) Market demand Vs. industry supply for electric vehicles [29]

This rapidly growing demand for EVs encourages researchers and developers to improve this technology to overcome the current challenges in electric and hybrid electric vehicles. The main issues and challenges for electrified vehicle deployment are its limited range and power performance. These challenges come from the energy storage system, power electronics, and electric motor technology. However, in the following sections, there will be a brief literature review on vehicle electrification advancement, energy storage systems modeling, different power electronics topologies, and hybrid energy storage system architectures.

2.2 Vehicles Electrification:

2.2.1   Overview

Vehicles electrification is the future alternative to conventional vehicles. The electrified vehicle is divided into two types i.e. the plug-in electric vehicle and hybrid electric vehicle. Both types are different in power sources and their internal configuration. However, energy storage systems like batteries and ultracapacitors are presented in both. A 3-phases AC motor is used to run the vehicle while rechargeable batteries become the source of energy. The bridge between the energy storage system and electric motors is the power electronics components. These power electronics components are capable of delivering high power from the battery to the motors in a proper control manner to accomplish a proper vehicle operation.

Moreover, these types of vehicles include cars, trucks, motorcycles, trains, scooters… etc. and each type has a separate configuration and power requirements. The following sub-sections will describe the complete internal configuration of electric and hybrid electric vehicles and how they work [29].

2.2.2   Types of vehicles electrification

In general, there are two types of electric vehicles which are a pure electric vehicle (EV) or plug-in electric vehicle (PEV), and the second type is a hybrid electric vehicle (HEV), and they are shown in Figure (2.3) and Figure (2.4), respectively [28]
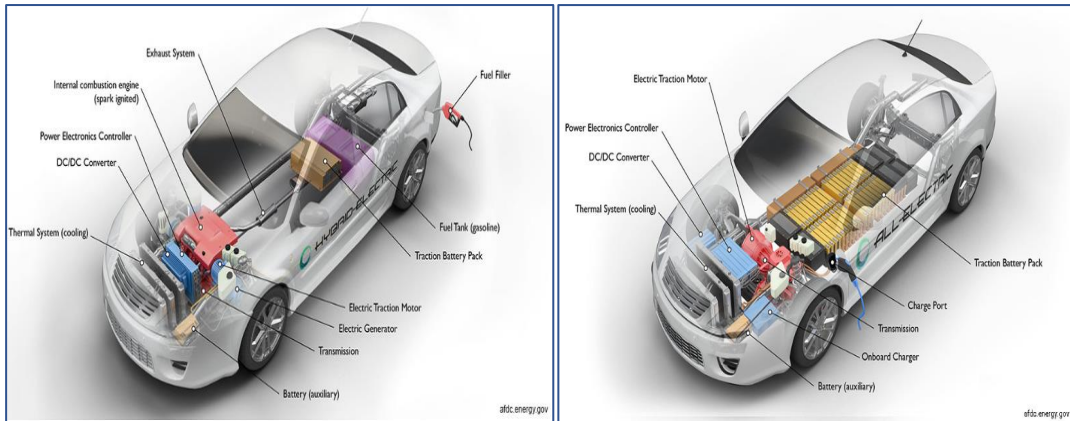
Figure (2.3) Hybrid electric vehicle (HEV) [28]   *Figure (2.4) Plug-in electric vehicle (PEV) [28]*

2.2.2.1 Plug-in Electric Vehicle (PEV)

This type of vehicle has no source of energy other than electrical power that comes from an energy storage device (usually batteries) to run the AC motor and all other circuitry inside the vehicles. Plug-in electric vehicle needs an external AC source to charge the battery pack since it has no source of energy other than electricity. However, the charging time and traveling range vary based on the architecture of the vehicle. PEV has its own advantages and disadvantages which are shown in the following Table.

Table (2.1) Advantages and disadvantages of PEV [30,32]

Advantages	Disadvantages
The battery pack can be charged from the electric grid.	Expensive.
Electric vehicle reduces fuel consumption compared to a conventional vehicle.	An electric vehicle requires a long charging time for the battery pack.
The used power source does not produce harmful particles or gases as conventional vehicle produces.	EV is not suitable for those places where the grid is not available.

PEV contains a quieter engine than ICE in conventional vehicles.	Battery's price is high, and its lifetime is limited.

2.2.2.1.1 Components of Electric Vehicle

EVs usually consist of a higher number of electronic components than conventional engine vehicles. The following are the major components used to drive vehicles without any interruption of external sources on the battery bank. First, a 3-phase electric motor and drives. Second, the energy storage system which usually includes a battery pack or battery pack combined with an ultracapacitor. Third, the control unit which includes a motor, battery, and charge controllers. Forth, regenerative braking system which uses the kinetic energy during braking mode to charge the energy storage system. Fifth, power electronics while the last one is the mechanical system that includes gearbox and the vehicle's body. The following diagram will elaborate on the major parts present in an electric car [28, 30].
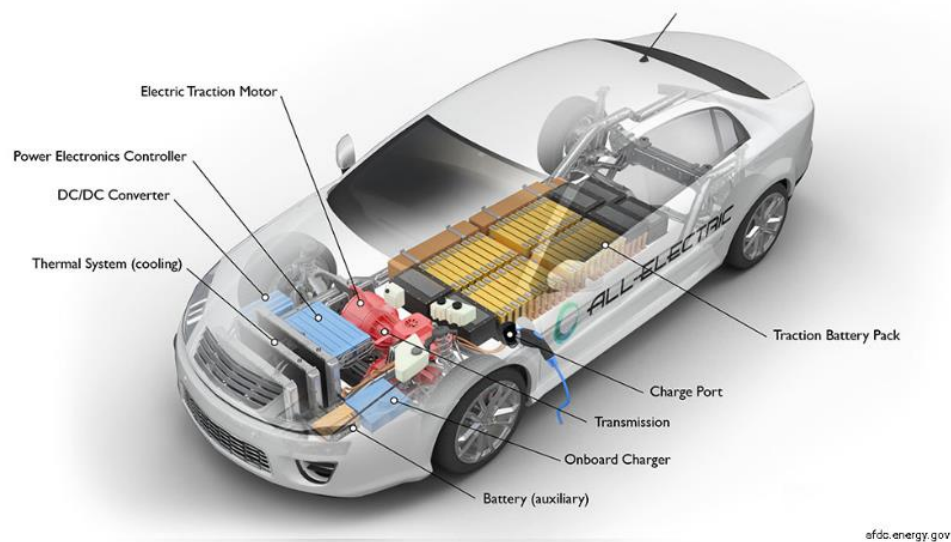
Figure (2.5) EV's major components [28]

2.2.2.1.2 Modes of Operation:

In general, an electric vehicle operates in two modes which are regenerative braking mode and motor only mode. In regenerative braking mode, the mechanical power (kinetic

energy) is used to charge batteries when power flows from the mechanical shaft to the batteries via the regenerative braking system. Whenever the brakes are pushed the mechanical energy is converted into electrical form to charge the battery. In motor only mode, the power flows from the battery pack to the mechanical shaft. In this mode, the battery power is used to drive the electric motor to move the vehicle. The following Figure will illustrate the operation modes in electric vehicles [31].
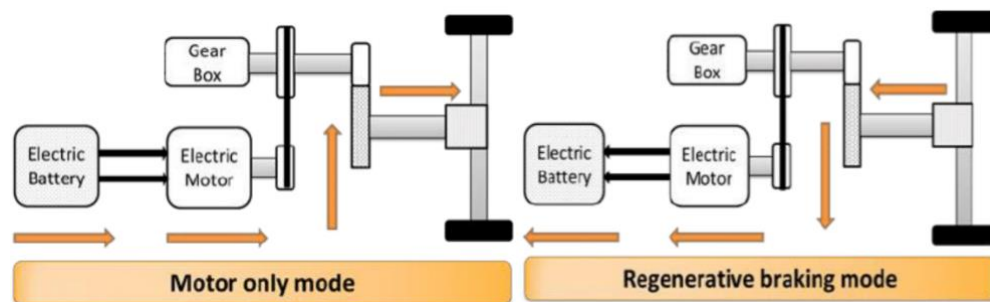
Figure (2.6) operation modes of PEV [31]

2.2.2.2 Hybrid Electric Vehicle

The hybrid electric vehicle is another type of electrified vehicles in which two different energy sources are electricity and fossil fuel. The main difference between Plug-in electric vehicles and hybrid electric vehicles is that HEV does not require any external source to charge the battery pack. HEV makes it sophisticated and reliable not only in the manner of efficient power generation but also in economic results as it consumes less amount of fuel than conventional vehicles. However, in another version of HEV that is known as "Hybrid Plug-in Electric Vehicle (HPEV)," the vehicle can be connected to the external grid to charge the batteries, which makes it more reliable than HEV, but the features of HPEV will not be discussed in this research. Moreover, HEV has its own advantages and disadvantages which are shown in the following Table [32].

Table (2.2) Advantages and disadvantages of HEV [30,32]

Advantages	Disadvantages
High efficiency.	It is not an economical vehicle as compared to PEV.
HEV produces less pollution than the conventional combustion engine.	Not environment-friendly as compared to PEV.
Environmentally friendly as compared to the conventional combustion engine vehicles.	The lifetime of batteries is limited, which will affect the overall performance of the system.
HEV does not require charging hours to charge the battery as PEV does.	It is much costly than conventional vehicles
The use of fossil fuel has enhanced the drawbacks present in the PEV.	Complex control system.

2.2.2.2.1   Components of Hybrid Electric Vehicle

HEVs usually consist of components that are used to drive the vehicles, but these components may vary based on the electrical power flow for each vehicle's architecture e.g. series, parallel, or series-parallel HEV. However, the major standard components used in these types are a 3-phase electric motor, generator, drives, conventional engine, energy storage system, DC-DC converter, power splitter, control unit, regenerative braking system, gearbox, and fuel tank. The following Figure will elaborate on the major parts in HEV [28].
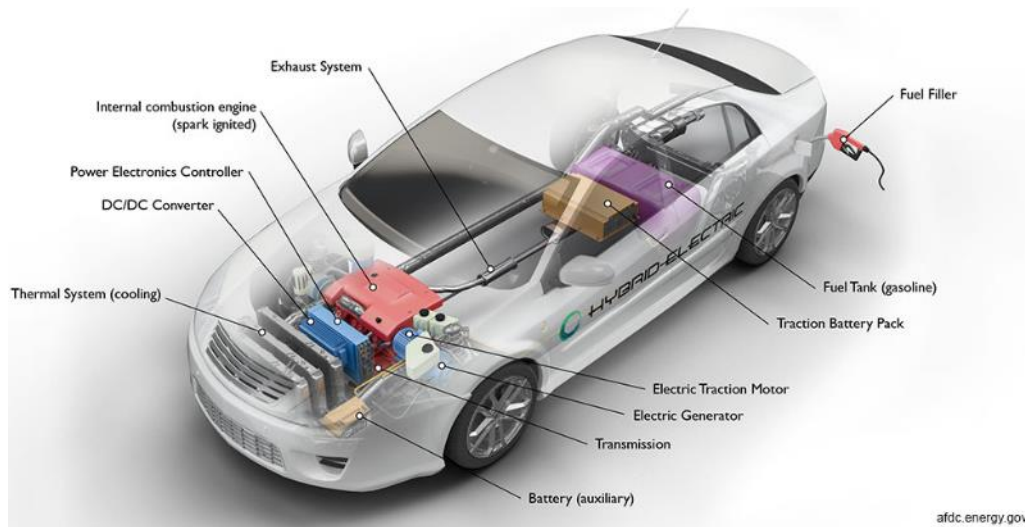
Figure (2.7) HEV's components [28]

2.2.2.2.1.1 Motors/ Generators

In electric and hybrid electric vehicles, there is an urgent need of advanced electric motors and generators to enhance the aggressive development of electrified vehicles. In literature, many types of motors and generators can be used for traction in EVs or HEVs. Figure (2.8) shows the classification of various motors used in traction applications [33].
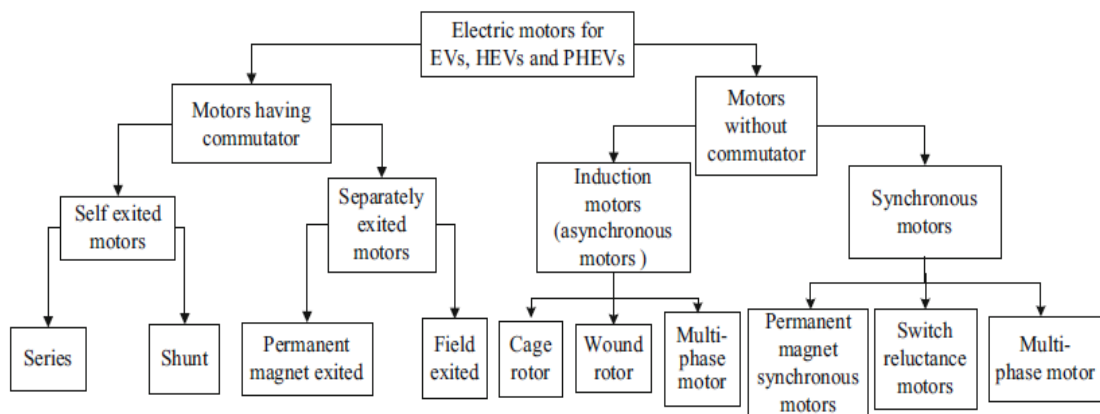
Figure (2.8) classification of motors used in traction applications [33]

For HEVs, there are many traction motors available in the market, such as switched reluctance motors, brushless DC motors, permanent magnet synchronous motors, induction motors, etc. However, based on the tradeoffs between cost, performance, robustness, and

reliability, induction motors (IM) and permanent magnet synchronous motors (PMSM) are the most common types used in HEVs [33, 34].

2.2.2.2.2 Architectures of hybrid electric vehicles

Hybrid electric vehicles can be categorized based on the electrical power flow into series, parallel, series-parallel, or complex HEV architectures. The first three configurations will be discussed in the following subsections, while the complex architecture, which is not commonly used, will not be addressed in this research.

2.2.2.2.2.1 Series hybrid electric vehicle

In series HEV architecture, the internal combustion engine is mechanically disconnected from the drivetrain of the vehicle, and energy is converted from fuel in the internal combustion engine into electrical energy to be stored in an energy storage system or converted back to mechanical energy by an electric motor. However, the efficiency of the overall system is limited due to energy conversion losses (between electrical and mechanical energy). Therefore, this architecture tends to be suitable for applications that do not require efficient electrical systems. Figure (2.9) shows a series HEV architecture in which an electric motor operates as the primary driving source [33, 35].
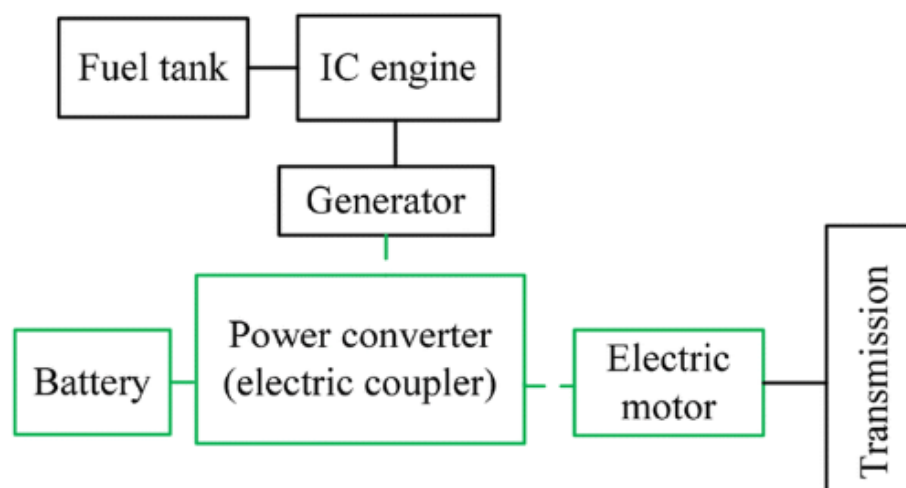
Figure (2.9) Series HEV architecture [33]

2.2.2.2.2.2 Parallel hybrid electric vehicle

In parallel HEV architecture, both electric motor and internal combustion engine, or one alone, can supply the traction power to the vehicle. The configuration that is demonstrated in Figure (2.10) has the mechanism that allows separate operation by one or more power sources. The flexibility in such systems makes it preferable for different operation conditions [33].
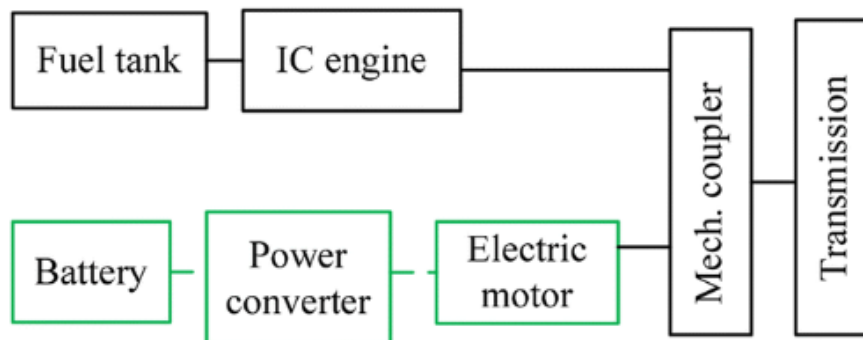
Figure (2.10) Parallel HEV architecture [33]

2.2.2.2.2.3 Series-Parallel hybrid electric vehicle

In series-parallel architecture, the internal combustion engine and electric motor are disconnected from drivetrain while a secondary motor remains connected to supply traction power to the vehicle. This configuration can operate in both series and parallel modes. This architecture is more complex than other configurations, but it is more flexible and reliable. The following Figure illustrates the series-parallel architecture of HEV [33, 36].
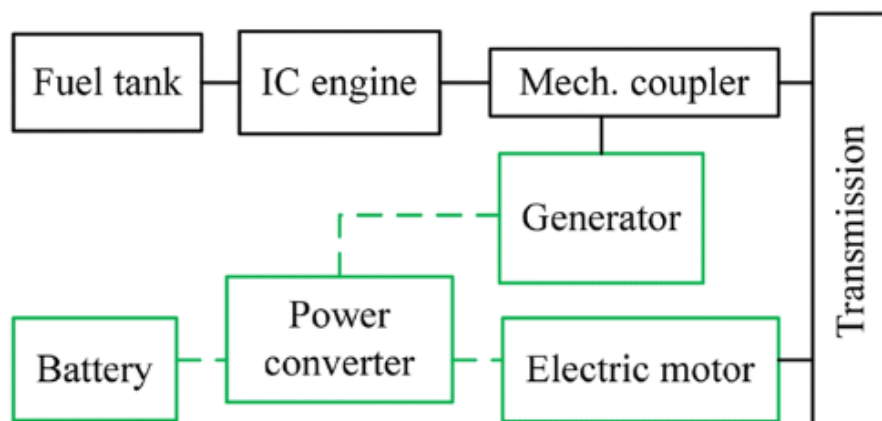
Figure (2.11) Series-Parallel HEV architecture [33]

2.2.2.2.3   Modes of operation

The working principle of an HEV is quite different from a PEV as two sources are present in the HEV. Therefore, HEV can operate in five different modes which are motor only mode, engine only mode, regenerative braking mode, trickle charge mode, and power assist mode. In all these modes the power flow of the system is controlled in a very frequent manner by the vehicle's controllers. Motor only mode works the same as in the PEV where only battery pack's power is used to drive the vehicle and the conventional engine is off. Engine only mode works the same as in traditional vehicles where all the power only comes from the engine. In regenerative braking mode, when the brake is pushed, the mechanical energy is used to charge the battery pack via a generator. In trickle charge mode, the engine power is used to charge batteries and to drive the vehicle simultaneously when it is desired such as during cruise mode. Moreover, in power assist mode, both engine and battery power are used to drive the vehicle during high power demand like in hill climbing or acceleration times. The following Figures will elaborate the working modes of HEV in a possible simplest form [31].
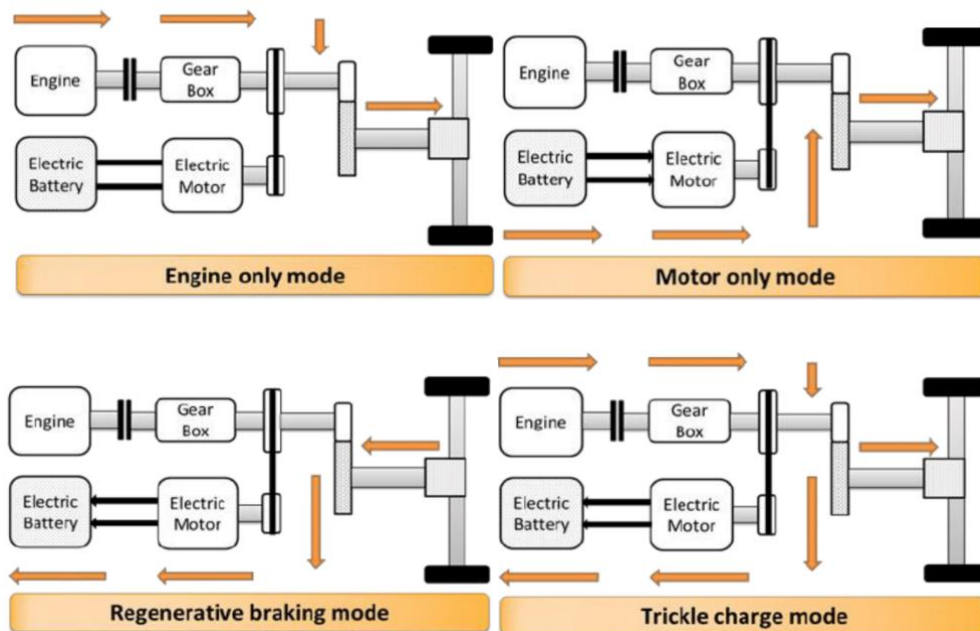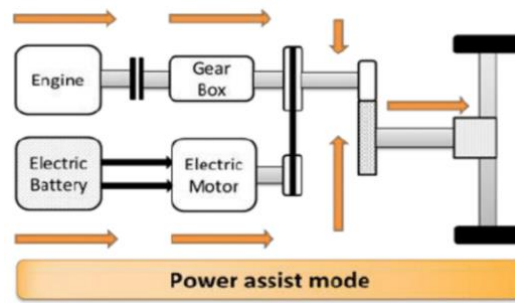
Figure (2.12) Various operation modes of an HEV [31]

The dual operation in the HEV makes it more economical and has enhanced the key feature of the conventional vehicles (CV) and the pure electric vehicles. Also, HEV has overcome some limitations in the PEV; for example, HEV has a more extended range of travel, and it can carry more weight than PEV. Also, it doesn't need a long charging duration for the battery pack as in PEV. However, the following table will give a brief comparison between PEV, HEV, and CV [32].

Table (2.3) Comparison of several types of vehicles [32]

Types of vehicles	Conventional Vehicle (CV)	Plug-in Electric Vehicle (PEV)	Hybrid Electric Vehicle (HEV)
Power Source	Engine	Motor	Engine and Motor
Battery pack	-	Large	Small
Gasoline	✓	✗	✓
Electricity	✗	✓	✓

2.3 Hybrid Energy Storage System

In electric and hybrid electric vehicles, the selection of ESS depends on various parameters, including energy density, power density, life expectancy, charging/discharging

time, cost, weight, and size. Also, each energy storage device has its own characteristics. However, in literature, flywheel, fuel cells, ultracapacitor, superconducting magnetic coils, rechargeable batteries, and near hybrid ESS are the most common energy storage systems used in EVs and HEVs [37].

For EVs and HEVs applications, the current trend shows that batteries and ultracapacitors remain as preferable choices. These technologies have some advantages and drawbacks where batteries have a low cost per watt-hour, high energy density but short cycle life and low specific power. On the other hand, ultracapacitors can maintain high peak power, long cycle life, high cost per watt-hour and low energy density [33]. The UCs are robust and have a quasi-infinite cycle life and fast response time which can sustain highly dynamic power profiles. In [38], Bruke and Zhao discussed the applications of ultracapacitor in electric and hybrid electric vehicles including transient buses, passenger cars, and stop-go hybrids vehicles. Since an individual energy storage device can't fulfill all the requirements, the combination of batteries and ultracapacitors will help to overcome their drawbacks, which will lead to the high stability of the entire system [36, 39].

2.3.1 Battery modeling

2.3.1.1 Overview:

This section covers fundamental background topics relating to technical aspects of battery modeling and general applications, especially for lithium-ion batteries since it is the most common type used in electrified vehicles. First, it is necessary to understand the basic battery's terminologies, which are tabulated in Table (2.4).

Table (2.4) Battery's terminologies [9]

Battery's terminologies	
Term	**Definition**

Cell	The basic electrochemical unit characterized by the anode (- electrode) and a cathode (+ electrode), used to receive, store, and deliver electrical energy.
Primary cells	The Electrochemical reaction is not reversible. (it can be used only once)
Secondary cells	The Electrochemical reaction is reversible. (it can be discharged and recharged many times)
Battery Pack	A group of cells electrically connected for producing electric energy.
Nominal Voltage	The manufacturers usually specify a cell or battery's nominal voltage into a given voltage class for the purpose of convenient designation. It depends on the combination of active materials used in the cell.
Operating voltage	The operating voltage of a cell or battery may vary above or below the nominal voltage value.
Cell's nominal charge capacity	The quantity of charge that a cell is rated to hold.
C-rate (cell current)	The constant current charge or discharge rate that the cell can sustain for 1-hour. (the relation between C rate and discharge time is not strictly linear due to the internal resistance and material characteristics).
Cell's nominal energy capacity	The quantity of electrical energy that the cell is rated to hold. ($cell's$ energy storage capacity $=$ $cell's$ nominal voltage $\times$ $cell's$ nominal charge capacity).
Power & energy	Energy and power are not the same at a specific rate of discharge. Power is the instantaneous rate of energy being released.

Specific energy	It measures the maximum amount of stored energy per unit weight.
Energy density	It measures the maximum amount of stored energy per volume.
Total charge capacity (Q)	The total amount of charge removed when discharging a cell from 100% to 0%.
Coulombic efficiency (η)	$\text{Charge out}/\text{Charge in}$
Energy efficiency	$\text{Energy out}/\text{Energy in}$
Depth of Discharge (DoD)	It is the converse of State of Charge $(\text{DoD} = 1 - \text{SoC})$

Any battery contains groups of cells electrically connected for producing electric energy. These cells can be connected either in series or parallel, as shown in Figure (2.13). When cells are connected in series, the battery voltage is the sum of the individual cell voltages, but the capacity is the same for the chain since the same current passes through all cells.
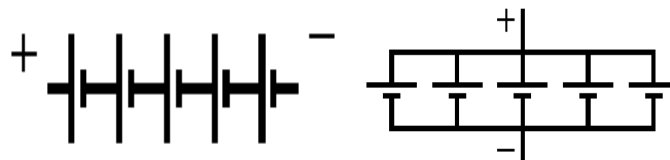
Figure (2.13) parallel-connection (Right) and series-connection (left)) of battery's cells [9]

When cells are connected in parallel, the battery voltage is equal to the cells' voltage, but the capacity is the sum of the cells' capacities since the battery current is the sum of all the cell currents. Moreover, Cells components and batteries principle of operation were illustrated in detail in Chapter 1 in Subsection 1.2.3.1.

2.3.1.2 Materials choice:

Chemical properties are different for each type of batteries; for example, Fluorine has the most positive number in the periodic table of elements (+2.87), while Lithium has the most negative number (-3.01). If we create a cell combining these materials, we will end up with a high voltage. In other words, the larger the difference between the positive and negative electrodes' potentials, the higher the cell voltage, but there is no electrolyte that will withstand that high voltage without decomposition. Also, the voltage generated across the terminals of a cell is directly related to the types of materials used in positive and negative electrodes. Therefore, material choice for batteries depends mainly on the application itself, and its economic and technical aspects [9].

2.3.1.3 Lithium-ion cell:

In electric and hybrid electric vehicles, lithium-ion cell is usually used in these applications due to many reasons such as its high energy density, low self-discharge rate, and abundance of lithium in our planet. According to Gregory L. Plett, considering the available supply of lithium, there is more than enough lithium available (over 200 billion tons) to satisfy the world's demand for high energy automotive batteries [9]. Also, in his book, Plett said that Li-ion batteries used in EVs and HEVs weigh about 7 kg/kWh, and so that the lithium content will be about 0.2 kg/kWh. Thus, a typical EV passenger vehicle may use batteries with capacities between 30 kWh and 50 kWh so that the lithium content will be about 6 kg to 10 kg per EV battery while the capacity of HEV batteries is typically less than 10% of the capacity of an EV battery and the weight of lithium used is correspondingly 10% or less of EV battery weight. Table (2.5) presents the advantages and drawbacks of Li-ion cells [9].

Table (2.5) Advantages and disadvantages of Li-Ion cell [9]

LITHIUM-ION CELL		
#	Advantages	Disadvantages

1	Operating at a higher voltage than other rechargeable cells, typically about (3.7V)	Li-ion cells are more expensive than similar capacity cells.
2	High energy density.	Li-ion is very sensitive to overcharge; therefore, it requires a protection circuitry, which will add to the cost and complexity of the design and manufacture.
3	Li-ion battery management circuitry is simpler than other types.	It is not available in standard cells sizes (AA, C, and D)
4	Li-ion cell has a lower self-discharge rate than other types of rechargeable cells (Li-ion cell usually retain most of their charge even after months of storage).	Li-ion cells require a specific matching charger designed to accommodate it because of their different shapes and sizes.

Li-ion cells can be manufactured in different shapes like cylindrical cells (Historically most common), prismatic cells, pouch cells, as shown in Figure (2.14) [9].

Figure (2.14) Manufacturing shapes of Li-Ion cells [9]

2.3.1.4 Classifications of battery modeling:

In the literature, battery cell models are usually categorized into three categorizations. First, physical-based models which describe the structure of the material and the electrochemical phenomena inside the cell. Second, empirical models which the empirical parameters which don't have any physical significance in some cases. The last one is the abstract models, also known as an electrical equivalent-circuit model, that represents the model as an electrical equivalent circuit. However, the tradeoff between complexity and accuracy is what determines the robustness of the model. The complexity depends on the computation unit and memory resources while the accuracy takes into consideration second-order effects like temperature, aging, and power and capacity fading. Table (2.6) shows a brief comparison between these models [9, 40].

Table (2.6) Comparison of battery models [10]

Battery cell models			
Model	**Physical**	**Empirical**	**Abstract**
Also known as	White boxes	Black boxes	Grey boxes
Accuracy	Remarkably high	Medium	Medium
Complexity	High, (requires more than 50 parameters).	Low, (2-3) Parameters.	Medium to Low. (2-30) Parameters.
Physical interpretability	High	Low	Limited to acceptable
Suited application	Battery system design stage	Prediction of lifetime and efficiency	Real-time monitoring and diagnosis
Limitations	A large number of parameters and high configuration effort.	The accuracy is limited.	-----------------

However, since physical model and empirical model require a sort of chemical background, dealing with electrical circuits and components are much easier for us (as electrical engineers) because it is adequate and simple for many applications, so the electrical equivalent-circuit model will be explained in the next section to describe the implementation of battery cell. Plett has demonstrated all these models and their state-space representations in his books, which can be referred to in [9, 40].

2.3.1.4.1   Electrical equivalent-circuit model:

The electric circuit model is designed from the phenomenological point of view by using electric circuit elements to observe electrical behaviors of battery cells. A simple equivalent-circuit model, as shown in Figure (2.15), has three main elements. First, Open-circuit voltage (OCV) source which is used instead of the terminal voltage to represent the battery's voltage since the terminal voltage of the battery when it is fully charged is not always higher than the voltage of a discharged cell because of that the terminal voltage of the cell depends on battery's recent usage. The OCV of a fully charged cell is higher than that of a discharged cell; therefore, we can say that OCV is a function of the state of charge, but neither a function of current nor past usage. The second element R_s is called equivalent series resistance of the cell, and it is added to the circuit to describe the cell's voltage drop and power dissipation as heat when it is under load. Equivalent series internal resistance is considered as a dynamic feature to the model because it is a function of the state of charge and temperature. At temperature below room temperature, chemical activity decreases, and internal resistance increases while at a temperature much higher than room temperature, a higher rate of chemical activity will induce a self-discharge effect because the internal resistance decreases. The last element is one or more parallel R-C sub-circuit (R_p, C_p) which represent cell's dynamics behavior at middle and higher frequencies which are caused by slow diffusion and hysteresis voltages process in the cell, and they are also a function of state of charge and internal temperature.; for example, when a cell is allowed to rest, its voltage does not immediately return to OCV, but decays gradually caused by these voltages effects [40, 41].
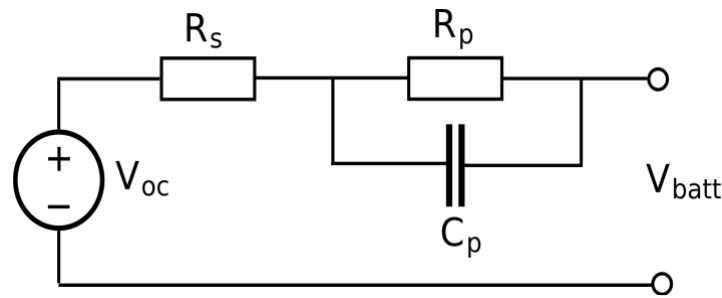
Figure (2.15) Basic electrical equivalent-circuit model [41]

Many factors may cause some failure modes to the model, such as overheating, aging, poorly controlled manufacturing process, cell design faults, overcharging and discharging, and other factors. Therefore, to improve the accuracy of the model, other effects must be taken into consideration like aging effect, capacity and power fading effect, self-discharge effect, …etc. Which on the other hand, will increase the model complexity [40, 42]. However, in [43] the authors have presented a detailed comparison between all concerns and the impact of battery modeling, also highlighted the issues and challenges regarding the safety, battery management system, and protection aspects. In addition, Song Ci [44] has presented a comprehensive survey on battery design challenges and techniques including thermal management, safety features, and fault tolerance, efficient sensing of the state of charge (SoC) and state of health (SoH). Moreover, in [45] Xiong presented a critical comparison of the state of charge estimation methods and techniques with a focus on their use in EVs and reviewed multi fusion modeling methods as well as capacity degradation and aging effects for batteries.

2.3.2   Ultracapacitor modeling

2.3.2.1 Overview:

Ultracapacitor (UC), also known as supercapacitor (SC) or electric double-layer capacitor (EDLC), is considered as a promising energy storage device due to its high-power density, low internal resistance, wide operating temperature range, fast response, and high lifecycle times. Therefore, an ultracapacitor can be independently suitable for applications, like EVs, HEVs, and others, that require high-power density, or it can be combined in a hybrid energy storage system with a high-energy device like batteries. The working principle of UC

was given in chapter 1 (subsection 2.7.1) with its advantages and disadvantages. However, in this section, the classifications of UC modeling will be introduced and a comparison between these models will be tabulated. Also, the electrical-equivalent circuit model will be explained in detail, similar to what has been done in battery modeling section [9, 46].

2.3.2.2 Classifications of ultracapacitor modeling:

Ultracapacitor models have trade-offs between model accuracy and complexity, similar to battery modeling. In literature, ultracapacitor models are categorized based on electrical behavior into four main categorizations which are electrochemical model, equivalent circuit model, fractional-order model, and intelligent model. The electrochemical model is the most accurate, but it requires many parameters to capture all the behaviors and dynamics inside UC's cell. In contrast, the equivalent circuit model represents the behavior of UC as electric circuit elements, and its accuracy is highly acceptable. Besides, the fractional-order model uses fractional-order calculus to describe UC's dynamics, and this model shows a stronger capability of capturing the UC dynamic behavior. Furthermore, the intelligent model employs artificial neural networks and fuzzy logic to predict and capture the behavior of UCs. Table (2.7) shows a brief comparison of these models [42,47,48].

Table (2.7) Comparison between ultracapacitor models [42,47,48]

Ultracapacitor modeling techniques		
Model	**Advantages**	**Disadvantages**
Electrochemical model	High accuracy.	Heavy computational.
Equivalent circuit model	Moderate accuracy. Easy to implement.	Other effects like thermal and aging, will increase the complexity of the model.

Fractional-order model	Few model parameters.	Heavy computational.
Intelligent model	Good modeling capability.	It requires a lot of training (Poor robustness).

2.3.2.2.1   Ultracapacitor's equivalent circuit model:

UC's electric equivalent circuit model is designed from the phenomenological point of view by using electric circuit elements to represent the electrical behaviors of UC's cells. Figure (2.16) illustrates a simple electrical equivalent-circuit model of the ultracapacitor. This model has three main elements which are capacitor, equivalent series resistance (ESR), and equivalent parallel resistance (EPR).
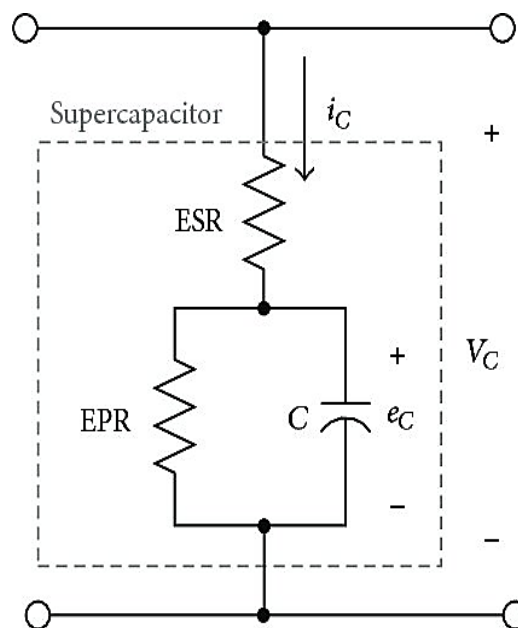
Figure (2.16) UC Equivalent-Circuit [46]

The capacitor describes the capacitance effect of UC, and ESR represents the overall resistance which is the dominant effect during charging and discharging processes. EPR describes the self-discharge effect that influences the performance of the UC [48,49,50]. In

addition, in [47] Tao has presented a mathematical model for UC based on the physical structure and dynamic electrical characteristics.

2.3.3 Hybrid energy storage system architectures

Several review papers [33,36,51] examine the diversity of electrified vehicles, various energy storage technologies, hybrid energy storage, and power electronics topologies, as well as the different kinds of energy management strategies.

2.3.3.1 Overview

In a battery ultracapacitor hybrid energy storage system, the tradeoff between the UC's cost and the battery's size and lifetime are what governs the selection of HESS architecture. There are various architectures to connect the HESS to electric motor drive via power electronics, which are discussed in the following subsections.

The boost half-bridge bi-directional DC-DC converter, which is also called the two-quadrant converter, can operate in boost mode in one direction and buck mode in the other direction, as shown in Figure (2.17). This converter is a suitable choice for battery/UC interface, but there are different types of bi-directional converters could also be used, as shown in Figure (2.18), and they are presented in [27,33,36,39].
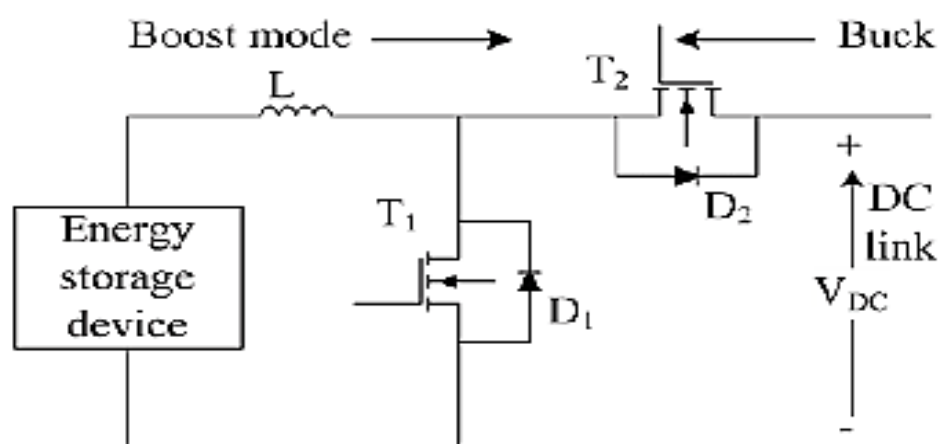
Figure (2.17) Half-bridge bi-directional dc-dc converter [36]

Isolated bidirectional converters		
(a) Boost-half bridge	*(b) Half bridge*	*(c) Full bridge*
Non-isolated bidirectional converters		
(d) SEPIC/Luo	*(e) Cuk*	*(f) Buck-boost (boost half-bridge)*
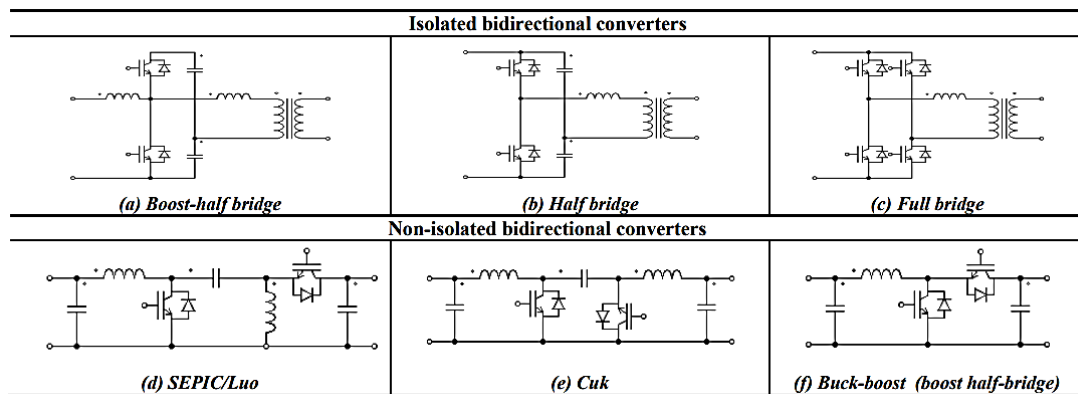
Figure (2.18) Bidirectional DC/DC converter topologies [27]

2.3.3.2 Battery/UC HESS connection topologies:

2.3.3.2.1   Passive parallel battery/UC connection

The passive parallel connection is the simplest topology with both the battery pack and the UC are directly connected to the motor drive without a DC/DC converter, as shown in Figure (2.19). This architecture may provide simplicity and cost-effectiveness, but the main issue in this topology is the absence of the voltage control on the DC bus. Therefore, this issue is resolved in the passive cascaded topology as presented in Figure (2.20), where the HESS has partially decoupled connection to the DC bus by the bidirectional DC/DC converter which controls the DC-bus voltage [33,36].
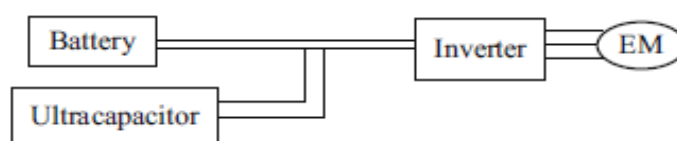
Figure (2.19) Directly passive parallel connection [33]

However, in this architecture, the UC is expected to provide transients and fast power variations while the battery supplies a relatively slow varying dynamic. Battery and UC are parallelly connected; consequently, there is no control over the battery current, which will be similar to the UC current because the UC will act faster than the battery because of its lower time constant. The main drawback of this topology is the lack of effective control on the battery current [36].
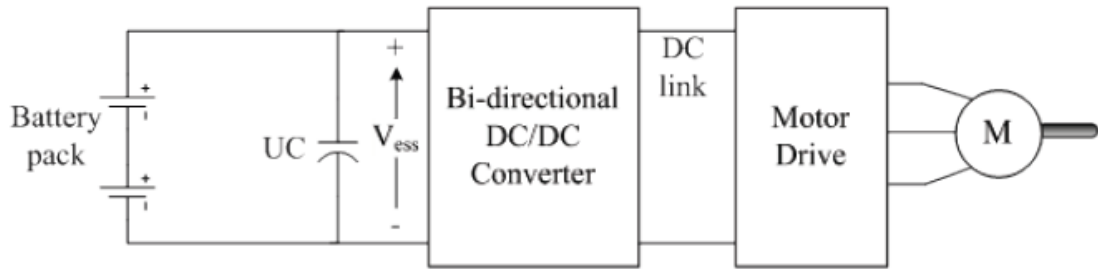
Figure (2.20) passive cascaded connection [36]

2.3.3.2.2   Active cascaded UC/battery connection

In this topology, the UC terminals are connected to the dc bus through a bi-directional dc-dc converter while the battery is directly connected to the dc bus, as shown in Figure (2.21). In this architecture, the power supply from the UC can be effectively controlled by the bi-directional dc-dc interface that also helps to recapture regenerative braking energy. However, the battery is not directly controlled and not protected against rapid power level changes, which are the drawbacks of this topology. The two advantages of this architecture are: first the UC voltage can be different from the nominal DC bus voltage which will provide flexibility to increase or decrease the UC energy capacity regardless of the system DC voltage; and second, the input voltage to the motor drive is relatively constant because the battery is directly connected to the DC bus, so there is no need to DC bus voltage regulation [36,51].
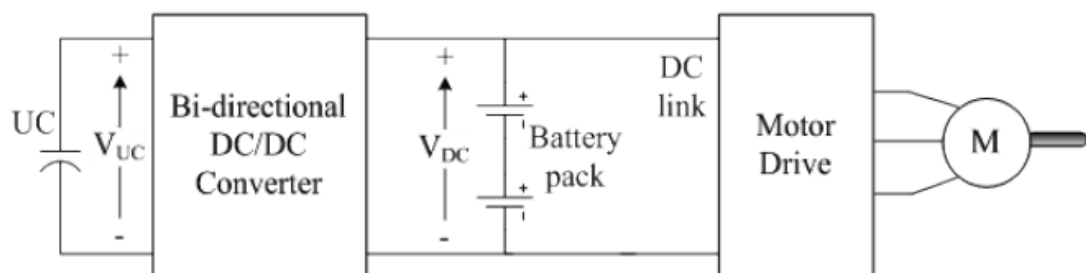
Figure (2.21) Active cascaded UC/battery connection [36]

2.3.3.2.3   Active cascaded battery/UC connection

In the battery/UC connection shown in Figure (2.22), the UC terminals are directly connected to the DC bus while the battery is connected through a bi-directional dc-dc converter to the same dc bus; therefore, the battery, in this case, is protected against rapid power changes

because the UC in this topology will act as a low-pass filter and takes care of fast load transients. Also, the battery voltage can be maintained at a lower level than the previous topology. During braking, the UC is recharged directly from the DC link and some portion of the braking energy can be transferred to the battery. In this architecture, the UC should be large enough to prevent DC bus voltage from large fluctuations which will affect the motor drive during frequent charging. This topology can be used to reduce conduction and switching losses and to improve the accuracy of the system [33,36,39].

In this architecture, the battery pack also should be controlled appropriately to preserve the voltage across the UC and DC bus. For simplicity and cost-effectiveness, the UC can be the only device responsible for capturing regenerative braking energy, which would prolong the lifetime of the battery. In [33], the author has explained some control strategies for this battery/UC architecture.
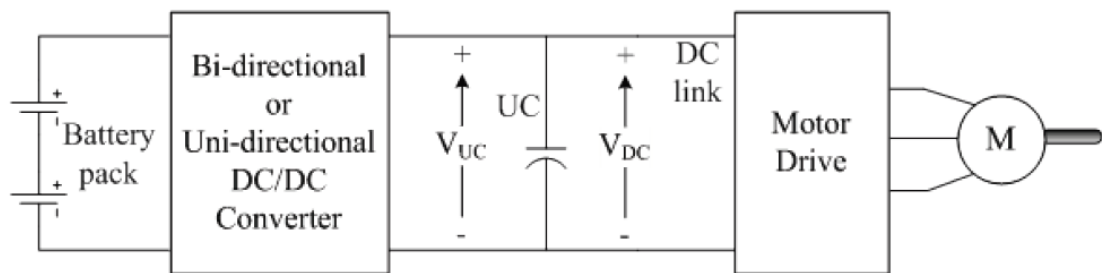
Figure (2.22) Active cascaded battery/UC connection [36]

2.3.3.2.4   Active cascaded HESS with two DC/DC converters

For the active cascaded HESS with two DC-DC converters, shown in Figure (2.23), one energy storage device can be cascaded to the motor drive through a dc-dc converter and the other cascaded through the first and second dc-dc converter. This architecture has a fully decoupled connection from the DC bus, so both battery and UC voltages can be decoupled from the system voltage and from each other. The positions of the UC and battery can be switched, leading to a slightly different cascaded architecture. However, the battery and UC converters must be appropriately controlled to provide stable operation over a wide input voltage range.

The major disadvantage of this architecture is that the system may encounter additional losses due to the two cascaded converters. Also, this topology will lead to a significant increase in the system budgeting.
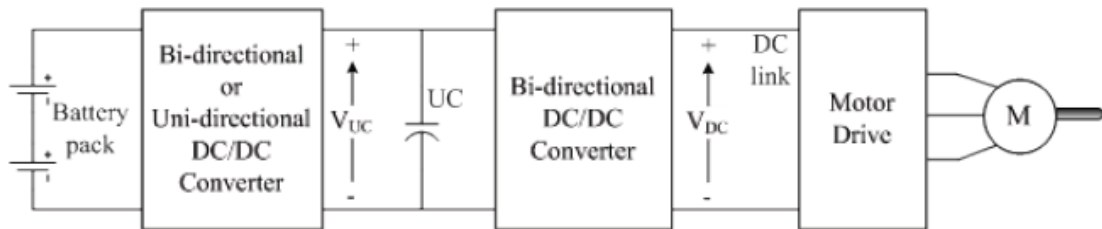
Figure (2.23) Active cascaded HESS with two DC/DC converters [36]

2.3.3.2.5 Multiple parallel converters configuration

In this architecture, each energy storage device is connected to the DC bus through its own bi-directional dc-dc converter. A connection diagram of this topology is shown in Figure (2.24). This architecture has a fully decoupled connection from the DC bus as well as between the battery and UC voltages. Therefore, this architecture shows superior performance, especially for the controllability of the current flow since it proposes more flexibility, functionality, and control simplicity than earlier architecture. In this topology, one source can keep operating even if another failed, which improves the system reliability [36]. This topology is chosen for the hybrid electric vehicle application developed in this chapter.
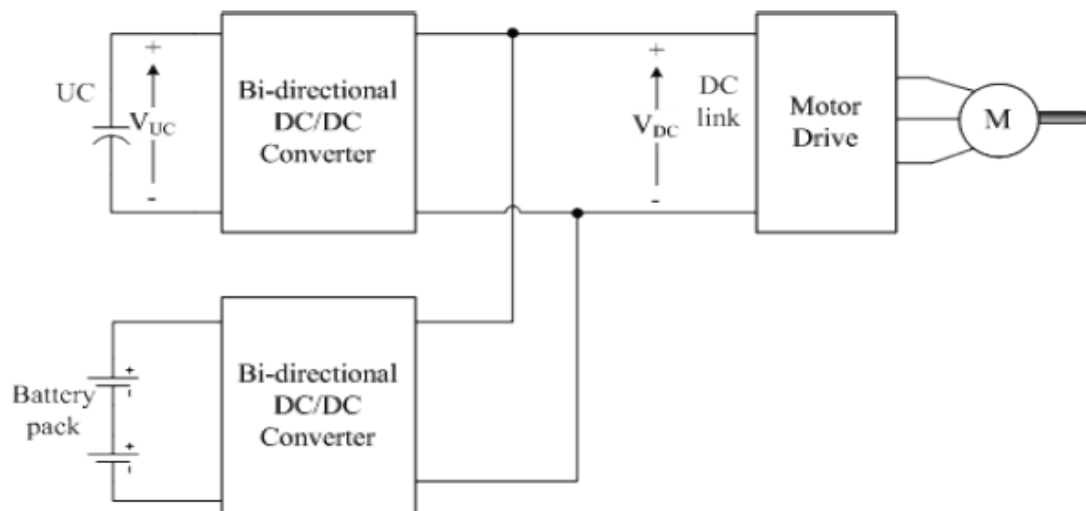
Figure (2.24) Multiple parallel-connected converters architecture [36]

2.3.3.2.6   Multi-input DC-DC converter architecture

In this architecture, the multi-input DC/DC converter is used for the integration between HESSs and the motor drive, as shown in Figure (2.25). The advantage of this architecture is that more than two energy storage devices can be used or combined with renewable energy sources, such as PV, in electric vehicles with a smaller number of components. Since this DC-DC converter can operate in different modes of operation such as boost, buck and buck/boost, this HESS architecture attains an essential role in the energy sources diversification in EVs and HEVs [33,52,53].
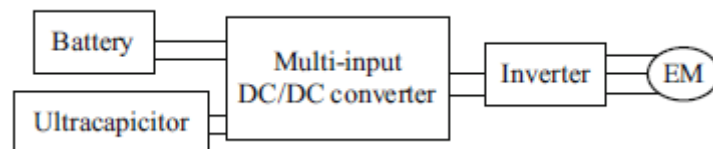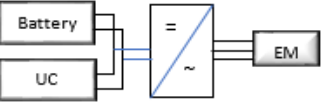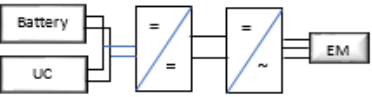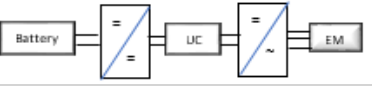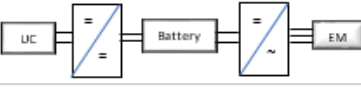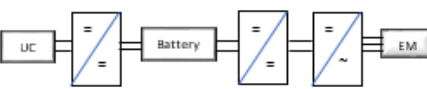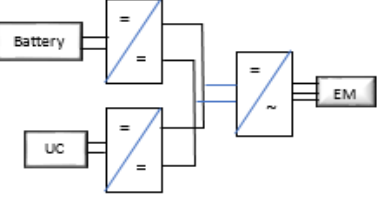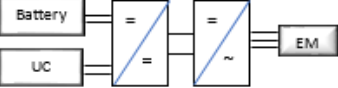
Figure (2.25) Multi-input DC/DC converter architecture [33]

Table (2.8) presents a comparison between previous architectures based on structure, control, size, and cost. These architectures graded on a color scale, with green indicating simple, yellow indicating average, and red indicating complex.

Table (2.8) Comparison of HESS architectures

Type	Architecture	structure	Control	Battery and UC size selection	Cost	Advantages	Disadvantages
Passive	Battery, UC, =/~, EM	🟢	🟢	Both are Restricted	Low	simplicity and cost effectiveness	Lack of DC-DC converter
Passive cascaded (semi-active)	Battery, UC, =/=, =/~, EM	🟢	🟢	Both are Restricted	Medium	DC link voltage regulation	No active battery current controller
Active cascaded battery/UC	Battery, =/=, UC, =/~, EM	🟡	🟡	UC size is Rectricted	Medium	Battry voltage can be low	DC-DC converter can be Unidirectional
Active Cascaded UC/Battery	UC, =/=, Battery, =/~, EM	🟡	🟢	UC size is flexiple	Low	UC and DC link voltages can be different	simplicity of control
Multiple cascaded converters	UC, =/=, Battery, =/=, =/~, EM	🟡	🔴	UC size is Restricted	High	DC link voltage regulation	High battery power losses
Multiple parallel converters	Battery, =/=, UC, =/=, =/~, EM	🟡	🔴	Both are flexible	High	Flexiplity, stability, efficiency, and reliability	control complixity
Multi-inputs DC-DC converter	Battery, UC, =/=, =/~, EM	🔴	🔴	Both are flexible	Medium	Less number of components	Not fault tolerant

2.4 Hybrid Electric Vehicle (HEV) Modeling in Simulink

In this section, a series-parallel hybrid electric vehicle will be illustrated and simulated by using MATLAB-SIMULINK to show the benefits of integrating a battery/ultracapacitor hybrid energy storage system in traction applications. This HEV model is available at MATLAB Central File Exchange [54].

2.4.1 Overview of the HEV model

In this model, a hybrid electric vehicle with a series-parallel architecture will be simulated by using MATLAB-SIMULINK (2019a) software. This model, which is shown in Figure (2.26), consists of a control system, a mechanical system, and an electrical system. Also, the model can be run for different standard drive cycles that are used to test hybrid electric vehicles. The model that we are working with has many options for balancing model fidelity and simulation speed.
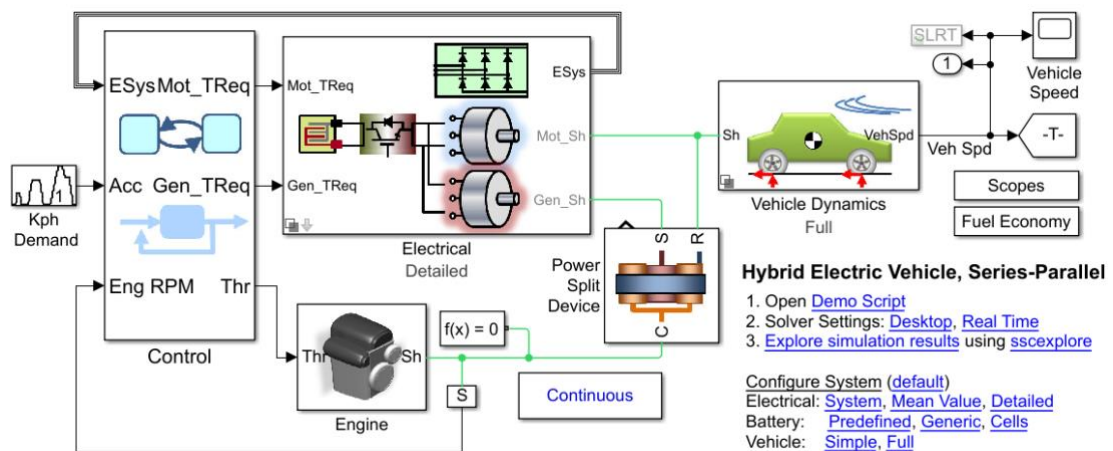
Figure (2.26) Overall series-parallel HEV model [54]

2.4.2 Electrical system

The electrical system has a motor, generator, DC-DC converter, and battery models, as shown in Figure (2.27). According to Miller in [54], the electrical model has three levels of variants of fidelity which are necessary for HEV development. These levels are system-level variant which you can use to test for integration issues and to optimize the entire system, and the model also has a mean-value level variant where you can perform tests on a three-phase

electrical system, and finally the detailed level variant which can be used to test the power quality on the different electrical networks in a hybrid electric vehicle. In this HEV model, all modeling levels have an identical structure, and each level includes different details [54].
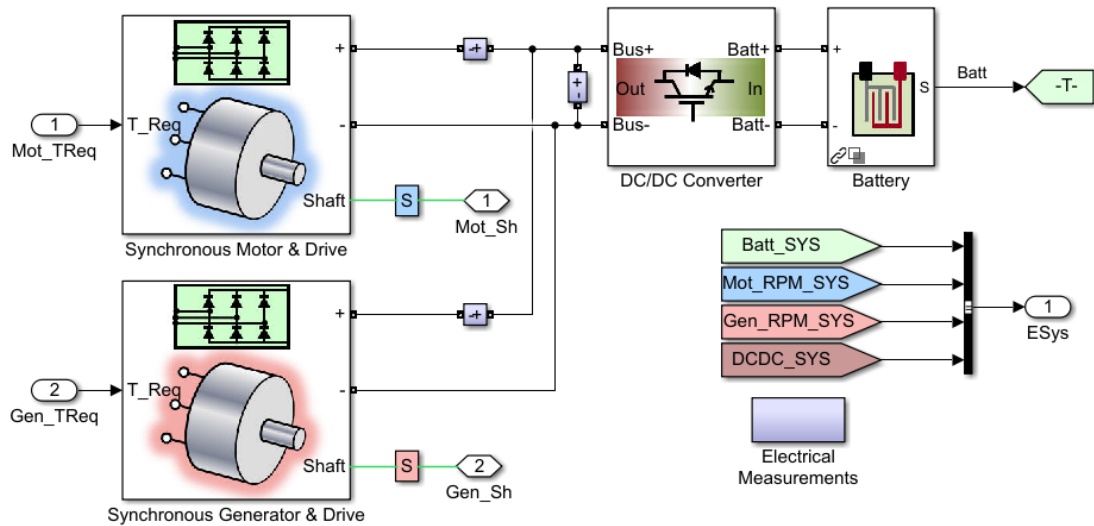
Figure (2.27) Detailed electrical system [54]

According to Miller, sometimes during the development process, you will need to iterate quickly, so you will need models that have fewer features but simulate fast; for example, using look-up tables to represent torque current relationship in motors and generators. At other times you will need to simulate the model with the entire details, so you will use a more detailed model that includes the whole switching dynamics and three-phase in the electrical network. Therefore, the ability to balance the trade-off between model fidelity and simulation speed is critical for efficient development [54].

2.4.2.1 Battery model

In the battery system block, you have the option of using predefined, generic, and custom cell models depending on which portion of the system you are focusing on. These battery models are shown in Figures (2.28), and the MATLAB documentation for these batteries can be found in MATLAB's documentation, which provides extensive details on how these batteries are modeled, the equations that were used, and the assumptions that have been made for each model.
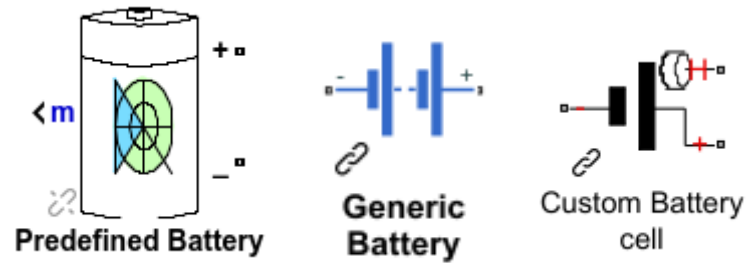
Figure (2.28) Battery models [54]

2.4.2.1.1   Predefined battery model

Sim-Power systems toolbox provides different predefined battery models for different chemistries, which can be found in the appendix. Figure (2.29) shows how the predefined battery block is used in our hybrid electric vehicle system model. Notice that all subsystems and source codes in this model are illustrated in detail in the appendix [54].
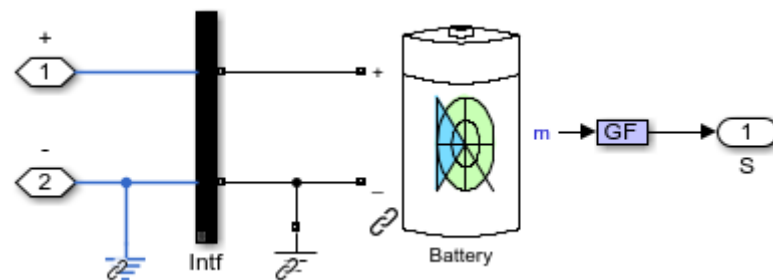
Figure (2.29) Predefined battery model [54]

2.4.2.1.2   Generic battery model

Sim-Electronics toolbox in MATLAB-SIMULINK provides a generic battery model that represents a charge dependent voltage source. The advantage of this battery model is that it can be used to represent many different types of batteries by using relatively few parameters. Figure (2.30) shows how the generic battery block is used in our hybrid electric vehicle system model. This model is chosen for the simulations in this chapter.
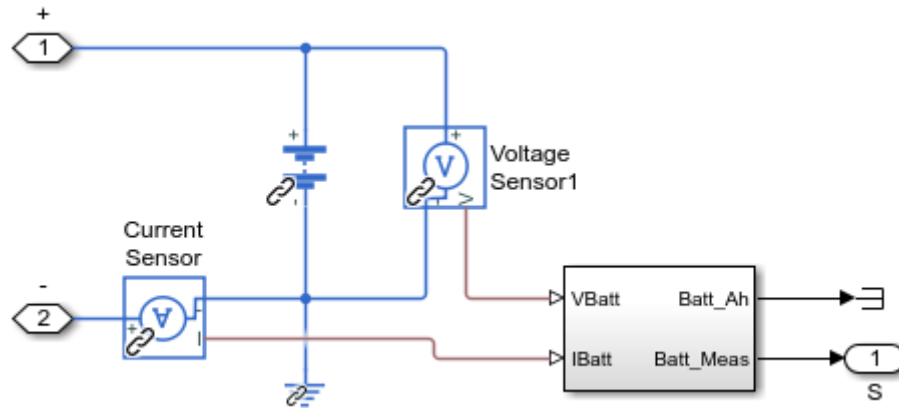
Figure (2.30) Generic battery model [54]

2.4.2.1.3 Custom battery cell model

A custom battery model can be created using the Simscape language in MATLAB-SIMULINK. A common way to create a battery model is to create a battery cell equivalent discharge circuit where many of the components in this circuit will be dependent upon the state of charge, depth of discharge, and temperature. Figure (2.31) shows how the custom battery cell block is used in our hybrid electric vehicle system model [54].
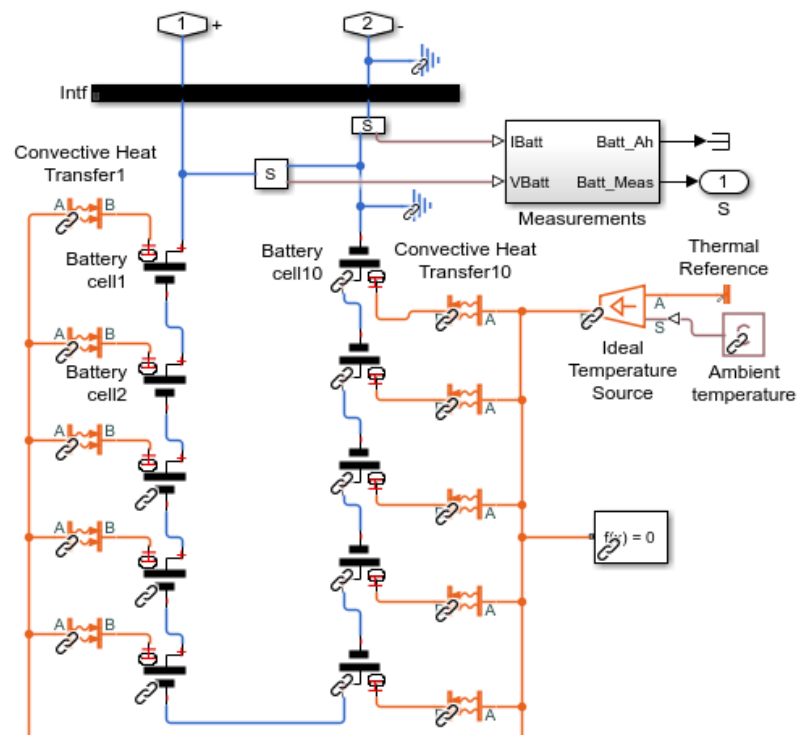
Figure (2.31) Battery cell model [54]

2.4.2.2 Ultracapacitor model

In the MATLAB-SIMULINK, you have the option of using predefined, generic, and custom cells to model an ultracapacitor depending on which portion of the system you are focusing on. These ultracapacitor models are shown in Figures (2.32), and the MATLAB documentation and source codes for these models can be found in the appendix, which provides extensive details on how these UCs are modeled, the equations that were used, and the assumptions that have been made [54].
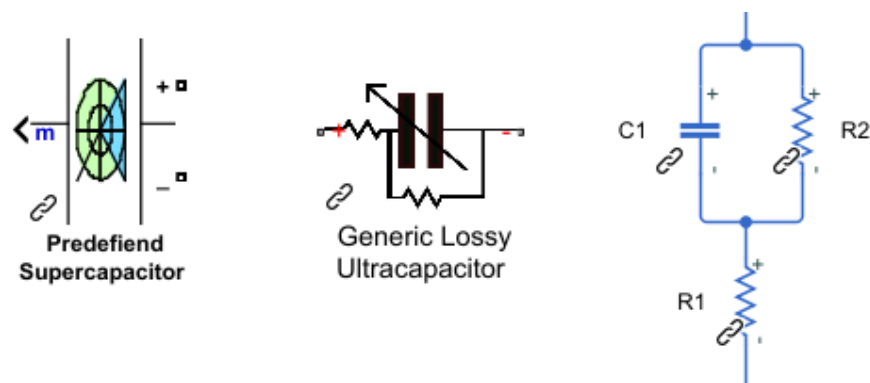

Figure (2.32) Ultracapacitor models [54]

2.4.2.2.1   Generic Lossy Ultracapacitor

This model describes an ultracapacitor with resistive losses where an equivalent series resistance added in series with the capacitor, and a self-discharge resistance is included in parallel with the capacitor. Source codes and equations used in this model are given in the appendix [54].

2.4.2.3 DC-DC- converter model

The DC-DC converter model contains power electronics to model the power electronics switching. This DC-DC- converter in this model is used to boost the voltage from the battery to the 500 Volts required on our DC link and calculating the pulse width modulated signal based on that voltage, according to Miller. Figure (2.33) shows how the DC-DC converter block is modeled in our hybrid electric vehicle system model [54].
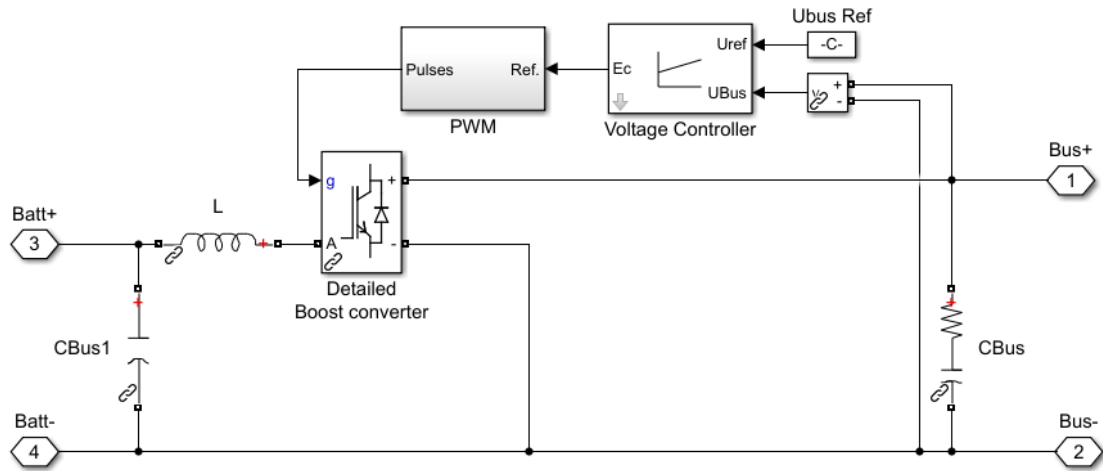
Figure (2.33) DC-DC converter model [54]

2.4.2.4 Motor and drive model

According to Miller, the motor model modeled by using Sim-power systems toolbox. The synchronous motor system model consists of a three-phase permanent magnet synchronous electric motor, a three-phase inverter to convert the DC electrical network to an AC electrical network, and a vector controller that is used to specify the pulse width modulation to the three-phase inverter. Also, it has a connection to the mechanical network. Figure (2.34) shows how the synchronous motor block is modeled in our hybrid electric vehicle system model. This model was modeled based on the (AC6 IPMSM) model in MATLAB-SIMULINK library [54].
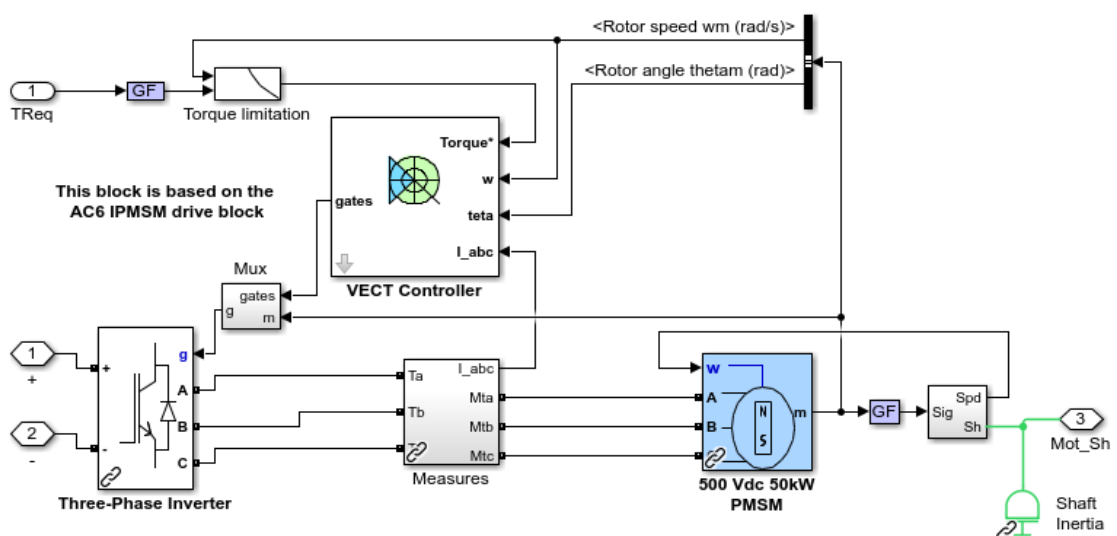
Figure (2.34) Motor and drive model [54]

2.4.2.5 Generator and drive model

The generator model is modeled by using Sim-power systems toolbox, and it has a similar structure to the motor model. The model has a three-phase permanent magnet synchronous generator, a three-phase inverter, and a vector controller as shown in Figure (2.35).
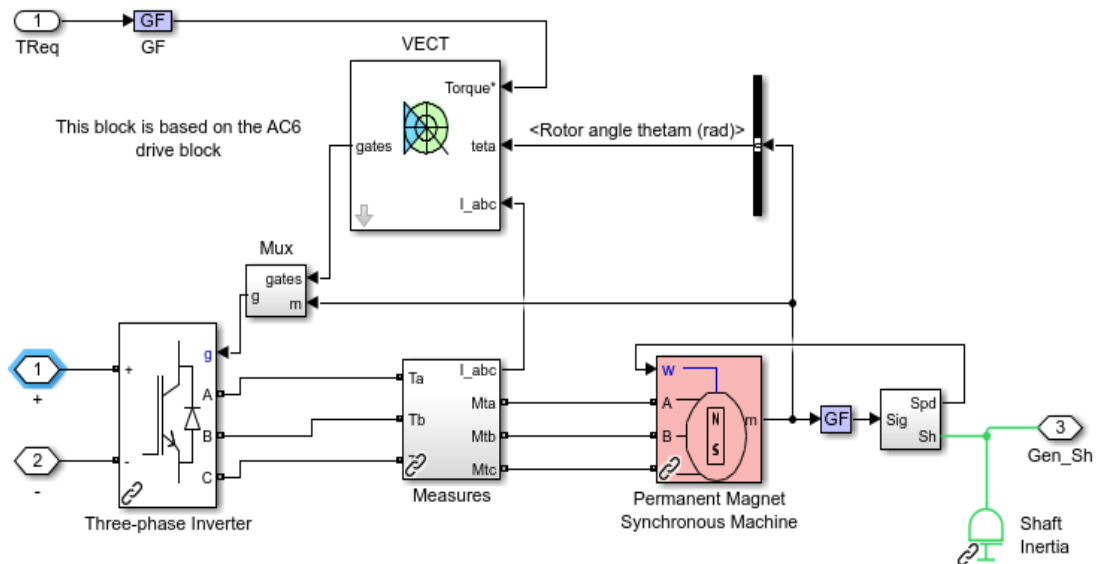
Figure (2.35) Generator and drive model [54]

2.4.3 Mechanical drivetrain system

The mechanical system contains the engine model, power split device, and the vehicle dynamics which are modeled in the SIM-Driveline toolbox in MATLAB-SIMULINK. A snapshot of the mechanical system components is presented in Figure (2.36).
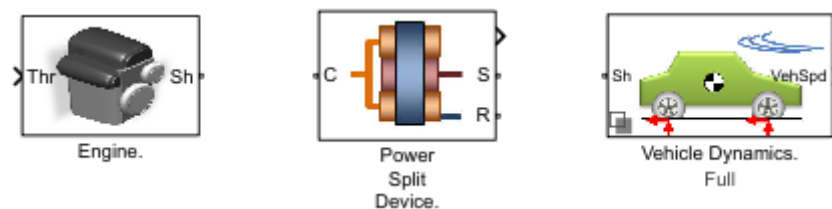
Figure (2.36) Mechanical system components [54]

2.4.3.1 Engine Model

The engine model is shown in Figure (2.37). As you can see, the input to the model is a throttle signal coming from the controller unit, and mechanical connections connected to the

rest of the drivetrain. The model has a generic model, mechanical rotational reference, rotational damper, engine shaft inertial and other components. In the appendix, MATLAB documentation and source codes for each element are illustrated [54].
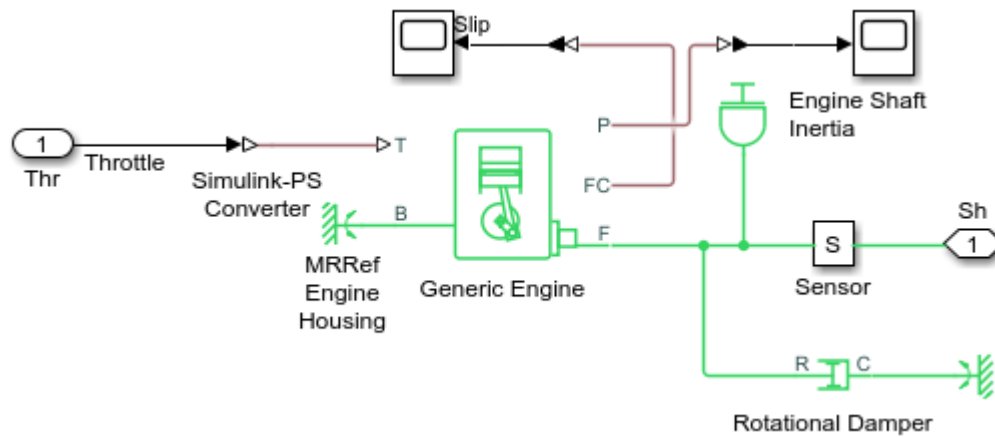
Figure (2.37) Engine model [54]

2.4.3.2 Power split device model

The power split device is modeled as a planetary gear using the gear libraries and Sim-driveline toolbox, as you can see in Figure (2.38). The planetary gear block has one input for the carrier, which is connected to the engine, and two outputs for the ring, which is connected to the vehicle and the electrical motor, and the other output for the sun, which is connected to the generator [54].
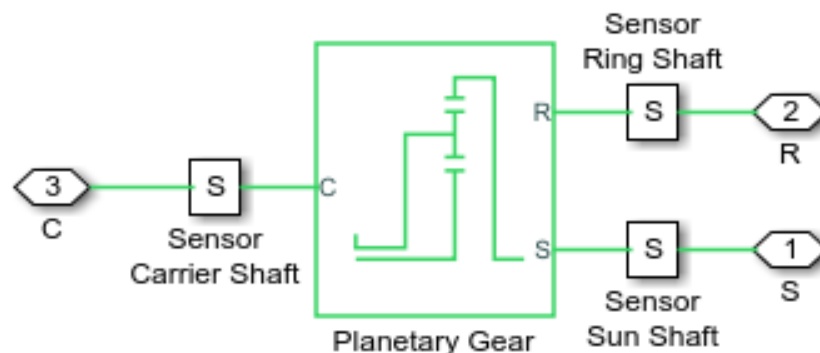
Figure (2.38) Power splitter model [54]

2.4.3.3 Vehicle dynamics model

The vehicle dynamics model has two different variants which are simple vehicle model and full vehicle model, as displayed in Figure (2.39).

Figure (2.39) Vehicle models [54]

The first variant is the simple vehicle model which includes simply inertial and aerodynamics effects, and it simulates very quickly. Second, the full vehicle model that includes tire models for transient and steady-state dynamics, differential for connecting the two left and right wheels, regenerative braking torque source, vehicle body, and other vehicle dynamics. The full vehicle model can be seen in Figure (2.40). To find out more information about what effects are captured in this model, you can look at the appendix., which has the different equations that were used, different parameters, and also references [54].
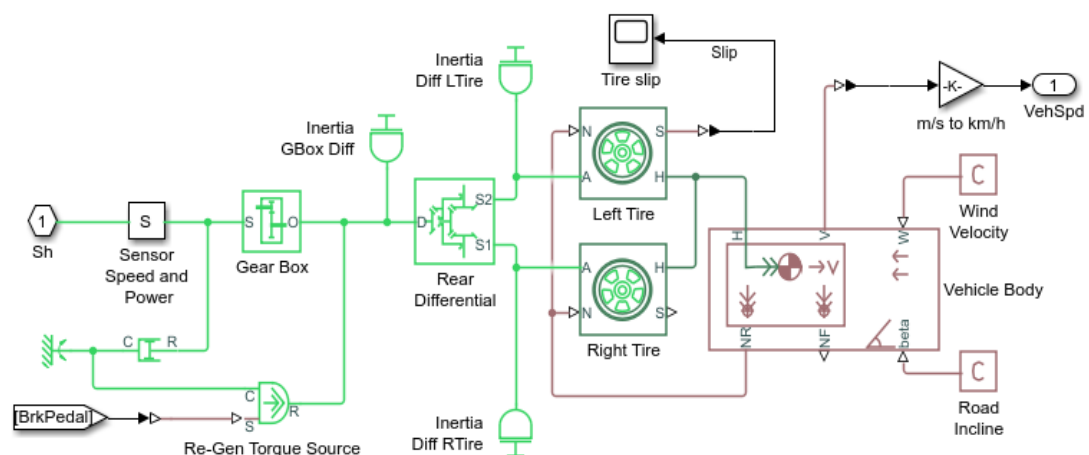
Figure (2.40) full vehicle model [54]

2.4.4   Control system

The control system consists of multiple proportional-integral (PI) controllers as well as mode logic programming state flow as shown in Figure (2.41). In the control subsystem, you can see that it has a mode logic state flow, engine speed controller, generator controller, motor controller, and battery charge controller. The control system takes the vehicle speed, brake input, battery state of charge, and engine speed as inputs and figures out the state of the vehicle, then either enables or disables the motor, the generator, or the engine [54].
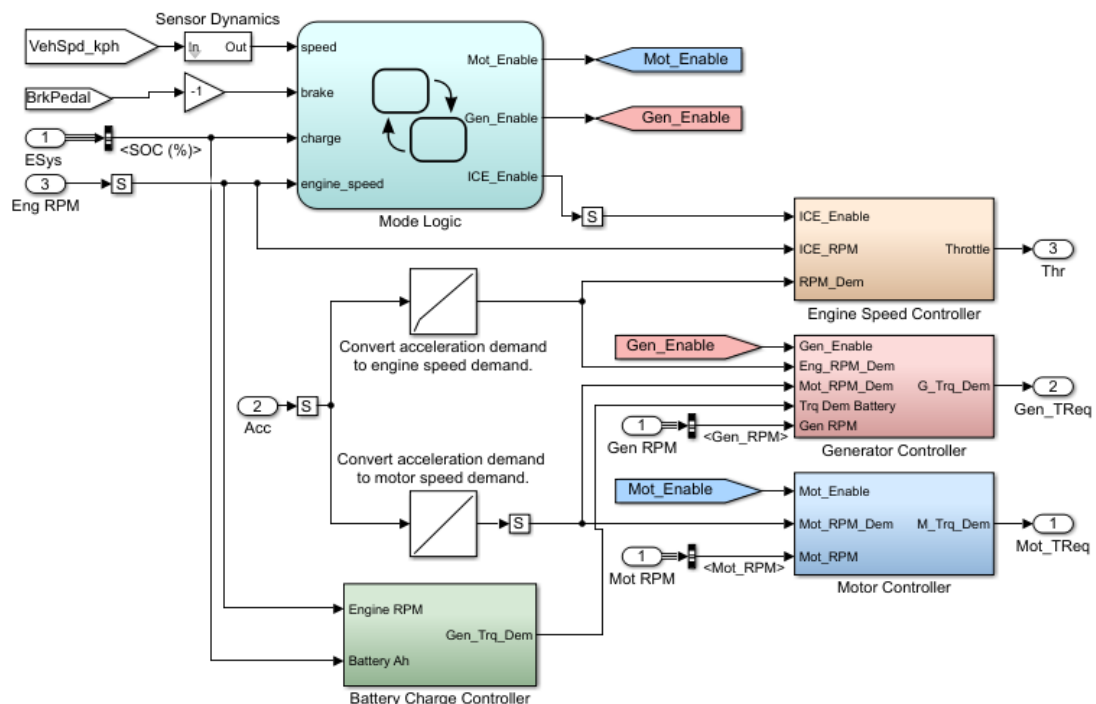
Figure (2.41) Control system [54]

2.4.4.1 System's mode logic

The specification for the mode logic state flow of our hybrid electric vehicle with the series-parallel architecture, shown in Figure (2.42). In this model, there are two main modes and states, which are: first motion mode including start mode, acceleration mode, and cruise mode, and the second mode is the braking mode. As you can see in Figure (2.42), hybrid electric vehicle driving requires different control states, different actions taken in each state, and when to transition between those states [54].
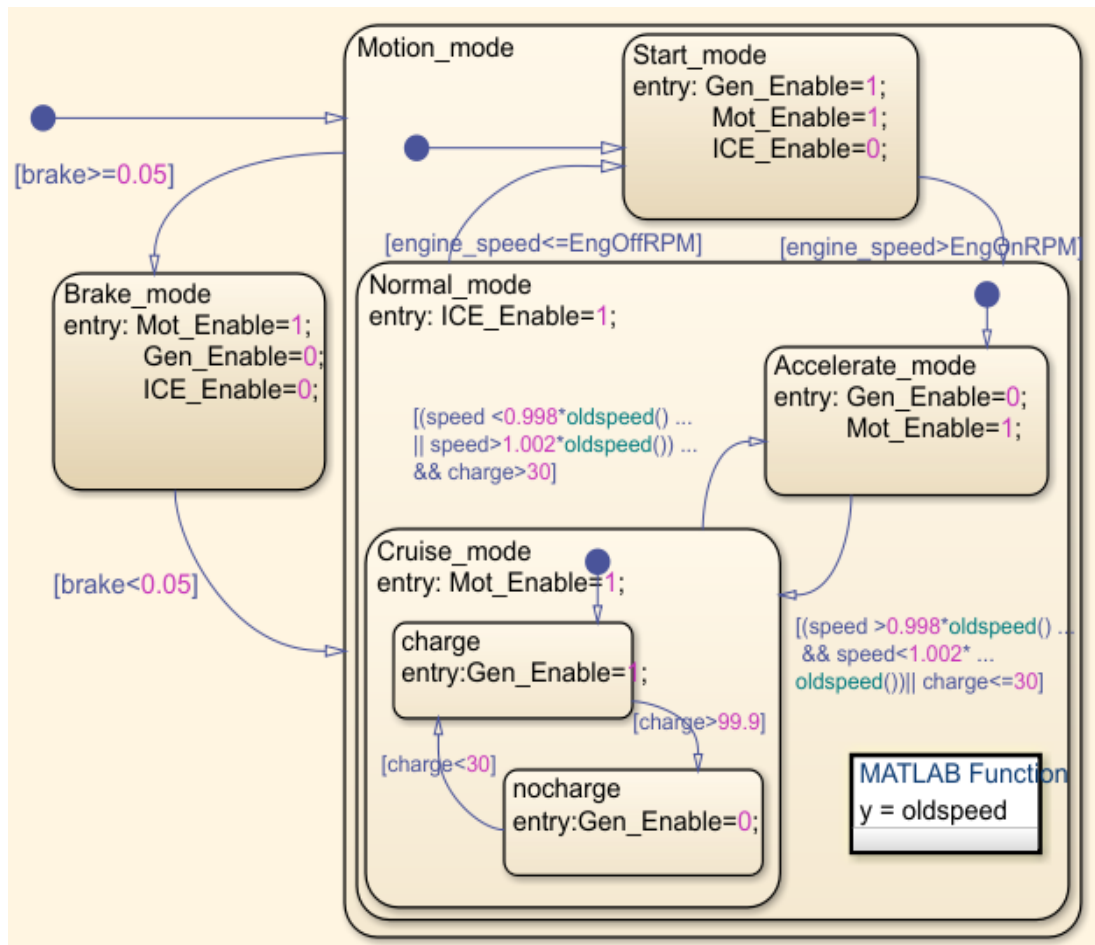
Figure (2.42) mode logic state flow [54]

According to Miller, when the vehicle is in motion, it may be in start mode. In start mode, the generator is used as a starter motor to start the engine, and the electrical motor is used to drive the vehicle. After that, when the engine gets above a certain threshold, the vehicle enters a normal mode where the engine is used to drive the vehicle and to charge the battery if its SoC less than 30%. If the driver wishes to accelerate, the vehicle enters the acceleration mode where the motor can be used to drive the vehicle even faster and the generator is turned off so that all of the engine's torque can be used to accelerate the vehicle.

Moreover, when the vehicle is in cruise mode, the generator may be used to charge the battery. Furthermore, there are also transitions to go back to acceleration mode and to start mode. However, if the driver applies the brakes, then the motor, in this case, is used via regenerative braking to charge the battery [54].

2.4.4.2 Engine speed controller

The following Figure (2.43) shows how engine speed is controlled during the starting time and running time. As an input, this controller takes the internal combustion engine enabling command from mode logic, engine speed demand from drive cycle acceleration, and engine speed feedback from the engine speed sensor. For demands below the idle speed of 800 rpm, the speed demand is set to zero. The output of this controller is throttle demand that specifies the torque demanded from the engine [54].
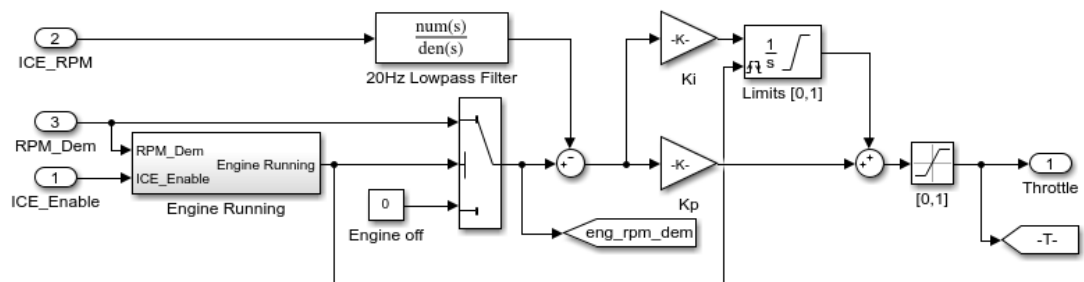
Figure (2.43) Engine controller [54]

2.4.4.3 Generator controller:

The generator controller controls the torque demanded from the generator for starting mode and charging the energy storage system. Figure (2.44) presents the controller model, which takes as inputs the generator enabling demand from mode logic, engine speed demand and motor speed demand from drive cycle acceleration, the torque required for charging the battery, and generator speed feedback from electrical system sensors [54].
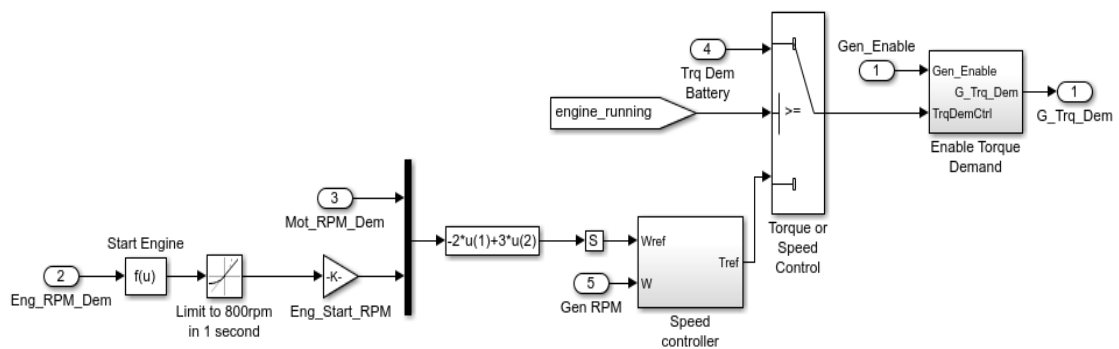
Figure (2.44) Generator controller [54]

2.4.4.4 Motor controller

In Figure (2.45), this loop controls motor speed by converting motor speed demand from drive cycle acceleration demand to volts where the maximum value is 5 volts, which is equivalent to a speed demand of 6500 rpm. The output of this controller is motor torque demand that specifies the torque demanded from the motor [54].
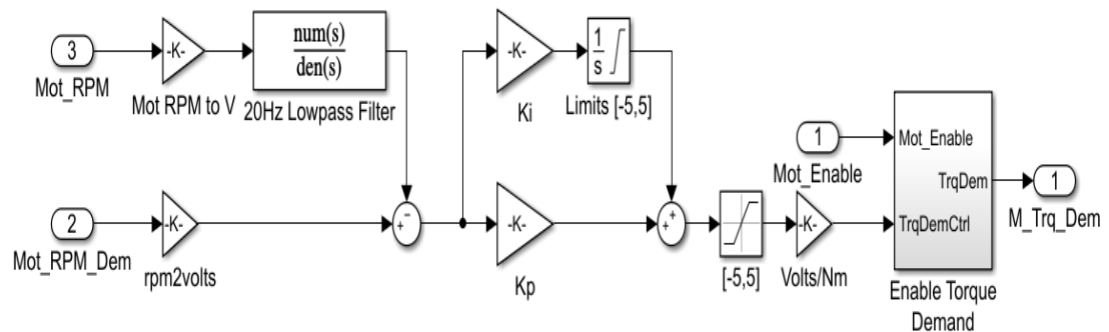
Figure (2.45) Motor controller [54]

2.4.4.5 Battery charge controller

This controller loop, shown below, is responsible for controlling the torque demanded from the generator for charging battery based on the state of charge. If the battery has more than 100% rated capacity, then no generation is required. And linearly ramp to using 20% of available engine torque for charging between 30% capacity and 100% capacity [54].
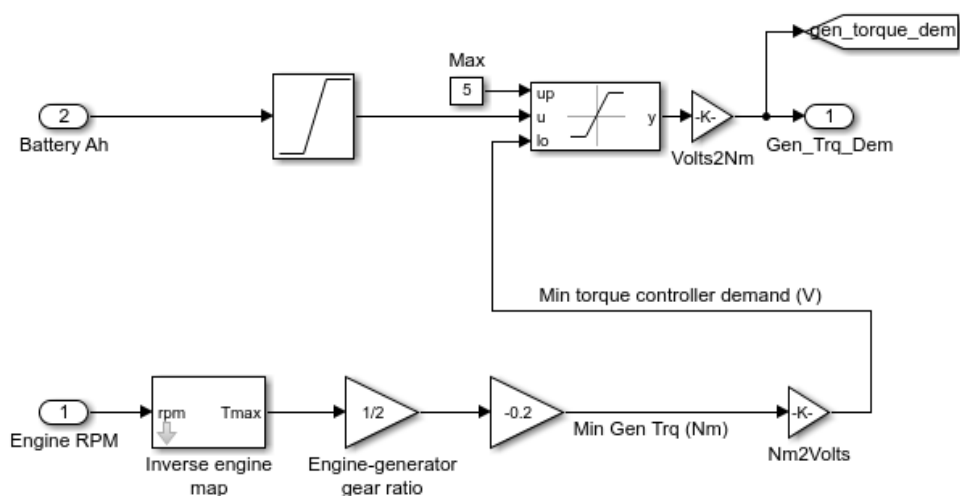
Figure (2.46) Battery controller [54]

2.4.5   Drive cycles

In general, drive cycles represent a set of vehicle speed points versus time, and they are used to compare and assess fuel consumption and pollutant emissions of different vehicles. There are two types of driving cycles, first modal cycles, which represent a combination of straight acceleration and constant speed periods, second transient cycles which are more realistic because they represent a real driver behavior by involving different speed variations. In this model, there are five different drive cycles, shown in the following Figures, to choose among them including modal cycles such as the European standard (NEDC, ECE, and EUDC), Japanese standard (10-15 mode), and transient cycles like the American drive cycles (FTP-75) [35,55,56].
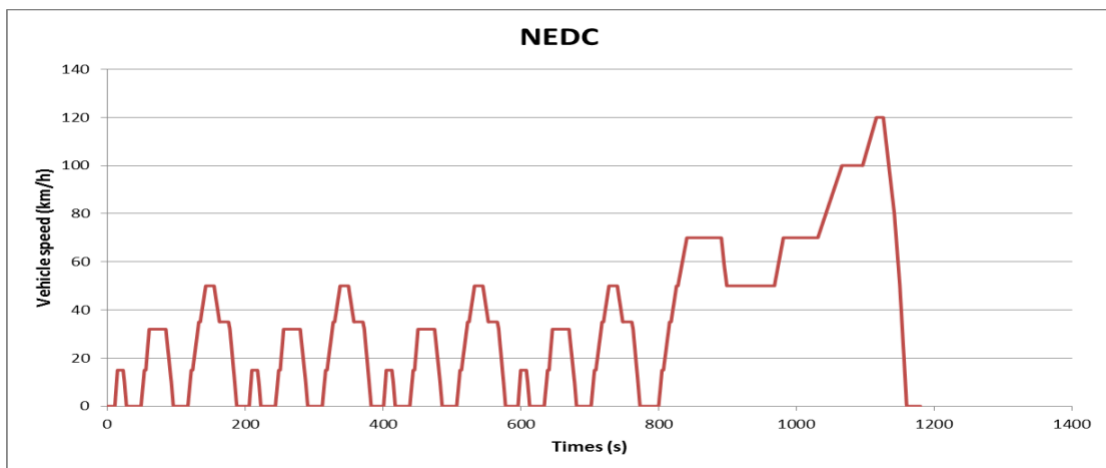
Figure (2.47) European Standard drive cycles [55]
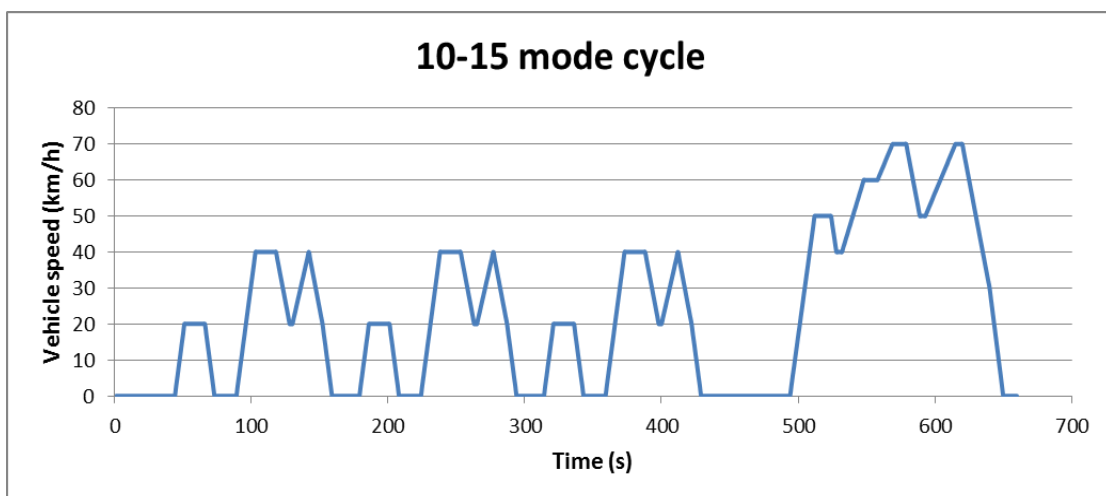
Figure (2.48) Japanese drive cycle [55]
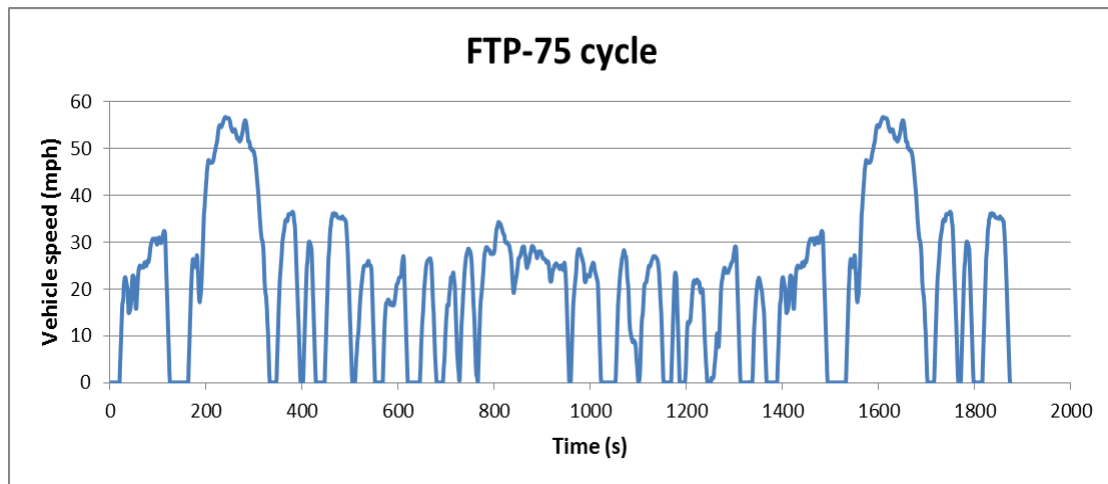
Figure (2.49) American drive cycle [55]

2.5 Battery/Ultracapacitor HESS Modeling in Simulink

2.5.1 Battery lone architecture

This architecture, shown in Figure (2.50), uses a generic battery that is directly connected to the DC link through a DC-DC converter. This architecture is not a hybrid energy storage system, but for comparison purposes, it will be simulated and compared with hybrid architectures in this Chapter [54].
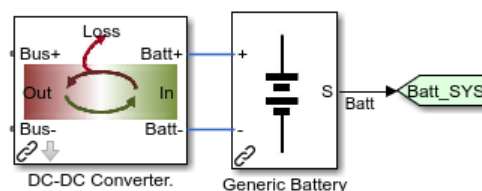
Figure (2.50) Battery Alone architecture [54]

2.5.2 Passive cascaded HESS architecture

This architecture, shown below, will be simulated, and it has a generic battery and lossy generic UC that connected in parallel and connected to the DC link through a DC-DC converter. This passive architecture does not have sufficient control over the battery and UC. The DC-DC converter is operating in boost mode during discharging and in buck mode during recharging. The DC link voltage (500 V) has to be maintained during the simulation period time [54].
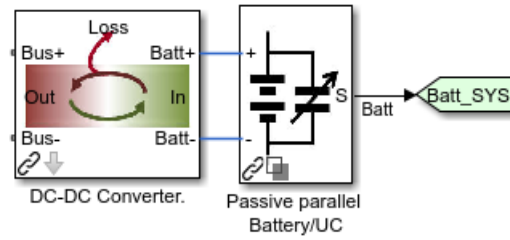
Figure (2.51) Passive cascaded HESS architecture [54]

2.5.3   Active HESS with two parallel DC-DC converters architecture

In this architecture, shown in Figures (2.52) and (2.53), the DC-DC converter was modeled using the Simscape library based on [54,57,58,59]. By setting the power from energy storage source equal to the power transmitted to the DC link plus the power lost to load dependent losses. The current through load-dependent losses is fed back to the controller to affect the mode logic of the whole system. This power balancing method is used to mimic the power exchange between both sources accomplished by a power converter.
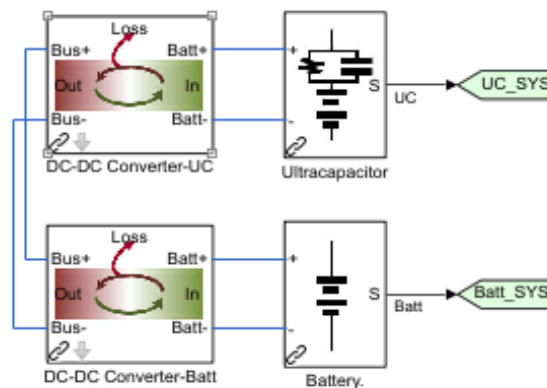
Figure (2.52) Active HESS with two parallel DC-DC converters [54]
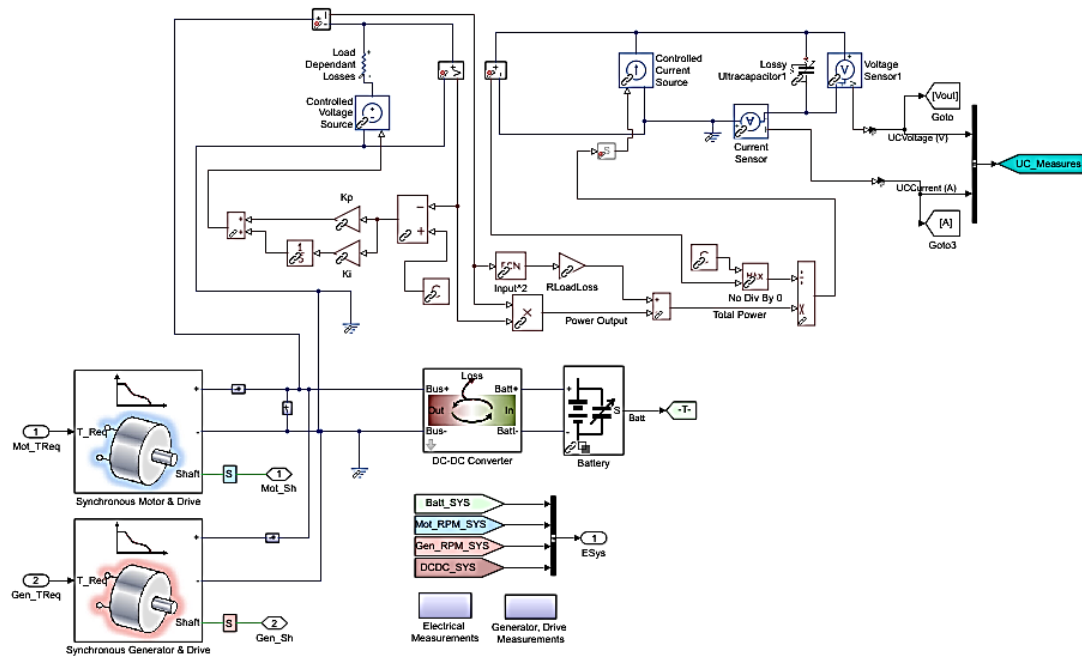
Figure (2.53) Active HESS with two parallel DC-DC converters

This HESS architecture has fully decoupled connections between the power sources and the DC link and from each other, so it has the flexibility to use two independent control strategies for battery and UC, which will increase the reliability of the system. During any failure in one of the power sources, the other source can still provide power to the DC link. This architecture allows the battery and UC to have lower voltage levels than the DC link [36,51].

In this model, the battery and UC converters are responsible for regulating DC link voltage by using a local PI controller where the proportional and integral gains for the UC's DC-DC converter are 0.0095 and 5, respectively; and for battery's DC-DC converter are 0.1 and 10. Besides, the minimum input voltage reference of UC's converter is 45 V, and 20 V for the battery's converter; as a result, ultracapacitor has a faster time response than battery to provide high voltage variations in the DC link. On the other hand, a rate limiter was added to the battery's DC-DC converter to limit the slope of the battery reference current and saturate the battery current value to $\pm 55\ A$. However, this is done by using system identification and PID tuning toolboxes in MATLAB, and some tuning of the battery current control.

Consequently, this model architecture showed a significant improvement to the overall system, and the results are reported at the end of this Chapter [36,51,54,59].

2.6 Overall HEV System Parameters:

In order to model a hybrid electric vehicle, there are numerous assumptions have to be made, and system requirements have to be met. In this model, the following requirements apply to the overall HEV system: First, dimensions of the vehicle are given as follows; Curb Weight = 1325 kg, Length = 4450 mm, Width = 1725 mm, and Height = 1490 mm. Second, the internal combustion engine should supply 57000 watts at 5000 rpm. Table (2.9) shows the specifications, parameters, assumptions, and requirements that were used in each part of the overall system [54].
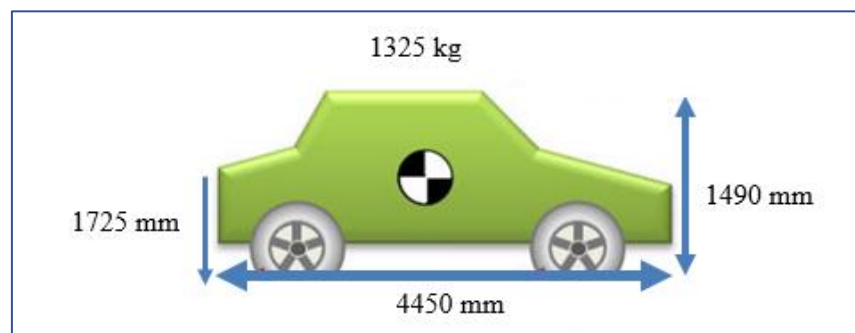

Figure (2.54) Vehicle's dimensions [54]

Table (2.9) Hybrid electric vehicle model parameters [54]

1- Mechanical System		
Vehicle and ICE parameters		
Specs.	Value	Unit
Mass	1200	kg
Wheel inertia	0.1	$kg\ m^2$
Engine vehicle gear ratio	1.3	-
Distance from Center of Gravity (CG)to rear axel	1.35	m
Distance from Center of Gravity (CG)to front axel	1.35	m
Distance from Center of Gravity (CG)to ground	0.5	m
Frontal area	2.16	m^2
Air density	1.18	kg/m^3
Tire Radius	0.3	m
Tire inertia	1e-2	$kg.m^2$
Rated vertical load	3000	N
Rated peak long force	3500	N
Slip at peak force	6	%
Inertia	0.5	$kg.m^2$
Max. Power	57	kW
Speed at Max. Power	5000	RPM
Max. speed	6000	RPM
Min. speed	1000	RPM
Stall speed	500	RPM
Torque at 4200 rpm	115	Nm
Friction	0.2079	$N.m.s/rad$
ICE fuel consumption per revolution	25	mg/rev
Gasoline density	750	kg/m^3

2.7 Selection of Architectures and Model Components

In this section, three cases of a series-parallel hybrid electric vehicle, which were described earlier, will be modeled and simulated: (1) with a battery alone, (2) a passive parallel battery/UC hybrid architecture, and (3) a parallel-connected multi-converters architecture. For the simulations, a portion of the American drive cycles (FTP-75) will be used for the time interval t= [0, 505]. This FTP-75, (Federal Test Procedure) driving cycle, represents frequent stops and a part of highway driving and includes acceleration, cruising, deceleration, and braking conditions. The system level, full vehicle, generic battery, and UC models will be used in all three simulations.

In all three simulations, the vehicle speed for interval [0, 505] seconds is shown in Figure (2.55). Also, the reference DC-link selected as 500 V, and the bi-directional converter was controlled so that it maintains the DC link voltage during discharging and recharging.
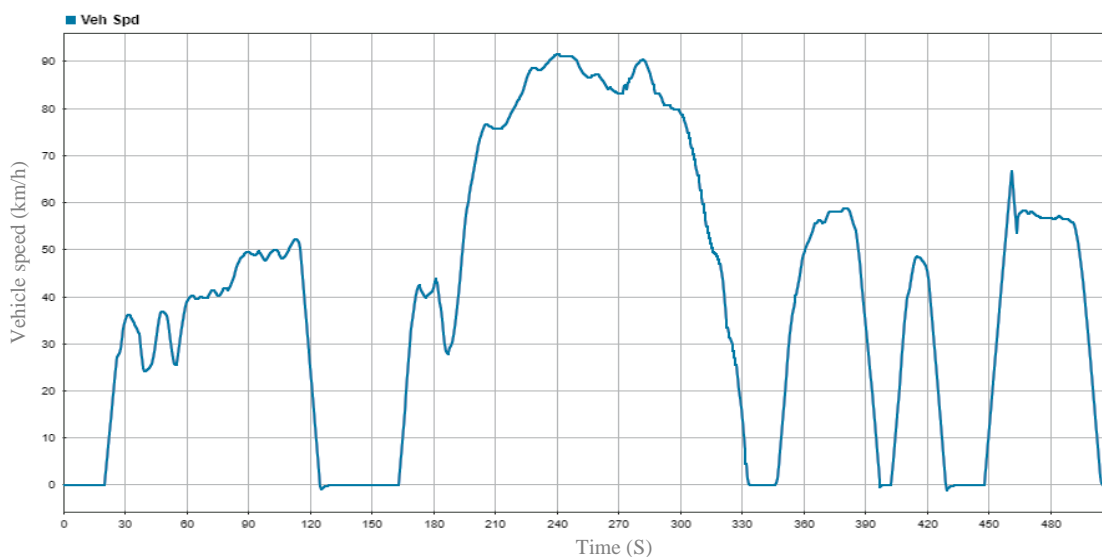
Figure (2.55) Vehicle speed

2.8 Simulations Results

2.8.1 Simulation of battery alone architecture

The first simulation was performed for a series-parallel hybrid electric vehicle that a battery energy storage connected to the electrical system through a bi-directional DC-DC

converter. Figure (2.56) presents the motor, generator, and engine speeds. The output power of the battery, motor, generator, and engine are shown in Figure (2.57). It can be seen that the power supply is mainly coming from the engine and electric motor.
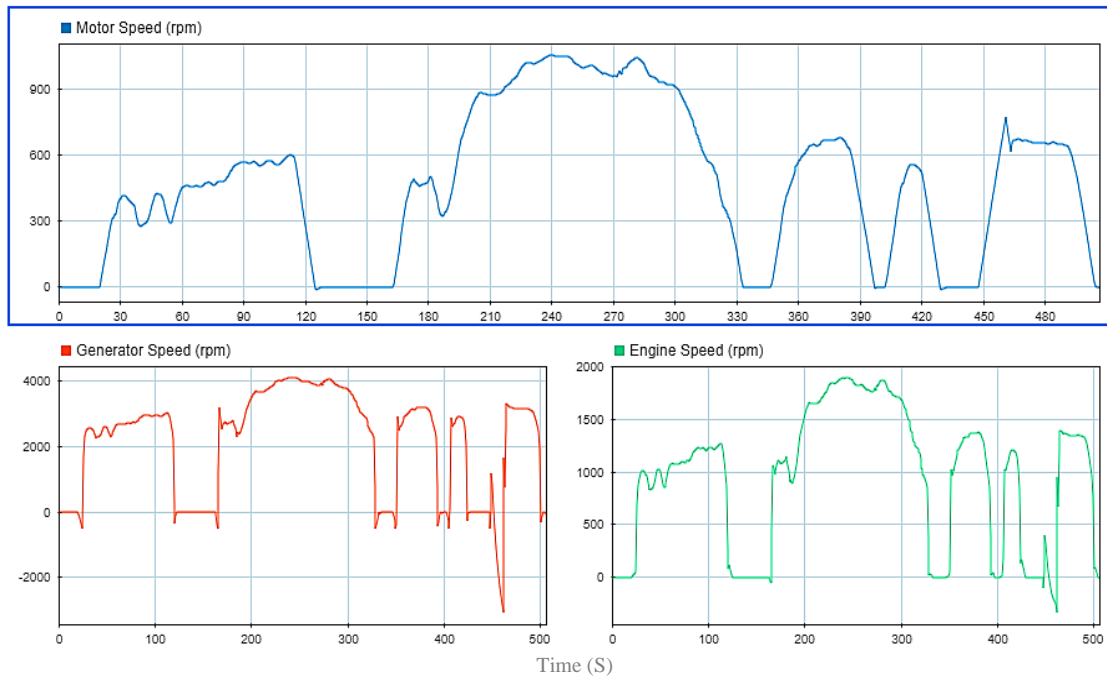
Figure (2.56) output speeds
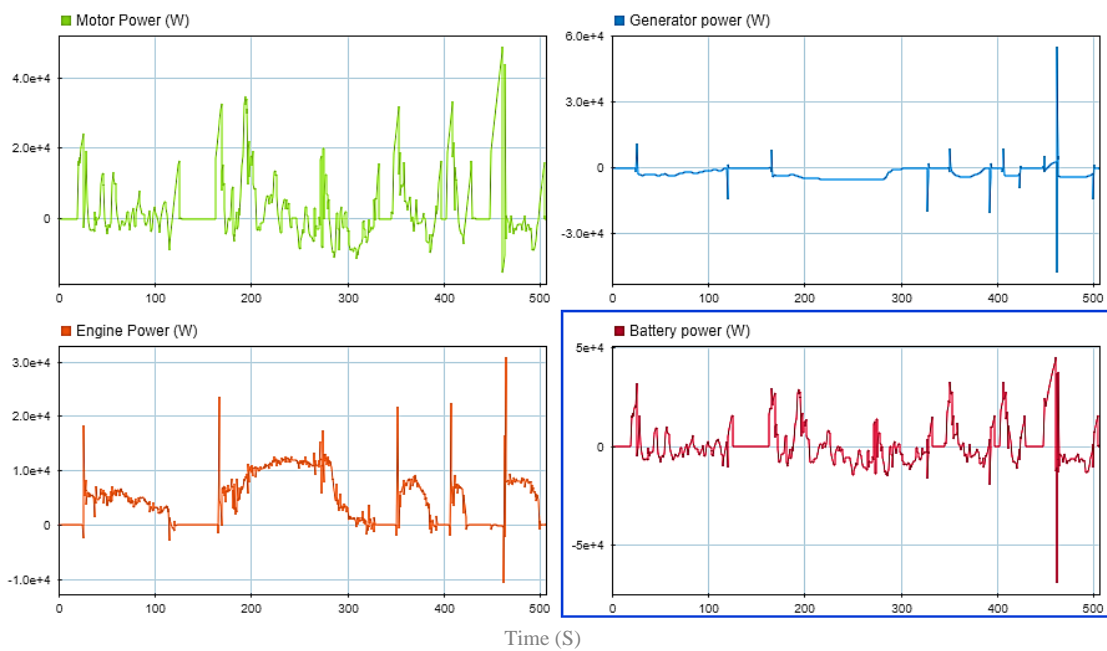
Figure (2.57) output powers

The battery current profile together with the battery voltage and state of charge are reported in Figure (2.58). The battery peak current and voltage are 330.9 A and 271.9 V, respectively, and the cycle end state of charge is about 88%. If the battery state of charge increased above 100%, that means no generation is required, and this was specified in the battery charge controller.
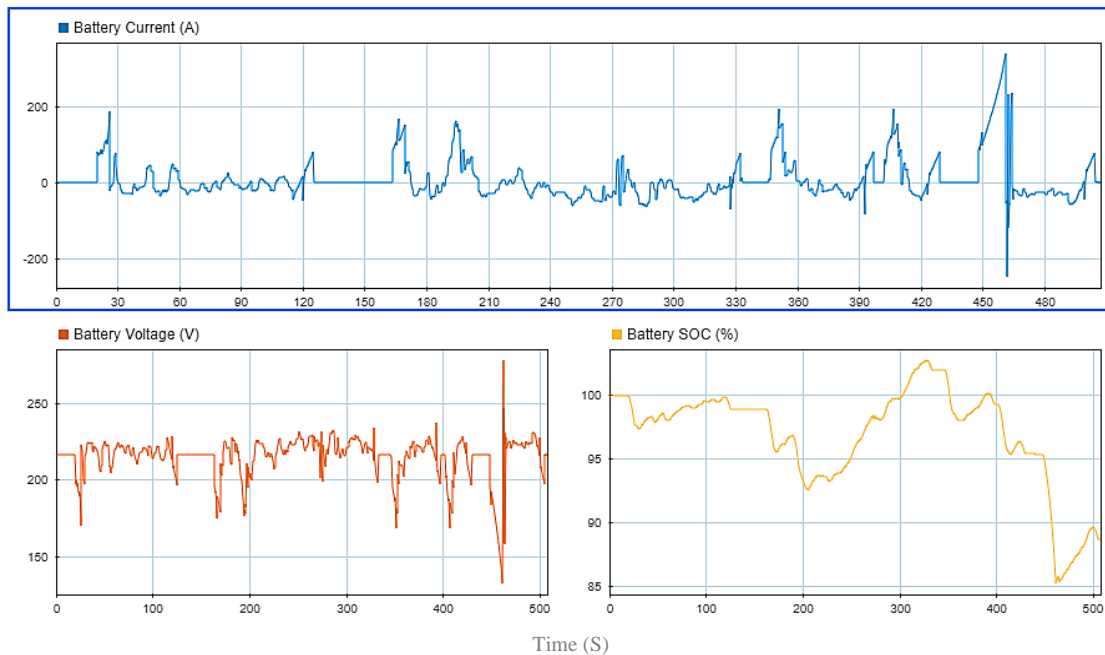
Figure (2.58) Battery current, voltage, SoC profiles

The DC link and battery voltages are presented in Figure (2.59). It can be seen that the DC link voltage varies around the reference DC voltage which is 500 V. the maximum voltage noticed at the DC link is 557 V, and the minimum is 431 V; therefore, the maximum voltage fluctuation range is 126 V, which is equal to 22.6%, over the simulation period. Moreover, the maximum battery voltage seen over the same period is 271.9 V, and the minimum is 120.9 V with a fluctuation range of 151 V. In addition, the reported total fuel economy of this architecture for the period [0, 505 s] is 46.31 MPG.
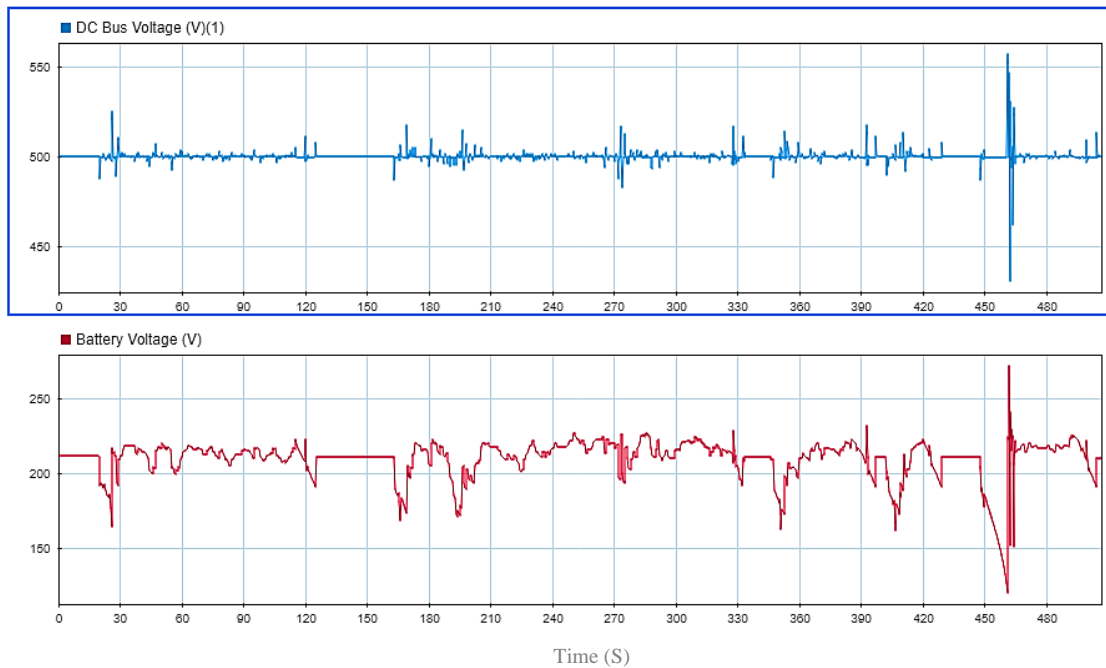
Figure (2.59) DC link and Battery voltage profiles

2.8.2 Simulation of passive parallel battery/UC architecture

In this architecture, the battery and ultracapacitor are connected in parallel to the DC link via a DC-DC converter. In literature, sometimes, this configuration is called passive or semi-active hybrid energy storage.

During the simulation of this configuration, the DC link voltage profile is not showing notable change, while the battery voltage profile affirmed the advantage of having HESS in reducing voltage variations. The voltage variations increase during high power demand and also during operation mode changes of the bi-directional DC-DC converter. At the output of the passive hybrid system, the maximum voltage observed is 278 V, and the minimum is 133.1 V, with a fluctuation range of 144.9 V.

The battery has a slower dynamic than ultracapacitor; therefore, it has to supply a smoother current profile than does the UC. However, the battery's current always follows the UC's current profile automatically because of the voltage balance between the battery and UC to keep the voltage terminal the same. As a result, the battery's current profile shows some fluctuations that can be reduced by performing other configurations.

By looking at the fuel economy, this architecture has increased the driving distance slightly compared to the battery alone architecture. The reported range per fuel unit is 46.74 MPG compared to 46.31 MPG in the previous simulation, and a higher number means more efficient, while a lower number indicates less efficient.

2.8.3   Simulation of two active parallel-connected converters architecture

In this architecture, both the battery and the ultracapacitor are connected parallelly to the DC link via two bi-directional DC-DC converters; therefore, the voltage and power flow are fully decoupled from each other. The same drive cycle used before is also used here over the same time interval. In this configuration, the ultracapacitor's bi-directional DC-DC converter is controlled to regulate the DC link voltage and minimize voltage variations, while the battery's converter is controlled so that it produces the average load required to the DC link. One of the key advantages of this configuration is that it can enhance the flexibility of manipulating battery and UC controllers as discussed earlier.

During the simulation of this configuration, the DC link voltage profile, shown in Figure (2.60), affirmed the advantage of having HESS in reducing voltage variations. The voltage variations increase during high power demand and also during operation mode changes of the bi-directional DC-DC converter. At the DC link, the maximum voltage observed is 513.6 V, and the minimum is 489.9 V; accordingly, the maximum DC link voltage ripple range is 23.67 V, which is equal to 4.6%. this is a significant reduction in the DC voltage fluctuation as compared to the previous architectures over the same simulation period.
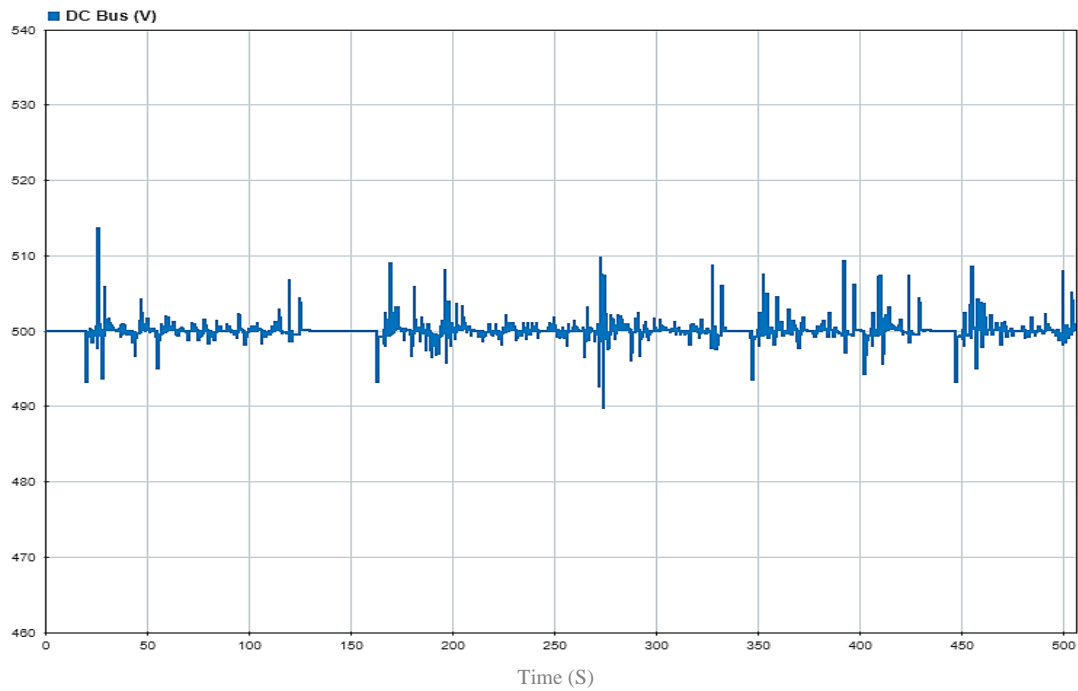
Figure (2.60) DC link voltage profile

As a result of this architecture, the battery current waveform, which is shown in Figure (2.61), has confirmed the advantage of using this configuration in supplying a smoother current profile than does the other configurations. Also, it has reported a further reduction in the battery current magnitude due to the current rate controller.

Moreover, the fuel economy in this architecture has further increased compared to the battery alone and passive HESS architectures. In this architecture, the fuel consumption is 68.72 MPG compared to 46.74 and 46.31 MPG in previous simulations. Therefore, the fuel economy improvement is about 20 miles per gallon, which is equal to 30%.

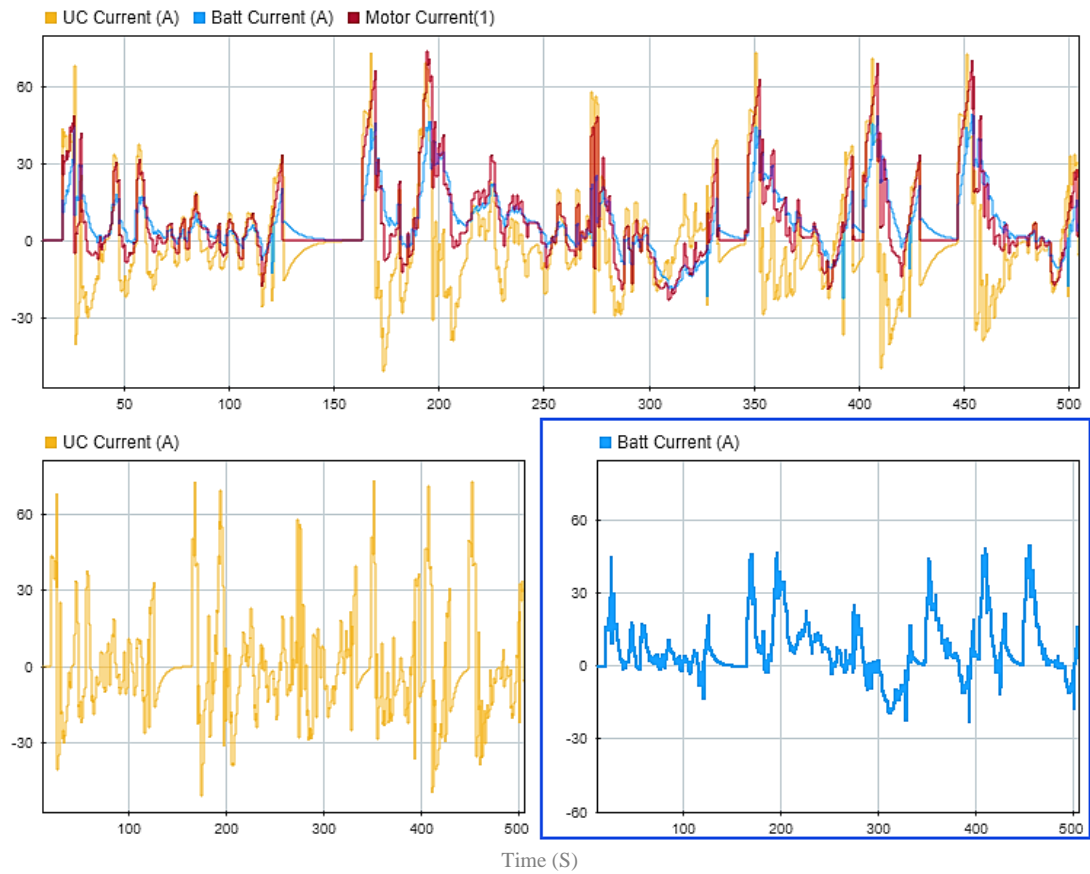*Figure (2.61) Motor, Battery, and UC current profiles*

2.9 Discussion and Comparison

Three different architectures with different components were modeled and simulated. One of the architectures was battery ESS only while others were the passive and active battery and UC hybridization architectures. The analysis results for these three architectures are presented for comparison in Table (2.10).

Table (2.10) Simulations results

Criteria	Battery Only ESS	Passive Cascaded HESS	Two parallel converters HESS
Structure	Simple	Average	Average
Control	Simple	Simple	Complex
Number of converters	1	1	2
Maximum DC link voltage (V)	557	550	513.6
Minimum DC link voltage (V)	431	437	489.9
DC link voltage ripple (V)	126	113	23.67
Maximum battery voltage (V)	271.9	278	229.5
Minimum battery voltage (V)	120.9	133.1	198.9
Battery voltage ripple (V)	151	144.9	30.63
Battery current ripple (A)	586.8	563.5	73.8
Battery SoC at the end of the cycle (%)	88	88.9	98.5
Fuel economy (L/100km)	5.08	5.03	3.423
Fuel economy (km/L)	19.69	19.87	29.22
Fuel economy (MPG)	46.31	46.74	68.72

From Table (2.10), the battery only architecture has the simplest structure and control strategy while the other architectures have different levels of structure and control complexity. Although active parallel architecture has two converters, the total inductor mass is smaller than that of the passive architecture because in active architecture, each converter carries only the current of one source. The total inductor mass is proportional to the current passes through inductor wiring. The DC link voltage fluctuations were slightly decreased in passive configuration compared to battery alone configuration and further decreased in the active architecture because of the control strategy used which allows the UC to take huge fluctuations. Also, because of the same strategy, the battery voltage and current ripples were reduced in the active architecture. Moreover, by comparing these architectures in terms of battery SoC, it can be seen that active parallel architecture is superior because the UC was utilized more in this architecture. Furthermore, if these architectures are compared based on the fuel economy, the active parallel architecture with two converters is outstanding because it increased the motor current and as a result, increased the motor torque.

From the results in Table (2.10), it is observed that the active architecture with two parallel converters and a modified control strategy reduced the battery current and current ripple, resulting in prolonging the battery lifetime. Also, this architecture reduced the DC link voltage ripple and improved the vehicle's driving range.

Chapter 3: Energy Storage Systems for Renewable Energy Applications

3.1 Introduction

This chapter will be focusing on energy storage systems for residential, commercial, and utility-scale in microgrids and renewable energy applications. There will be three cases for three different states, which will be simulated by a software called Hybrid Optimization Model for Electric Renewables (HOMER) to investigate ESS's economic and sizing aspects. However, storing energy efficiently and cost-effectively has long been studied by scientists and researchers that led to accelerating the developments in most of ESS technologies. By the end of 2019, the global energy storage deployment capacity is expected to hit 30 GWh which is more than doubling the growth in 2018. According to the energy storage outlook report 2019, in the next five years, the global energy storage capacity is expected to reach 158 GWh led by the US and China, as shown in Figure (3.1) [60]. This growth will be driven by utility-scale storage deployment. Also, residential-scale storage is prospected to increase caused by the high demand for residential renewable energy systems like solar PVs and small wind turbines [61]
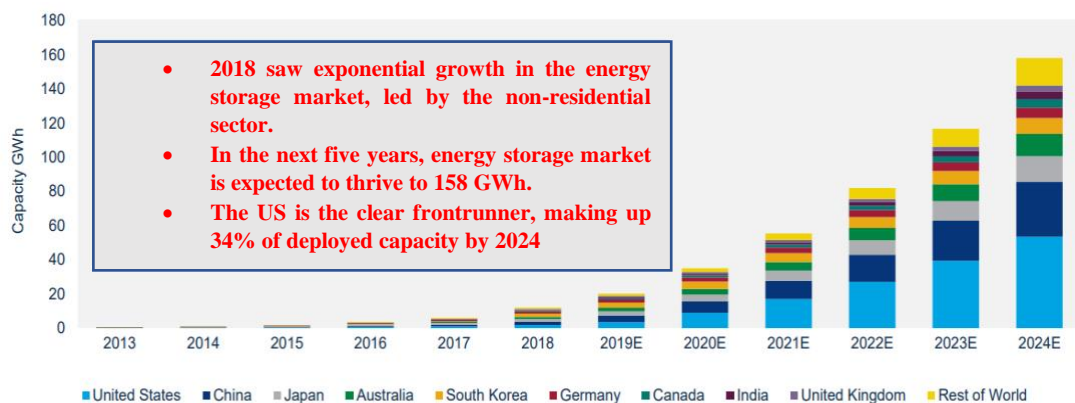

Figure (3.1) Global ESS outlook (2013-2024) [60]

Many energy storage technologies have been studied by researchers aiming to find the best suitable ESS for different applications, such as integrating ESS with an existing power grid or microgrids that contain renewable energy distribution sources like solar PV and wind turbines. For those stationary systems, an energy storage system can provide services for long,

medium, or short duration, such as load leveling, arbitrage, peak shaving, renewable penetration, intermittency mitigation, frequency and voltage regulation, transient stability, etc. In [3,4], these energy storage services and applications are classified based on the storage duration, power rating, response time, and suitable ESS options for each scale.

Microgrids are small-scale power networks that operate independently or in tandem with utility-scale electrical supplies. In other words, microgrids are a combination of distributed energy resources and energy storage devices to serve a set of loads through a distributed network. Generally, microgrids contain conventional sources like diesel generators, renewable sources like solar photovoltaic or wind turbines, energy storage devices, power electronics, control units, and AC or DC loads. Figure (3.2) shows a basic example of a microgrid structure. Microgrids can operate in different modes, such as grid-connected mode, an isolated mode that is also known as islanded mode, or transition mode. There are three microgrid structures known as DC, AC, and hybrid microgrids. In DC microgrids, all distributed generators (DGs), energy storage devices, DC loads, and power electronics connected to a DC bus line which is connected to the low voltage distribution system. If all these components are connected to the AC bus line, then it is called AC microgrid. The hybrid AC-DC microgrid is a combination of AC and DC microgrids [62].
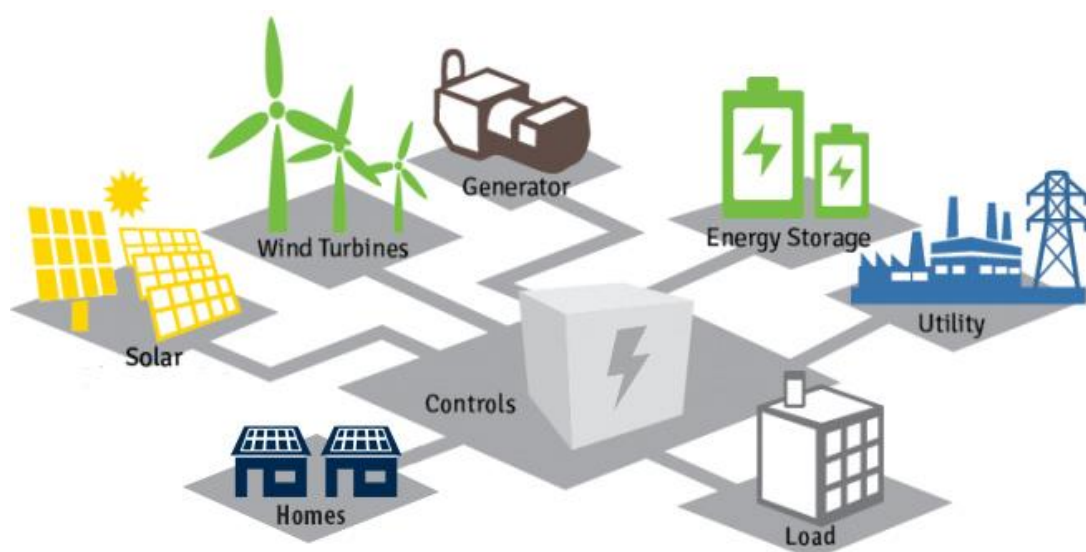

Figure (3.2) Microgrid structure [63]

Microgrids or hybrid renewable energy system could be helpful in remote areas or isolated islands where there is no existing power infrastructure. Microgrids provide an excellent alternative to frequently used backup generators, which as a result, increase the grid reliability. However, even in places with more reliable power grids, outages can have a very high cost, particularly for sites with critical loads, such as data centers or research facilities. Therefore, there is a strong potential for microgrids for emergency response and reliable power during and following extreme outage events.

3.2 System Modeling in HOMER Software

3.2.1   Overview

HOMER software developed originally at the National Renewable Energy Laboratory (NREL), starting with their village power program back in 1992, later in 2000, they expanded it to look at larger systems (100 MW or larger). In 2009, NREL spun off Homer as a sperate private company with 100,000 users in 193 countries. Homer software is a tool for rapid assessment of least-cost solution for clean, reliable, and distributed power. It compares thousands of possible combinations as either standalone or grid-connected systems of conventional generators, solar, wind, storage systems, and load management including demand-side management and energy efficiency. Also, it allows users to sort feasible systems by optimizing different variables including interest rates, tariffs, sell back rates, emission goals, renewable resources and equipment, fuel prices …etc. [64,65]

HOMER software contains most of the features that are required to analyze a microgrid or a hybrid renewable power system along with an energy storage system such as batteries and flywheels. This software can model a range of loads, including electrical loads as well as thermal loads. It can also model a variety of generator options including reciprocating units, turbines, fuel cells, and they can run on different fuel options including diesel natural gas, hydrogen, or biomass. Besides, you can model renewable generation options, such as solar PVs, wind turbines, hydrokinetic, or tidal turbines. Those systems can be connected to the utility grid with a range of reliability or in islanded or isolation modes. Regarding energy storage

technologies, you can model a wide range of battery technologies including Lead-Acid, Lithium-ion, redox flow batteries, and more, or you can model different technologies, such as flywheels, supercapacitor, fuel cells, pumped hydroelectric, and hydrogen storage systems [64].

3.2.2   Natural resources, components, and cost data:

3.2.2.1 Natural resources

Since the proposed models have solar and wind renewable energy sources, NASA Surface meteorology and Solar Energy database is used to download solar radiation and wind speed in those three locations. Figure (3.3) illustrates a sample of the monthly averaged solar radiation and clearness index in Orlando-Florida. According to NASA Surface meteorology and Solar Energy database, the monthly averaged global horizontal solar radiation, for this particular location, is about 4.65 kWh/m^2/day over a 22-year period (July 1983- June 2005). the monthly averaged solar radiation in Milwaukee and San Diego are 3.8 and 5.07 kWh/m^2/day, respectively [65].

Figure (3.3) Monthly averaged solar radiation [65]

Based on the NASA Surface meteorology and Solar Energy database, the monthly averaged wind speed at 50 meters above the surface of the earth is 4.63 m/s over ten year period in Orlando-Florida, and the bar chart shown below gives the monthly averaged wind speed for one year in Orlando. The monthly averaged wind speed in Milwaukee and San Diego are 5.7 and 5.46 m/s, respectively [65].
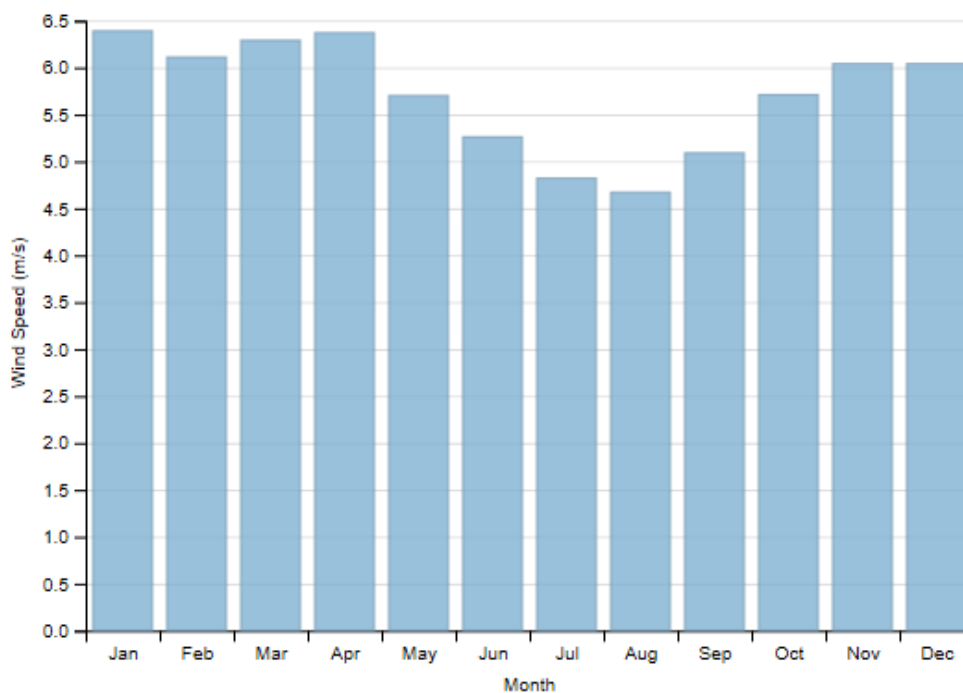
Figure (3.4) Monthly averaged wind speed [65]

3.2.2.2 Electrical loads

As mentioned before, the purpose of this chapter is to investigate energy storage economic and sizing aspects for residential, commercial, and utility-scale hybrid renewable energy systems in islanded and grid-connected modes. Those three cases are taken for distinct locations in San Diego-California, Orlando-Florida, and Milwaukee-Wisconsin. The load profiles for residential and commercial cases are built based on the average electricity consumption in location. Table (3.1) shows the average daily bill in kWh given by the U.S. Energy Information Administration (EIA) [66]. A random variability of 10 % day-to-day and 20% timesteps are introduced to make the load profile looks more practical [65].

Table (3.1) Electrical load consumption [66]

Load consumption						
Location	San Diego - CA		Orlando - FL		Milwaukee - WI	
Type	Residential	Commercial	Residential	Commercial	Residential	Commercial
Average daily consumption (kWh/day)	18.2	187.56	37	217.46	23.1	188.73
Scaled peak load (kW)	3.3791	26.9307	6.8696	31.2249	4.2889	27.0987
Load factor	0.2244	0.2902	0.2244	0.2902	0.2244	0.2902

In commercial cases, a more realistic load profile for a hospital and large office in Orlando-Florida is proposed to show the effect of peak change during the day on sizing and cost. The hospital load profile represents a hospital with 241,351 square feet and five floors that consumes 28672.13 kWh/day and 1593.67 kW peak, while the large office (498588 square feet and 12 floors) consumes 21225.16 kWh/day and 1815.67 kW peak. Figures (3.5) and (3.6) elaborate daily load profiles for the hospital and large office in Orlando-Florida. In utility-scale, a synthetic community load profile, shown in Figure (3.7), is scaled based on the average electricity consumption in Orlando where the average daily consumption is 751 MWh/day and 100 MW of peak demand, and the average baseline is 6.9 kW. A random variability of 10 % day-to-day and 20% timesteps are introduced to make the load profile looks more practical. July month is the peak month in all cases [65].
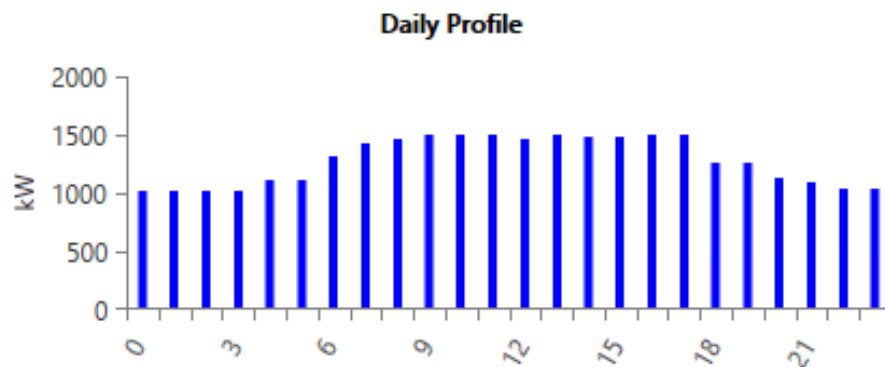
Figure (3.5) Hospital's daily load profile [65]
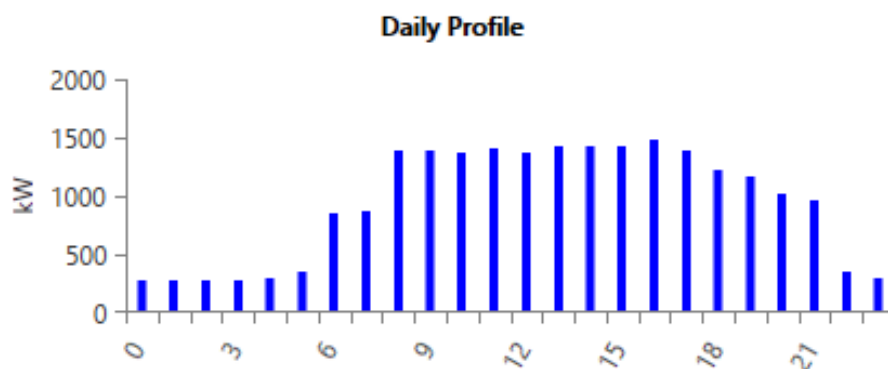
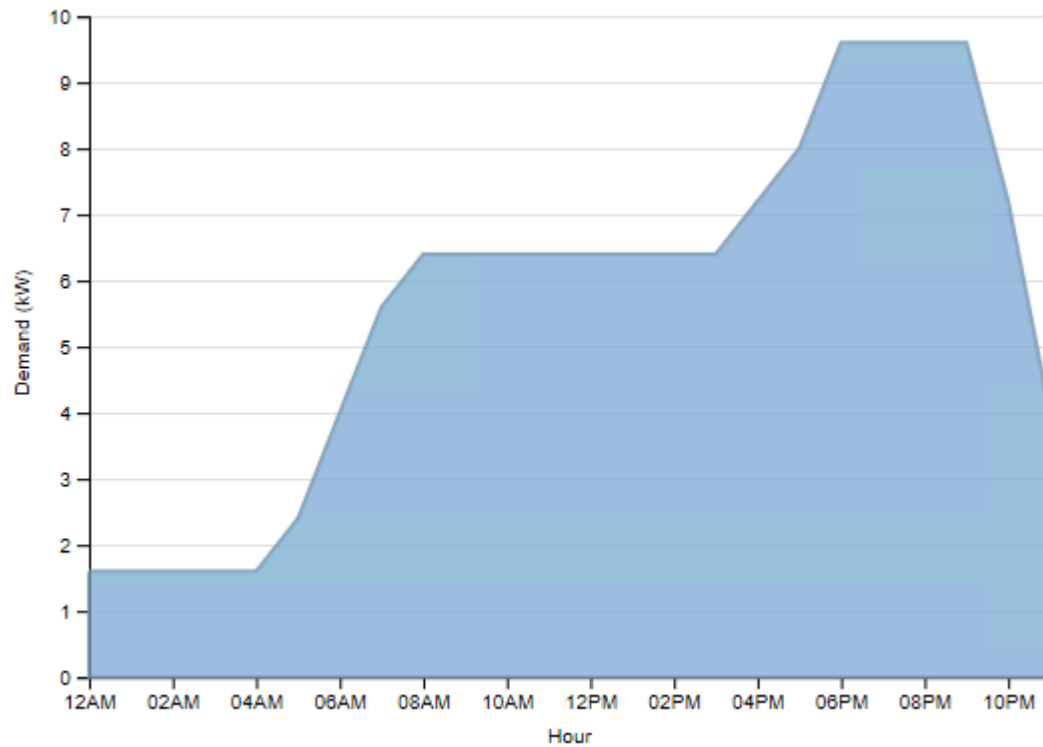*Figure (3.6) Large office daily load profile [65]*

Figure (3.7) Daily community load profile in utility-scale [65]

3.2.2.3 Energy sources

There are five main components connected to the AC or DC buses designed for hybrid renewable-based isolated or grid-connected systems. These components are electric load, wind turbine, solar PVs, energy storage systems, and power converter. The system schematic, shown in Figure (3.8), used for both residential and commercial cases, while Figure (3.9) shows the utility-scale grid-connected system. Five energy storage systems with different technical and economic characteristics are used to find the most optimal mix of these components for each case, and those energy storage systems are Lithium-ion battery, Lead-Acid battery, Zinc-bromine flow battery, flywheel, and supercapacitor. PV modules can be connected to the AC or DC buses, and the power converter's size and cost will change based on the topology [65].
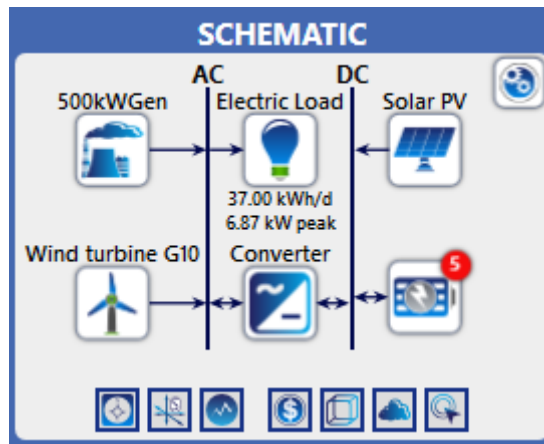
Figure (3.8) Residential system's schematic [65]
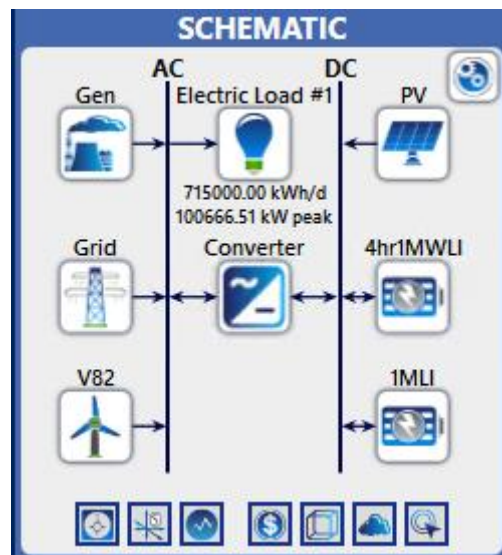
Figure (3.9) Utility system's schematic [65]

3.2.2.3.1   Solar PVs

The solar PVs utilized in all cases are assumed to be automatically sized by HOMER software. A PV with 1 kW initial capacity and 0.1 variations are the assumptions the need to be considered in the study. The PV's lifetime is 25 years, and no tracking system is assumed in all cases. Also, a ground reflectance of 20 % is considered in all cases. Temperature effect on PV's operation is takin into consideration in this study, and the temperature data is obtained from the NASA Surface meteorology and Solar Energy database which was measured over a 22-year period (July 1983 - June 2005) [65]. Finally, Table (3.3) shows the costs of solar PVs on each scale based on the costs from the Levelized Cost of Energy (LCOE) report [67,68,69]

3.2.2.3.2 Wind turbines

Two generic wind turbines with 3 kW and 10 kW are used in residential and commercial scale to give the system the flexibility of using the most suitable components. These wind turbines have a lifetime of 20 years, and a hub height of 17 and 24 meters, respectively. The initial capital cost and replacement cost of generic wind turbine with 3 kW are 18,000 US dollars, and the operation and maintenance cost is 180 US dollars per year [65].

A Vestas wind turbine (V47-660 kW), with a hub height of 50 meters, is used in combined hospital and large office commercial cases, and Vestas V82-1.65 MW for utility-scale with a hub height of 79 meters. Table (3.3) illustrates the costs of each wind turbine used in each case [65].

3.2.2.3.3 Energy storage systems

Energy storage systems with different technical and economic aspects are used to find the optimum option for each case. Lithium-ion battery, Lead-Acid battery, Zinc-bromine flow battery, flywheel, and supercapacitor are used in residential and commercial scale, and the large lithium battery used in utility-scale. Table (3.3) illustrates lifetime, capital, replacement, and maintenance costs for each device.

In residential and commercial-scale cases, Lithium-ion battery has 167 Ah nominal capacity and 6 V nominal voltage. The round-trip efficiency is 90%. The minimum state of charge and the initial state of charge are assumed to be 20 and 100 percent, respectively. Table (3.2) summarizes the technical characteristics of lead-acid battery, zinc-bromine flow battery, flywheel, and supercapacitor used in residential and commercial cases [65].

Table (3.2) Technical characteristics of different ESSs [65]

Component	Nominal Voltage (V)	Nominal Capacity (Ah)	Roundtrip efficiency (%)	Max. Charge current (A)	Max. Discharge	Initial SoC (%)	Min. SoC (%)
Lead-Acid Battery	12	83.4	80	16.7	24.3	100	40
Zinc-Bromine Flow Battery	48	207	75	50	100	100	0
Flywheels	825	30.3	85	121	121	100	0
Super-Capacitor	3	3.75	-	2200	2200	100	0

In utility-scale, a large Lithium-ion battery with 1 MWh energy capacity, 600 nominal voltage, 250kW nominal capacity, and 4 hours storage duration is used because it is the only available option with high storage. It has a round-trip efficiency of 90 %, initial SoC of 100%, Min. SoC of 20%, and a lifetime of 15 years. Pumped hydroelectric and flow batteries are neglected in this case since they have a site and technical limitations [65].

3.2.2.3.4   Diesel generator

In all cases, a diesel generator with 500 kW capacity is used for baseload generation in islanded mode. The software is allowed to size the generator generation to meet the load demand automatically. This diesel generator has a lifetime of 15,000 hours of operation. Its initial capital cost and replacement cost are 500 US dollars ($) per kW of capacity, while the operation and maintenance cost are 0.03 US dollars per operating hour [65].

3.2.2.3.5   Grid

Storage is needed when there is a high renewable penetration system, but in cases like if a deficient penetration system is used or if you have a big grid like in North America or Europe, renewables can be installed without any storage system where the grid can be used as storage by using net metering. In all cases, net metering purchases are calculated monthly, and the grid power price is allowed to vary from 0.1 to 1 $/kWh [65].

3.2.2.3.6   Power converter

In microgrids, there are AC and DC components that need power converter to convert the AC to DC and vice versa. The capital and replacement costs of the power converter used in all cases are assumed to be 300 US dollars per kW ($/kW). The maintenance cost is 10 dollars per year, and the lifetime is assumed to be 15 years. Moreover, power conversion efficiency (inverter/rectifier efficiency) is assumed to be 95 %, and the rectifier relative capacity is 100 %. Also, the inverter is allowed to operate in parallel with the AC generator [65].

3.2.3   Cost information

HOMER is considered as an economic modeling software; therefore, cost information for each component is central to its analysis. Accurate cost information is important for a precise result. HOMER has the ability to run different fixed and variable capital costs, replacement costs, and maintenance costs for each component. Based on the costs given in the latest report for the Levelized cost of energy and storage (LCOE and LCOS), Table (3.3) elaborates the components' costs used in each study case [65].

Table (3.3) Components' costs and lifetime [67,68,69]

Component	Scale	Rated capacity (kW)	capital Cost ($)	Replacement Cost ($)	O&M Cost ($/year)	Lifetime (Years)
Components' cost data per rated capacity						
PV (Flat plate)	Residential	1	3,110	3,110	10	25
	Commercial	1	2,900	2,900	10	25
	Utility	1	1,300	1,300	10	25
Wind Turbine	Residential	10	50,000	50,000	500	20
	Commercial	660	1,000,000	1,000,000	30,000	20
	Utility	1,650	2,475,000	2,475,000	50,000	20
Lithium Ion Battery	Residential	1	550	440	10	15
	Commercial	250	500,000	500,000	10,000	15
	Utility	250	500,000	500,000	10,000	15
Lead-Acid Battery	Residential	1	300	300	10	10
	Commercial	1	300	300	10	10
	Utility	Not Used				
Zinc-Bromine Flow Battery	Residential	9.93	8,800	8,800	500	40
	Commercial	9.93	8,800	8,800	500	40
	Utility	Not Used				
SuperCapacitor	Residential	3,000	100	100	5	30
	Commercial	Not Used				
	Utility					
Flywheel	Residential	25	300,000	200,000	5	20
	Commercial	Not Used				
	Utility					
Power Converter	Residential	1	300	300	10	15
	Commercial	1	300	300	10	15
	Utility	1	300	300	10	15

3.3 Simulation Settings

HOMER uses an hour-by-hour down to minute-by-minute time steps to dispatch the model components to ensure adequate energy supply is available to meet the load demand. Controller set up is based on a chronological dispatch strategy, which is critical for modeling renewable systems to accurately capturing the best technical and economic performance.

HOMER load following and cycle charging controlling strategies are used to determine the optimum dispatch strategy for our three cases [65].

Optimization in HOMER allows you to compare different simulations by automatically sizing PVs, wind turbines, batteries, and converters, which will allow you to find the design with the lowest cost. Also, you can perform sensitivity analysis on each part of the system, such as components size and value, grid power price, fuel prices, wind speed, and solar radiation.

Table (3.4) Simulation settings [65]

Economics and Constraints			
Annual real interest rate (%)	6	Allow systems with multiple generators	Yes
Project lifetime (years)	25	Battery autonomy threshold (hours)	4
Timestep length (minutes)	1	Maximum renewable penetration threshold (%)	55
Time steps per year	525,600	System design precision	0.01
NPC precision	0.01	Maximum annual capacity shortage	5
Operating reserve as percentage of hourly load (%)	10	inflation rate (%)	0
Operating reserve as percentage of solar power output (%)	80	Cycle Charging Setpoint SoC	80
Operating reserve as percentage of wind power output (%)	50	Minimization strategy	Economic

3.4 Results and Discussions

3.4.1 Case 1: Synthetical residential and commercial-scale systems in islanded mode

This case represents residential and commercial synthetical loads in San Diego-California, Orlando-Florida, and Milwaukee-Wisconsin. Those cases are assumed to be in an islanded mode, which means no grid connection is available. The main objective of the simulation is to find the optimum mix of renewable energy sources and storage in those locations, so 100% renewable penetration is assumed in all cases. As mentioned previously, the load profiles are built for residential and commercial cases based on the average electricity consumption in these locations. Table (3.5) shows the optimization results for the residential-scale case. In all cases, the software is allowed to automatically size the solar PV modules, wind turbines, batteries, power converters, and diesel gensets.

Table (3.5) Optimization results for residential-scale systems in different states

Residential systems		CA	FL	WI
Location	**State**	**CA**	**FL**	**WI**
Architecture	PV (kW)	6.36	16.56	14.45
	Li-Battery (kWh)	18	44	37
	Converter (kW)	3.42	6.22	5.99
	Dispatch	CC	CC	CC
Cost	NPC ($)	36.87 K	92.52 K	79.81 K
	COE ($)	0.454	0.560	0.773
	Operating cost ($/yr)	483.1	1169.5	994.7
	Initial capital ($)	30.7 K	77.6 K	67.1 K
PV	Capital Cost ($)	19.8 K	51.5 K	44.9 K
	Production (kWh/yr)	10.7 K	24.5 K	18.7 K
Battery	Autonomy (hr)	18.99	22.83	30.75
	Annual Throughput (kWh/yr)	3.61 K	7.32 K	4.56 K
	Nominal Capacity (kWh)	18	44	37
	Usable Nominal Capacity (kWh)	14.4	35.2	29.6
Converter	Rectifier Mean Output (kW)	0.433	0.877	0.545
	Inverter Mean Output (kW)	0.372	0.753	0.469

This table illustrates the optimum system design in each state based on the system size and cost. In California, the winning system includes 100% renewable sources and storage, which is based exclusively on solar PV and lithium-ion batteries. It has a 6.358 kW of solar PVs, 18 kWh lithium-ion battery, 3.416 kW power converter, and a cycle charging (CC) dispatch strategy. The system's total net present cost (NPC) is 36873.23 ($) over the 25 years project lifetime, while the Levelized cost of energy (COE) is around 0.454 $ per kWh. The annual operating cost is 483.1 $/year, and the initial capital cost at the beginning of the project including all system's components is 30697.56 $. It can be noticed that solar PVs capital cost represents 64.4% of the system capital cost with 19772.7 $. The rest of the table summarizes the operational characteristics of each component. It can be noticed that the PV and battery sizes are dramatically different across those states, and that comes from the variation of the average solar radiation in each location. Also, it can be noticed that wind turbines are not considered as a suitable option for residential-scale systems. However, in commercial-scale systems, which consumes a larger amount of electricity than residential-scale systems, wind

turbines became feasible especially in Wisconsin where averaged wind speed is high; therefore, whenever you got high average annual wind speed, intuitively you would want to consider adding wind turbines to your system. Table (3.6) shows the optimization results for the two optimum systems in the commercial-scale scenario.

Table (3.6) Optimization results for commercial-scale systems in different states

Commercial systems							
Location	State	CA		FL		Wi	
	Ranking	1	2	1	2	1	2
Architecture	PV (kW)	65.0	63.2	89.2	96.3	78.6	70.8
	Wind Gen (10 kW)	-	-	-	-	2	2
	Li-Battery (kWh)	-	175	271	-	197	-
	LA- Battery (kWh)	-	-	-	-	-	334
	Zcell Battery (9.93 kWh)	16	-	-	23	-	-
	Converter (kW)	23.0	25.2	29.5	29.2	32.8	25.8
	Dispatch	CC	CC	CC	CC	CC	CC
Cost	NPC ($)	357.9 K	359.5 K	504.3 K	514.8 K	557.1 K	584.4 K
	COE ($)	0.421	0.424	0.639	0.652	0.653	0.685
	Operating cost ($/yr)	.6 K	4.6 K	6.7 K	.4 K	7.4 K	12.2 K
	Initial capital ($)	349.8 K	300.3 K	435.4 K	510.6 K	462.6 K	428.0 K
PV	Capital Cost ($)	202.1 K	196.5 K	277.4 K	299.4 K	244.4 K	220.1 K
	Production (kWh/yr)	109.3 K	106.3 K	131.7 K	142.1 K	101.9 K	91.8 K
Wind	Capital Cost ($)	-	-	-	-	100.0 K	100.0 K
	Production (kWh/yr)	-	-	-	-	26.5 K	26.5 K
	O&M Cost ($)	-	-	-	-	1.0 K	1.0 K
Battery	Autonomy (hr)	20.34	17.91	23.93	25.22	20.04	25.50
	Annual Throughput (kWh/yr)	23.56 K	21.65 K	24.31 K	25.88 K	16.29 K	18.00 K
	Nominal Capacity (kWh)	158.9	175.0	271.0	228.5	197.0	334.3
	Usable Nominal Capacity (kWh)	158.9	140.0	216.8	228.5	157.6	200.6
Converter	Rectifier Mean Output (kW)	3.09	2.59	2.91	3.39	1.94	2.27
	Inverter Mean Output (kW)	2.21	2.23	2.50	2.43	1.68	1.75

Overall, this table presents the optimization results for commercial-scale systems in San Diego-California, Orlando-Florida, and Milwaukee-Wisconsin. In this case, two optimization results are presented to highlight the effect of size, cost, and natural resources on deciding which system is optimal in each location. The assumptions and constraints are kept similar to residential scale cases.

The key findings from this table are: first, the size of the components has increased as compared to the residential case because the peak load profile increased; as a result, different hybrid systems became more economically feasible while in previous case PV and battery hybrid renewable system was the most economical option. Second, solar PVs are a cost-effective contributor in all cases. Third, lithium batteries are not the most economical option in all cases, as in residential-scale systems. In this commercial-scale scenario, different types of batteries with different sizes became considerable options; for example, lead-acid batteries in Wisconsin's case is used in the second optimum system, and zinc-bromine flow batteries in California's case is used in the first ranked system.

3.4.2   Case 2: Real commercial-scale system in islanded and grid-connected modes

This case represents a commercial system for a hospital and a large office building in Orlando-Florida. The total average daily consumption is 49,897.29 kWh/day, with a 3,409.41kW of peak load. The main goal of this simulation is to find the optimum mix of energy sources and storage in islanded and grid-connected modes. In this case, a sensitivity analysis is carried out to find the impact of several variables on the system's overall cost. The sensitivity inputs are diesel fuel price, renewable penetration fraction, average solar radiation, and average wind speed. The diesel fuel price is assumed to vary from 0.5 to 10 US dollars per liter, and renewable energy penetration is allowed to vary between 0 and 50%. As mentioned earlier, the averaged global horizontal solar radiation and averaged wind speed in Orlando-Florida are about 4.65 kWh/m^2/day and 4.63 m/s, respectively. However, solar radiation will change between 1 and 8 kWh/m^2/day while wind speed will vary from 3 to 8 m/s.

Figure (3.10) illustrates what type of system is optimal in islanded mode across the range of sensitivity values we considered. The X-axis represents the range of diesel fuel prices in (\$/L), and the y-axis represents the range of wind speed averages in (m/s). Renewable energy penetration is kept at 0% while the solar radiation is chosen to be at 4.65 kWh/m^2/day which is the averaged solar radiation in this particular location.

In this optimal system type graph, the red region represents a diesel Genset, solar PV, and lithium-ion battery system. The green region represents a diesel generator, solar PV, wind turbines, and lithium-ion battery system, while the orange area represents a solar PV and a Li-ion battery system. The blue area represents solar PV, wind generators, and lithium-ion battery system.
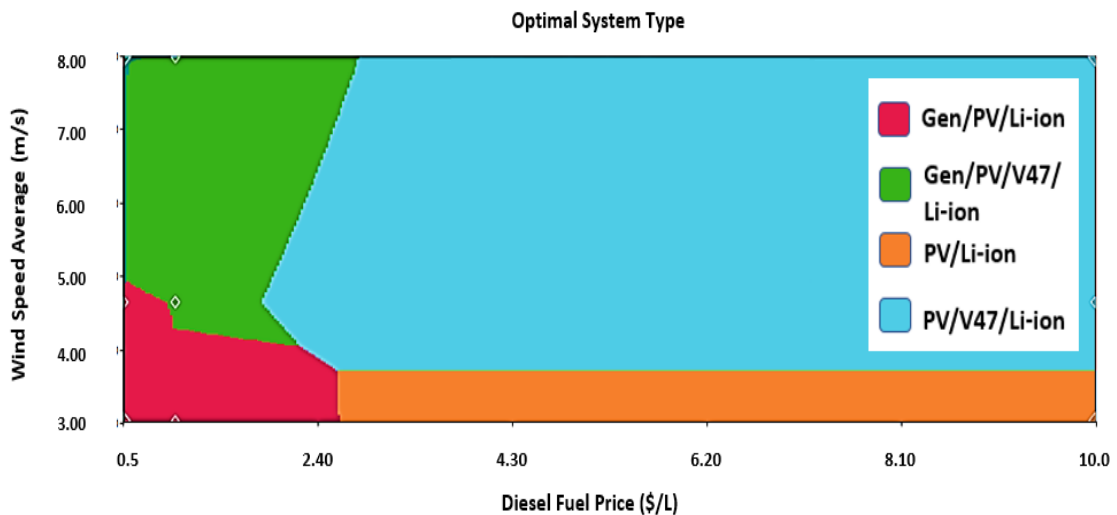

Figure (3.10) Optimal system type graph (islanded mode)

The key findings from this graph are: first, solar PV exists in all optimal system types except in the area at the top left corner, which has very high wind speed. In general, Florida, the sunshine state, has high average solar radiation over the year, which makes solar PV system a suitable choice for residential and commercial-scale systems. Second, lithium-ion battery with 1 MWh capacity and 4 hours storage duration is indispensable in all optimal system types. The reason is that lithium battery has high energy density and relatively long lifetime which makes it an essential component for hybrid renewable systems that experience high intermittency or islanded mode operations. Third, it can be seen that the diesel fuel price has an impact on whether renewable energy sources can be a suitable option for the system. When diesel fuel prices approximately surpassed 2.7 dollars a liter, renewable energy sources plus storage became a more cost-effective option than diesel generators.

In grid-connected mode, a grid block connected to the AC bus was added to the same model. A grid power price and sellback rate sensitivity inputs were included in the previous sensitivity analysis. The grid power price assumed to vary from 0.1 to 1 \$/kWh while the sellback rate is kept fixed at 0.05 \$/kWh. Figure (3.11) shows the optimal system types for grid-connected situation across the considered range of sensitivity inputs where X-axis represent the range of grid power prices in (\$/kWh), and the y-axis represents the range of solar radiation averages in (kWh/m^2/day). Renewable energy penetration is kept at 0% while the wind speed is chosen to be at 4.63 (m/s), which is the averaged wind speed in this particular location. Diesel fuel price was neglected because it did not show any effect on the optimization results.

In this optimal system type graph, shown below, the very tiny red region on the left side of the graph represents a grid only system, which means that all the power generation is coming from the grid and no other sources are used. The green region represents a grid and wind turbines system. The orange area represents a solar PV, and grid system, while the small gold region represents a solar PV, lithium-ion battery, and grid system. The blue area represents solar PV, wind generators, and grid systems.
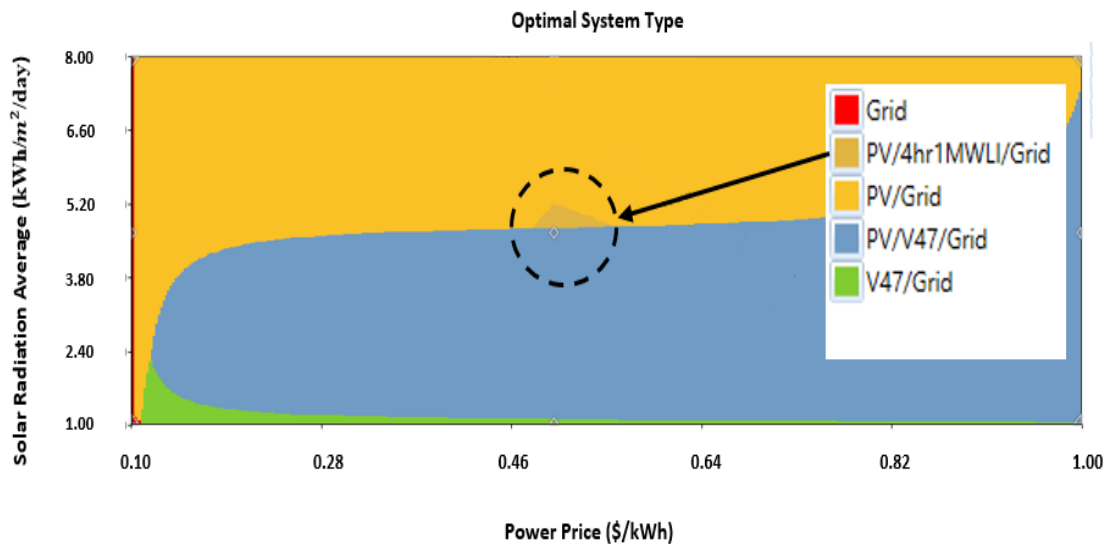
Figure (3.11) Optimal system type graph (grid-connected mode)

The key findings from this figure are: first, the grid only system is the optimal system type, and it appeared in all sensitivity regions. Second, the grid played a significant role as a

storage system for low and high renewable penetration. System; therefore, net metering or selling the surplus power from renewables back to the grid became cheaper than installing a lithium-ion battery system. However, Tables (3.7) and (3.8) illustrate the optimum systems at different sensitivity cases for both islanded and grid-connected modes, respectively. Also, those tables show the optimization results including each component size, systems cost statistics, renewable energy penetration percentages, and total annual fuel usage.

Table (3.7) Optimization results for commercial-scale system (islanded mode)

| Commerical system for Hospital and Large office in Orlando-Florida (islanded mode) | | | | | | | | | | | | | | |
| Sensitivity | | | | Architecture | | | | | Cost | | | | System | |
Renewable Fraction (%)	Diesel Fuel Price ($/L)	Solar Scaled Average (kWh/m²/day)	Wind Scaled Average (m/s)	PV (kW)	Wind turbine (V47-660kW)	Desiel Genset (kW)	4hr-Li-Battery (MWh)	Converter (kW)	NPC ($)	COE ($/kWh)	Operating cost ($/yr)	Initial capital ($)	Renewable Fraction (%)	Total Fuel (L/yr)
0	0.5	1	3	-	-	3.8 K	4	2.36 K	52 M	0.225	3.7 M	4.6 M	0	4.9 M
0	0.5	1	8	-	7	3.8 K	4	3.13 K	34 M	0.147	1.8 M	11.8 M	63.7	1.7 M
0	0.5	8	3	9.20 K	-	3.8 K	10	3.43 K	47 M	0.202	1.0 M	34.6 M	78.8	1.0 M
0	0.5	4.65	4.63	4.06 K	-	3.8 K	4	3.56 K	51 M	0.221	2.7 M	16.7 M	24.0	3.5 M
20	0.5	4.65	4.63	4.03 K	-	3.8 K	4	3.51 K	51 M	0.221	2.7 M	16.6 M	23.8	3.5 M
50	0.5	4.65	4.63	6.02 K	4	3.8 K	6	3.70 K	54 M	0.233	2.1 M	27.5 M	50.1	2.3 M
0	1	1	3	-	-	3.8 K	4	2.35 K	83 M	0.358	6.2 M	4.6 M	0	4.9 M
0	1	4.65	4.63	10.10 K	3	3.8 K	13	3.43 K	65 M	0.279	1.8 M	41.7 M	76.8	1.1 M
50	1	4.65	4.63	10.10 K	3	3.8 K	13	3.43 K	65 M	0.279	1.8 M	41.7 M	76.8	1.1 M
0	10	1	3	66.37 K	22	-	33	3.89 K	266 M	1.180	2.6 M	232.0 M	100	0
50	10	4.65	4.63	13.47 K	3	-	26	3.50 K	67 M	0.295	0.8 M	56.1 M	100	0

Table (3.8) Optimization results for commercial-scale system (Grid-connected mode)

| Commerical system for Hospital and Large office in Orlando-Florida (Grid-connected mode) | | | | | | | | | | | | | | | |
| Sensitivity | | | | | | Architecture | | | | | Cost | | | | System |
Power Price ($/kWh)	Sellback Rate ($/kWh)	Renewable Fraction (%)	Diesel Fuel Price ($/L)	Solar Scaled Average (kWh/m²/day)	Wind Scaled Average (m/s)	PV (kW)	Wind turbine (V47-660kW)	Grid (kW)	Converter (kW)	Dispatch	NPC ($)	COE ($/kWh)	Operating cost ($/yr)	Initial capital ($)	Renewable Fraction (%)
0.1	0.05	0	0.5	1	3	-	-	1,000 K	-	CC	23.3 M	0.1	1.82 M	0	0
0.1	0.05	0	0.5	1	8	-	9	1,000 K	-	CC	15.9 M	0.046	.54 M	9 M	75.7
0.1	0.05	0	0.5	4.65	4.63	-	-	1,000 K	-	CC	23.3 M	0.1	1.82 M	0	0
0.1	0.05	20	0.5	4.65	4.63	2.62 K	-	1,000 K	2.02 K	CC	27.4 M	0.117	1.50 M	8.2 M	20.0
0.1	0.05	50	0.5	4.65	4.63	7.59 K	-	1,000 K	6.56 K	CC	35.3 M	0.130	.89 M	24.0 M	50.1
0.1	0.05	50	1	4.65	4.63	7.59 K	-	1,000 K	6.56 K	CC	35.3 M	0.130	.89 M	24.0 M	50.1
0.1	0.05	50	10	4.65	4.63	7.59 K	-	1,000 K	6.56 K	CC	35.3 M	0.130	.89 M	24.0 M	50.1
0.5	0.05	0	0.5	4.65	4.63	13.25 K	2	1,000 K	8.17 K	LF	47.7 M	0.136	.37 M	42.9 M	69.3
0.5	0.05	50	0.5	4.65	4.63	13.25 K	2	1,000 K	8.17 K	LF	47.7 M	0.136	.37 M	42.9 M	69.3
1	0.05	50	0.5	4.65	4.63	13.63 K	2	1,000 K	8.17 K	CC	48.3 M	0.136	.34 M	44.0 M	69.8

3.4.3   Case 3: Utility-scale system

This case represents a utility-scale system for a community load profile in Orlando-Florida. The total average daily consumption is 715 MWh/day with a 100 MW of peak load. Similar to the previous cases, the main goal of this simulation is to find the optimum mix of energy sources and storage in islanded and grid-connected modes. In islanded mode, the sensitivity analysis has four sensitivity inputs, including diesel fuel price, renewable penetration fraction present, solar radiation, and wind speed. The diesel fuel price is assumed to vary from 1 to 5 US dollars per liter ($/L), and renewable energy penetration is allowed to vary between 0 and 50. Moreover, the solar radiation is assumed to change between 1 and 8 kWh/m^2/day where the averaged global horizontal solar radiation is about 4.65 kWh/m^2/day, while wind speed is allowed to change from 3 to 8 m/s, and the averaged wind speed is 4.63 m/s.

Figure (3.12) shows the optimal system type across the range of sensitivity values in islanded mode. The X-axis represents the range of diesel fuel prices in ($/L), and y-axis represents the range of solar radiation in kWh/m^2/day. HOMER is allowed to choose the most suitable renewable energy penetration which means that the renewable penetration fraction is kept at 0 %. This figure shows the results at 4.63 m/s of wind, which is the averaged wind speed in Orlando-Florida. In this optimal system type graph, the green region represents a diesel Genset, solar PV, (Vestas-82) wind turbines, and lithium-ion battery system. The orange region represents a solar PV, and lithium-ion battery system, while the blue area represents a solar PV, (Vestas-82) wind turbines, and lithium-ion battery system.
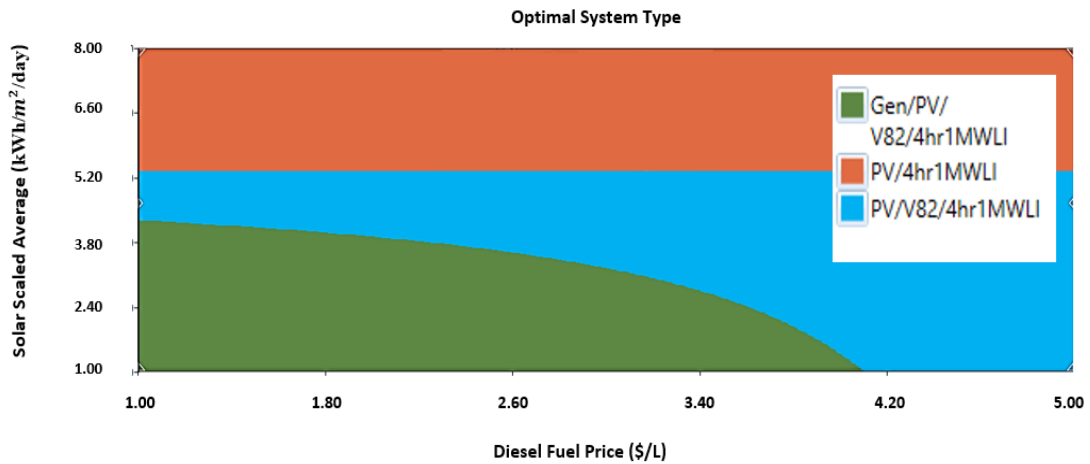
Figure (3.12) Optimal system type graph for the utility-scale system (islanded mode)

In grid-connected mode, the sensitivity analysis includes the grid power price, sellback rate, diesel fuel price, renewable penetration fraction present, solar radiation, and wind speed. The grid power price assumed to vary from 0.1 to 1 \$/kWh, and from 0.01 to 0.1 \$/kWh for the sellback rate while other sensitivity inputs are kept the same as in the islanded case. Figure (3.13) shows the optimal system types for grid-connected situation across the range of sensitivity inputs where X-axis represent the range of grid power prices in (\$/kWh), and y-axis represents the range of wind speed in (m/s). Renewable energy penetration is kept at 0% while the solar radiation is at 4.65 (kWh/m^2/day), which is the averaged solar radiation in this particular location. The blue sky region on the left side of the graph represents a grid only system. The green region represents wind turbines (Vestas-82), and grid system. The red area represents a solar PV, lithium-ion battery, and grid system. The gray region represents a solar PV, and grid system while the large blue region represents solar PV, wind generators, and grid system.
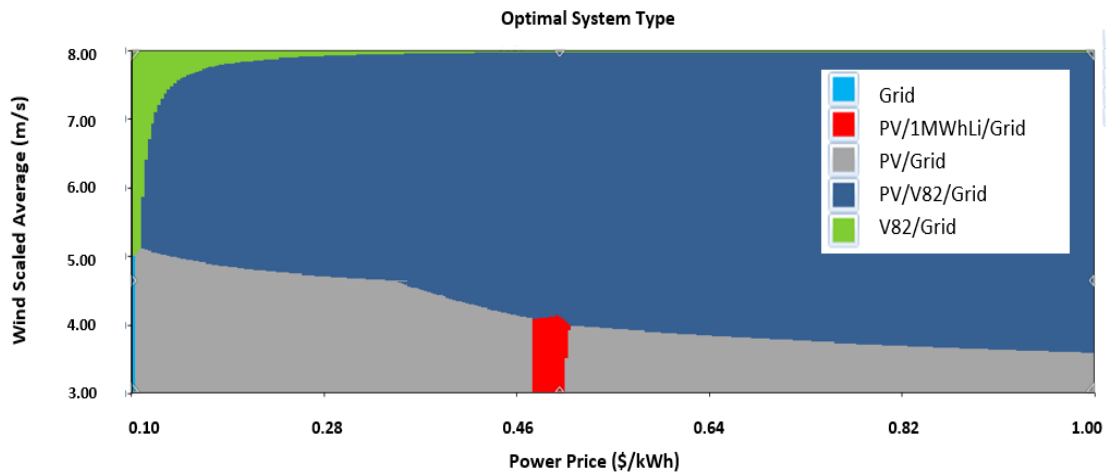
Figure (3.13) Optimal system type graph for a utility-scale system (Grid-connected mode)

Two cases were simulated by HOMER software. The first case is a utility-scale system operating in islanded mode while the second case is in grid-connected mode. In islanded mode, the most outstanding result is the reduction of the Levelized Cost Of Energy (LCOE) to almost 46% of that of diesel-based systems by using hybrid renewable energy and storage system. Table (3.9) shows which technologies and which sizing are economically feasible for each sensitivity cases.

In grid-connected mode, the grid played a significant role as a storage system for either low or high renewable penetration regions, as shown in the optimal system type graph. However, if we consider the grid only system is the base case and compare its economics to the winning renewable system. The winning system is defined as the lowest net present cost system (NPC). The optimization results show that the winning system has a grid combined with 705 vestas wind turbines (Vestas-82) at 0.1 $/kWh sellback rate, 0% renewable fraction, 1 $/L diesel fuel price, and averaged wind speed and solar radiation. Figure (3.14) demonstrates how the hybrid system saves money over the project lifetime as compared to the base cases (grid only system). The gray line represents the base case, while the blue line represents the hybrid system.
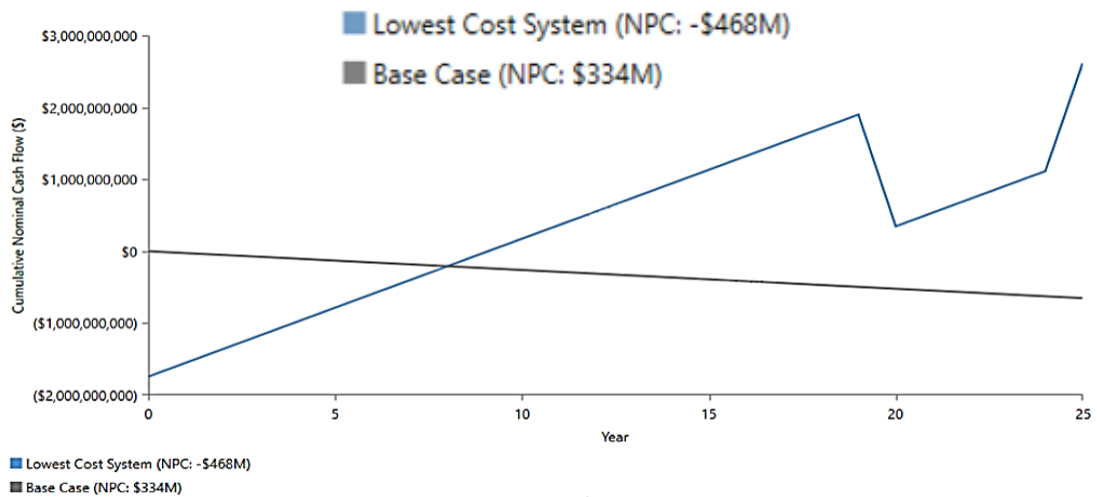
Figure (3.14) Hybrid system's overall savings

This figure compares between the base case and the winning case, and it also shows the initial capital cost for both systems and the year-over-year prices. When those lines cross, that is the expected payback time which is, in this case, eight years. In addition, the hybrid system shows significantly high overall savings by the end of the project lifetime compared to the grid only case.

The optimization results, shown in Tables (3.9) and (3.10), illustrate the optimum systems at different sensitivity cases for both islanded and grid-connected modes, respectively. Those results include the optimal component sizes, systems cost statistics, renewable energy penetration percentages, and total annual fuel usage.

Table (3.9) Optimization results for utility-scale system (islanded mode)

Utility-scale systems in Orlando-Florida (Islanded mode)														
Sensitivity				Architecture					Cost				System	
Renewable Fraction (%)	Diesel Fuel Price ($/L)	Solar Scaled Average (kWh/m²/day)	Wind Scaled Average (m/s)	PV (kW)	Wind turbine (V82-1.65MW)	Desiel Genset (kW)	4hr-Li-Battery (MWh)	Converter (kW)	NPC ($)	COE ($)	Operating cost ($/yr)	Initial capital ($)	Renewable Fraction (%)	Total Fuel (L/yr)
0	1	1	3	-	-	120 K	73	80.2 K	1,340 M	0.401	95.3 M	121 M	0	74.6 M
0	1	4.65	4.63	243 K	3	-	284	81.5 K	598 M	0.185	8.5 M	490 M	100	0
20	1	4.65	4.63	243 K	3	-	284	81.5 K	598 M	0.185	8.5 M	490 M	100	0
50	1	4.65	4.63	243 K	3	-	284	81.5 K	598 M	0.185	8.5 M	490 M	100	0
20	5	4.65	4.63	243 K	3	-	284	81.5 K	598 M	0.185	8.5 M	490 M	100	0
50	5	4.65	4.63	243 K	3	-	284	81.5 K	598 M	0.185	8.5 M	490 M	100	0

Table (3.10) Optimization results for utility-scale system (Grid-connected mode)

Utility-scale systems in Orlando-Florida (Grid-connected mode)																
Sensitivity					Architecture						Cost				System
Sellback Rate ($/kWh)	Renewable Fraction (%)	Diesel Fuel Price ($/L)	Solar Scaled Average (kWh/m²/day)	Wind Scaled Average (m/s)	PV (kW)	Wind turbine (V82-1.65MW)	4hr-Li-Battery (MWh)	Grid (kW)	Converter (kW)	Dispatch	NPC ($)	COE ($)	Operating cost ($/yr)	Initial capital ($)	Renewable Fraction (%)
0.01	0	1	1	3	-	-	-	1,000 K	-	CC	334 M	0.1	26 M	0	0
0.01	20	1	4.65	4.63	-	21	-	1,000 K	-	CC	317 M	0.092	21 M	52 M	28.7
0.01	30	1	4.65	4.63	2.9 K	21	1	1,000 K	1.65 K	LF	317 M	0.092	20 M	57 M	30.2
0.01	50	1	4.65	4.63	31.0 K	27	10	1,000 K	15.93 K	LF	327 M	0.092	16 M	117 M	50.1
0.05	0	1	4.65	4.63	-	31	-	1,000 K	-	CC	310 M	0.085	18 M	77 M	40.0
0.05	50	1	4.65	4.63	-	43	-	1,000 K	-	CC	312 M	0.079	16 M	106 M	50.8
0.1	0	1	4.65	4.63	-	705	-	1,000 K	-	CC	-468 M	-0.014	-173 M	1,745 M	97.4
0.1	50	1	4.65	4.63	-	705	-	1,000 K	-	CC	-468 M	-0.014	-173 M	1,745 M	97.4
0.01	0	5	4.65	4.63	-	21	-	1,000 K	-	CC	317 M	0.092	21 M	52 M	28.7
0.01	50	5	4.65	4.63	31.0 K	27	10	1,000 K	15.93 K	LF	327 M	0.092	16 M	117 M	50.1
0.01	50	5	4.65	8	-	29	7	1,000 K	6.71 K	LF	246 M	0.064	13 M	77 M	62.8
0.05	50	5	4.65	4.63	-	43	-	1,000 K	-	CC	312 M	0.079	16 M	106 M	50.8
0.05	50	5	4.65	8	-	632	-	1,000 K	-	CC	-284 M	-0.005	-145 M	1,564 M	99.1

Chapter 4: Conclusions and Future Work

4.1 Conclusions

This thesis focused on evaluating hybrid energy storage options for traction and renewable energy applications. Energy storage technologies have a wide range of characteristics and specifications. Like any other technology, each type of energy storage has its advantages and disadvantages; therefore, a comprehensive and a thorough literature review of the various energy storage options was presented to choose the optimal solution based on the key performance objectives and various aspects of those technologies. Also, a comparison table of a total of 19 energy storage systems based on 20 technical, economical, and operational characteristics has been presented. In addition, this literature review provides extensive background material for people who are interested in learning more about the different types of energy storage systems that exist. In addition, by having this information together, it will help engineers and researchers decide which energy storage systems to choose for their applications.

A hybrid electric vehicle is one key application space driving breakthroughs in energy storage technologies; consequently, in the second Chapter, a series-parallel hybrid electric vehicle was modeled and simulated by using MATLAB-SIMULINK to show the benefits of integrating a battery-ultracapacitor hybrid energy storage system in traction applications. The results have revealed the advantages of utilizing hybrid energy storage system (battery-ultracapacitor) in reducing the battery's voltage and current fluctuations, which would prolong the lifetime of the storage system. Based on the fuel consumption results, the active parallel battery/UC architecture with two converters showed an outstanding improvement as compared to the battery alone architecture.

The second key application space is renewable energy especially wind and solar. Due to the intermittent nature of renewable energy sources, energy storage is a must to achieve the required power quality. Therefore, in Chapter three, different cases of hybrid renewable energy (wind and solar) combined with energy storage systems were carried out using Hybrid

Optimization Model for Electric Renewables (HOMER) software to investigate the economic and sizing aspects. The concept of using energy storage systems combined with wind and solar systems in islanded mode has the potential to reduce the cost of the overall system in residential and commercial scales. In the utility scale systems, the grid played a significant role as a storage system for both low and high renewable penetration in grid connected-mode; therefore, net metering or selling the surplus power from renewable sources back to the grid became more economical than installing a lithium-ion battery system, at the current price point for lithium ion batteries.

4.2 Future Scope of Work

Based on the work that has been done in this thesis, the following research areas are recommended for future work:

1. Identifying the best energy storage systems for aerospace applications and modeling them.

2. Looking at different control strategies for the series-parallel hybrid electric vehicle with two energy storage devices.

3. Investigating the effects of hybrid energy storage on medium and heavy-duty electrified vehicles.

4. Investigating additional combinations of energy storage system for stationary applications.

Bibliography

1. Energy Agency, International. *Scaling-up the Transition to Electric Mobility M a y 2 0 1 9.*

2. US Department of Energy. *Alternative Fuels Data Center: How Do All-Electric Cars Work?* https://afdc.energy.gov/vehicles/how-do-all-electric-cars-work

3. Nadeem, Furquan, et al. "Comparative Review of Energy Storage Systems, Their Roles, and Impacts on Future Power Systems." *IEEE Access*, 2019, doi:10.1109/ACCESS.2018.2888497.

4. Politechnika Warszawska. Instytut Techniki Cieplnej., Pavlos, and Andreas Poullikkas. "A Comparative Review of Electrical Energy Storage Systems for Better Sustainability." *Journal of Power Technologies*, 2017.

5. Letcher, Trevor M. "Storing Energy, with Special Reference to Renewable Energy Sources." *Chemistry International*, vol. 38, no. 6, Elsevier Inc., 2016, doi:10.1515/ci-2016-0627.

6. ARES Nevada. *Advanced Rail Energy Storage*. 2019, p. 27, http://www.aresnorthamerica.com/about-ares-north-america.

7. Mallick, Kaustav, et al. *Modern Mechanical Energy Storage Systems and Technologies*. http://www.ijert.org.

8. Faisal, Mohammad, et al. "Review of Energy Storage System Technologies in Microgrid Applications: Issues and Challenges." *IEEE Access*, 2018, doi:10.1109/ACCESS.2018.2841407.

9. Plett, Gregory L. *Battery Management Systems. Volume 1 : Battery Modeling*.

10. Saidani, Fida, et al. "Lithium-Ion Battery Models: A Comparative Study and a Model-Based Powerline Communication." *Advances in Radio Science*, vol. 15, Copernicus GmbH, Sept. 2017, pp. 83–91, doi:10.5194/ars-15-83-2017.

11. Hariprakash, B., et al. "Comparative Study of Lead-Acid Batteries for Photovoltaic Stand-Alone Lighting Systems." *Journal of Applied Electrochemistry*, 2008, doi:10.1007/s10800-007-9403-4.

12. Wen, Zhaoyin, et al. "Research on Sodium Sulfur Battery for Energy Storage." *Solid State Ionics*, 2008, doi:10.1016/j.ssi.2008.01.070.

13. Bank, Asian Development. *Handbook on Battery Energy Storage System*. no. December, 2018.

14. Yang, Fengchang, et al. "Sodium–Sulfur Flow Battery for Low-Cost Electrical Storage." *Advanced Energy Materials*, 2018, doi:10.1002/aenm.201701991.

15. Rijssenbeek, Job, et al. "Sodium-Metal Halide Batteries in Diesel-Battery Hybrid Telecom Applications." *INTELEC, International Telecommunications Energy Conference (Proceedings)*, 2011, doi:10.1109/INTLEC.2011.6099819.

16. Henriksen, G. L., and D. R. Vissers. "Lithium-Aluminum/Iron Sulfide Batteries." *Journal of Power Sources*, 1994, doi:10.1016/0378-7753(94)01965-7.

17. Au, Climatecouncil Org. *FULLY CHARGED: RENEWABLES AND STORAGE POWERING AUSTRALIA Thank You for Supporting the Climate Council*. 2018.

18. Luo, Xing, et al. "Http://Wrap.Warwick.Ac.Uk Overview of Current Development in Electrical Energy Storage Technologies and the Application Potential in Power System Operation Q." *Applied Energy*, vol. 137, 2015, pp. 511–36, doi:10.1016/j.apenergy.2014.09.081.

19. EASE/EERA. *DRAFT-FOR PUBLIC CONSULTATION 2 EASE/EERA European Energy Storage Technology Development Roadmap The European Association for Storage Of*. www.eera-set.eu.

20. Cambridge, University of. *Zinc/Carbon Batteries*. 2018, https://www.doitpoms.ac.uk/tlplib/batteries/batteries_zn_c.php.

21. EPEC Engineered Technologies. *Battery Comparison of Energy Density - Cylindrical and Prismatic Cells*. https://www.epectec.com/batteries/cell-comparison.html. Accessed 10 Oct. 2019.

22. Schrøder, Allan, and Aksel Hauge. *General Rights Thermo-Mechanical Electricity Storage*.

23. Farhadi, Mustafa, and Osama Mohammed. "Energy Storage Technologies for High-Power Applications." *IEEE Transactions on Industry Applications*, vol. 52, no. 3, IEEE, 2016, pp. 1953–62, doi:10.1109/TIA.2015.2511096.

24. Ogunniyi, E. O., and H. C. V. Z. Pienaar. "Overview of Battery Energy Storage System Advancement for Renewable (Photovoltaic) Energy Applications." *Proceedings of the 25th Conference on the Domestic Use of Energy, DUE 2017*, Cape Peninsula University of Technology, 2017, pp. 233–39, doi:10.23919/DUE.2017.7931849.

25. Söderström, Felix. *Energy Storage Technology Comparison From a Swedish Perspective*. 2016, http://www.diva-portal.org/smash/record.jsf?pid=diva2%3A953027.

26. Hesaraki, Arefeh, et al. "Seasonal Thermal Energy Storage with Heat Pumps and Low Temperatures in Building Projects-A Comparative Review." *Renewable and Sustainable Energy Reviews*, vol. 43, 2014, pp. 1199–213, doi:10.1016/j.rser.2014.12.002.

27. Kollmeyer, Phillip J. *Development and Implementation of a Battery-Electric Light-Duty Class 2a Truck Including Hybrid Energy Storage*. 2015, p. 475.

28. *The History of the Electric Car | Department of Energy*. https://www.energy.gov/articles/history-electric-car.

29. Woodward, Mike. *New Market. New Entrants. New Challenges. Battery Electric Vehicles Contents*. 2017.

30. Wong, J. Y. (Jo Yung). *Theory of Ground Vehicles*. John Wiley, 2001.

31. Enang, Wisdom, et al. "Modelling and Heuristic Control of a Parallel Hybrid Electric Vehicle." *Proceedings of the Institution of Mechanical Engineers, Part D: Journal of Automobile Engineering*, vol. 229, no. 11, SAGE Publications Ltd, 2015, pp. 1494–513, doi:10.1177/0954407014565633.

32. *Advantages and Disadvantages of Electric Cars - Conserve Energy Future*. https://www.conserve-energy-future.com/advantages-and-disadvantages-of-electric-cars.php.

33. Singh, Krishna Veer, et al. "A Comprehensive Review on Hybrid Electric Vehicles: Architectures and Components." *Journal of Modern Transportation*, vol. 27, no. 2, Springer Science and Business Media LLC, June 2019, pp. 77–107, doi:10.1007/s40534-019-0184-3.

34. Groen, Benjamin Carson. *Investigation of DC Motors for Electric and Hybrid Electric Motor Vehicle Applications Using an Infinitely Variable Transmission*. 2011.

35. Ganji, Behnam, et al. "Drive Cycle Analysis of the Performance of Hybrid Electric Vehicles." *Lecture Notes in Computer Science (Including Subseries Lecture Notes in Artificial Intelligence and Lecture Notes in Bioinformatics)*, vol. 6328 LNCS, no. PART 1, 2010, pp. 434–44, doi:10.1007/978-3-642-15621-2_48.

36. Miller, John M. *Annual Progress Report for the Power Electronics and Electric Motors Program*. 2013.

37. Hannan, M. A., et al. "Review of Energy Storage Systems for Electric Vehicle Applications: Issues and Challenges." *Renewable and Sustainable Energy Reviews*, 2017, doi:10.1016/j.rser.2016.11.171.

38. Burke, Andrew, and Hengbing Zhao. "Applications of Supercapacitors in Electric and Hybrid Vehicles Applications UCD-ITS-RR-15-09." *5th European Symposium on Supercapacitor and Hybrid Solutions*, no. April, 2015.

39. Xiang, Changle, et al. "A New Topology and Control Strategy for a Hybrid Battery-Ultracapacitor Energy Storage System." *Energies*, vol. 7, no. 5, 2014, pp. 2874–96, doi:10.3390/en7052874.

40. Plett, Gregory L. *Battery Management Systems. Volume II, Equivalent-Circuit Methods*. ArtTech House, 2016.

41. Mu, Dazhong, et al. "Online Semiparametric Identification of Lithium-Ion Batteries Using the Wavelet-Based Partially Linear Battery Model." *Energies*, vol. 6, no. 5, MDPI AG, 2013, pp. 2583–604, doi:10.3390/en6052583.

42. Stiene, Tyler. *Analysis of a Hybrid Energy Storage System and Electrified Turbocharger in a Performance Vehicle*. McMaster University, 2016.

43. Hannan, Mahammad A., et al. "State-of-the-Art and Energy Management System of Lithium-Ion Batteries in Electric Vehicle Applications: Issues and Recommendations." *IEEE Access*, vol. 6, IEEE, 2018, pp. 19362–78, doi:10.1109/ACCESS.2018.2817655.

44. Ci, Song, et al. "Reconfigurable Battery Techniques and Systems: A Survey." *IEEE Access*, vol. 4, IEEE, 2016, pp. 1175–89, doi:10.1109/ACCESS.2016.2545338.

45. Xiong, Rui, et al. "Critical Review on the Battery State of Charge Estimation Methods for Electric Vehicles." *IEEE Access*, vol. 6, IEEE, 2017, pp. 1832–43, doi:10.1109/ACCESS.2017.2780258.

46. Huang, Yu Pei, and Peng Fei Tsai. "Improving the Output Power Stability of a High Concentration Photovoltaic System with Supercapacitors: A Preliminary Evaluation." *Mathematical Problems in Engineering*, vol. 2015, Hindawi Limited, 2015, doi:10.1155/2015/127949.

47. Tao, Yi, and Zhimei Li. "Study on Modeling and Application of Ultracapacitor." *Proceedings - 2014 IEEE Workshop on Advanced Research and Technology in Industry Applications, WARTIA 2014*, Institute of Electrical and Electronics Engineers Inc., 2014, pp. 999–1002, doi:10.1109/WARTIA.2014.6976443.

48. Yang, Fuyuan, et al. "Characterization, Analysis and Modeling of an Ultracapacitor." *World Electric Vehicle Journal*, vol. 4, no. 1, 2011, pp. 358–69.

49. Devillers, Nathalie, et al. "Review of Characterization Methods for Supercapacitor Modelling." *Journal of Power Sources*, vol. 246, Jan. 2014, pp. 596–608, doi:10.1016/j.jpowsour.2013.07.116.

50. Zhang, Lei, et al. "A Review of Supercapacitor Modeling, Estimation, and Applications: A Control/Management Perspective." *Renewable and Sustainable Energy Reviews*, vol. 81, Elsevier Ltd, 1 Jan. 2018, pp. 1868–78, doi:10.1016/j.rser.2017.05.283.

51. Chemali, Ephrem, Matthias Preindl, et al. "Electrochemical and Electrostatic Energy Storage and Management Systems for Electric Drive Vehicles: State-of-the-Art Review and Future Trends." *IEEE Journal of Emerging and Selected Topics in Power Electronics*, vol. 4, no. 3, IEEE, 2016, pp. 1117–34, doi:10.1109/JESTPE.2016.2566583.

52. Stg, Wenlong, Chean Hung Lai, Shung Hui Wallace Wong, et al. "Battery-Supercapacitor Hybrid Energy Storage System in Standalone DC Microgrids: Areview." *IET Renewable Power Generation*, vol. 11, no. 4, Institution of Engineering and Technology, 15 Mar. 2017, pp. 461–69, doi:10.1049/iet-rpg.2016.0500.

53. Kouchachvili, Lia, et al. "Hybrid Battery/Supercapacitor Energy Storage System for the Electric Vehicles." *Journal of Power Sources*, vol. 374, Elsevier B.V., 15 Jan. 2018, pp. 237–48, doi:10.1016/j.jpowsour.2017.11.040.

54. Mathworks. *Hybrid-Electric Vehicle Model in Simulink - File Exchange "Steve Miller"- MATLAB Central.* https://www.mathworks.com/matlabcentral/fileexchange/28441-hybrid-electric-vehicle-model-in-simulink. Accessed 24 Sept. 2019.

55. Nicolas, Romain. *The Different Driving Cycles*. 2013, http://www.car-engineer.com/the-different-driving-cycles/#prettyPhoto.

56. NREL. *ADVISOR Documentation*. http://adv-vehicle-sim.sourceforge.net/

57. Camara, Mamadou Baïlo, et al. "Design and New Control of DC/DC Converters to Share Energy between Supercapacitors and Batteries in Hybrid Vehicles." *IEEE Transactions on Vehicular Technology*, vol. 57, no. 5, 2008, pp. 2721–35, doi:10.1109/TVT.2008.915491.

58. Chemali, Ephrem, Lucas McCurlie, et al. "Minimizing Battery Wear in a Hybrid Energy Storage System Using a Linear Quadratic Regulator." *IECON 2015 - 41st Annual Conference of the IEEE Industrial Electronics Society*, Institute of Electrical and Electronics Engineers Inc., 2015, pp. 3265–70, doi:10.1109/IECON.2015.7392603.

59. Santucci, Alberto, et al. "Power Split Strategies for Hybrid Energy Storage Systems for Vehicular Applications." *Journal of Power Sources*, vol. 258, Elsevier, July 2014, pp. 395–407, doi:10.1016/j.jpowsour.2014.01.118.

60. Mackenzi, Wood. "Global Energy Storage Markets Will Grow 13-Fold from 2018 to 2024 to Reach 158 Gigawatt-Hours and Billion in Investment, Wood Mackenzie Power & Renewables Reports." *Power & Renewables Reports*, 2019, https://www.greentechmedia.com/articles/read/global-energy-storage-to-hit-158-gigawatt-hours-by-2024-with-u-s-and-china.

61. *5 Predictions for the Global Energy Storage Market in 2019 | Greentech Media*. https://www.greentechmedia.com/articles/read/five-predictions-for-the-global-energy-storage-market-in-2019?utm_medium=email&utm_source=Daily&utm_campaign=GTMDaily#gs.UEZE4hzz.

62. Carlos, Antonio, and Zambroni De Souza. "Microgrids Design and Implementation." *Microgrids Design and Implementation*, 2019, doi:10.1007/978-3-319-98687-6.

63. Contracting, Totem. *Microgrids | Totem Contracting*. https://www.totemcontracting.com/service/microgrids/.

64. Hoffman, M. G., et al. *Analysis Tools for Sizing and Placement of Energy Storage in Grid Applications A Literature Review*. 2010, http://www.ntis.gov/ordering.htm.

65. HOMER (The Hybrid Optimization Model for Electric Renewables). Retrieved from http:// www.homerenergy.com/

66. Administration, Energy Information. *Electric Sales, Revenue, and Average Price - Energy Information Administration*. 2019, https://www.eia.gov/electricity/sales_revenue_price/.

67. Lazard. *L a z a r d ' s l e v e l i z e d c o s t o f e n e r g y a n a Ly s i s*. 2019, https://www.lazard.com/media/451086/lazards-levelized-cost-of-energy-version-130-vf.pdf.

68. "L a z a r d ' s l e v e l i z e d c o s t o f e n e r g y a n a Ly s i s — v e r s i o n 1 2 . 0." *Lazard*, no. 12, 2018, pp. 0–19, https://www.lazard.com/media/450784/lazards-levelized-cost-of-energy-version-120-vfinal.pdf.

69. Lazard. "Levelized Cost Of Storage." *JLTA Journal*, vol. 21, no. 0, 2018, p. 0, doi:10.20622/jltajournal.21.0_0.

70. Adib, Andrew, and Rached Dhaouadi. "Modeling and Analysis of a Regenerative Braking System with a Battery-Supercapacitor Energy Storage." *2017 7th International Conference on Modeling, Simulation, and Applied Optimization, ICMSAO 2017*, Institute of Electrical and Electronics Engineers Inc., 2017, doi:10.1109/ICMSAO.2017.7934897.

71. *Battery Comparison of Energy Density - Cylindrical and Prismatic Cells*. https://www.epectec.com/batteries/cell-comparison.html.

72. Boicea, Valentin A. "Energy Storage Technologies: The Past and the Present." *Proceedings of the IEEE*, vol. 102, no. 11, IEEE, 2014, pp. 1777–94, doi:10.1109/JPROC.2014.2359545.

73. Brekken, Ted K. A., et al. "Optimal Energy Storage Sizing and Control for Wind Power Applications." *IEEE Transactions on Sustainable Energy*, vol. 2, no. 1, Jan. 2011, pp. 69–77, doi:10.1109/TSTE.2010.2066294.

74. Chen, S. X., et al. "Sizing of Energy Storage for Microgrids." *IEEE Transactions on Smart Grid*, vol. 3, no. 1, Mar. 2012, pp. 142–51, doi:10.1109/TSG.2011.2160745.

75. *Microgrids / Totem Contracting*. https://www.totemcontracting.com/service/microgrids/.

76. Das, Choton K., et al. "Overview of Energy Storage Systems in Distribution Networks: Placement, Sizing, Operation, and Power Quality." *Renewable and Sustainable Energy Reviews*, vol. 91, Elsevier Ltd, 1 Aug. 2018, pp. 1205–30, doi:10.1016/j.rser.2018.03.068.

77. *Developing HEV Control Systems Video - MATLAB & Simulink*. https://www.mathworks.com/videos/developing-hev-control-systems-1562928642827.html.

78. Eldeeb, Hassan H., et al. "Hybrid Energy Storage Sizing and Power Splitting Optimization for Plug-In Electric Vehicles." *IEEE Transactions on Industry Applications*, vol. 55, no. 3, Institute of Electrical and Electronics Engineers Inc., May 2019, pp. 2252–62, doi:10.1109/TIA.2019.2898839.

79. *Electric Sales, Revenue, and Average Price - Energy Information Administration*. https://www.eia.gov/electricity/sales_revenue_price/.

80. https://www.eia.gov/electricity/sales_revenue_price/.

81. *Energy Storage*. https://www.iea.org/tcep/energyintegration/energystorage/.

82. Escovale Inc. *GBES-Ground-Breaking Energy Storage Introduction (GBES-01)*. www.escovale.com

83. *Getting the Most out of Your HOMER Pro Trial - YouTube*. https://www.youtube.com/watch?v=8uJLnNKsogg&t=614s.

84. Gopikrishnan, M. "Battery/Ultra Capacitor Hybrid Energy Storage System for Electric, Hybrid and Plug-in Hybrid Electric Vehicles." *Middle-East Journal of Scientific Research*, vol. 20, no. 9, 2014, pp. 1122–26, doi:10.5829/idosi.mejsr.2014.20.09.114067.

85. Jing, Wenlong, Chean Hung Lai, Shung Hui, et al. *IET Renewable Power Generation Battery-Supercapacitor Hybrid Energy Storage System in Standalone DC Microgrids: Areview*. 2016, doi:10.1049/iet-rpg.2016.0500.

86. Khaki, Bahman, and Pritam Das. *Sizing and Placement of Battery Energy Storage Systems and Wind Turbines by Minimizing Costs and System Losses*.

87. Krupke, Christopher, et al. "Modeling and Experimental Study of a Wind Turbine System in Hybrid Connection with Compressed Air Energy Storage." *IEEE Transactions on Energy Conversion*, vol. 32, no. 1, IEEE, 2017, pp. 137–45, doi:10.1109/TEC.2016.2594285.

88. Liu, Yi, et al. "Sizing a Hybrid Energy Storage System for Maintaining Power Balance of an Isolated System with High Penetration of Wind Generation." *IEEE Transactions on Power Systems*, vol. 31, no. 4, Institute of Electrical and Electronics Engineers Inc., July 2016, pp. 3267–75, doi:10.1109/TPWRS.2015.2482983.

89. Mathwork. *Creating HEV Plant Models Video - MATLAB & Simulink*. https://www.mathworks.com/videos/creating-hev-plant-models-1562933346702.html.

90. *Developing HEV Control Systems Video - MATLAB & Simulink*. https://www.mathworks.com/videos/developing-hev-control-systems-1562928642827.html.

91. *Modeling HEVs Using Simscape - Video - MATLAB & Simulink*. https://www.mathworks.com/videos/modeling-hevs-using-simscape-89115.html.

92. Mukoyama, S., et al. "Load Test of Superconducting Magnetic Bearing for MW-Class Flywheel Energy Storage System." *Journal of Physics: Conference Series*, vol. 871, no. 1, IEEE, 2017, pp. 1–4, doi:10.1088/1742-6596/871/1/012090.

93. Sufyan, M., et al. "Sizing and Applications of Battery Energy Storage Technologies in Smart Grid System: A Review." *Journal of Renewable and Sustainable Energy*, vol. 11, no. 1, American Institute of Physics Inc., Jan. 2019, doi:10.1063/1.5063866.

94. Tan, Boon Kai, et al. "Design of a Battery-Ultracapacitor Hybrid Energy Storage System with Power Flow Control for an Electric Vehicle." *International Journal of Power Electronics and Drive Systems (IJPEDS)*, vol. 9, no. 1, Mar. 2018, p. 286, doi:10.11591/ijpeds.v9.i1.pp286-296.

95. Thomas, John, et al. "INTRODUCTION Fuel Consumption Sensitivity of Conventional and Hybrid Electric Light-Duty Gasoline Vehicles to Driving Style." *J. Fuels Lubr*, vol. 10, no. 3, 2017, p. 2017, doi:10.4271/2017-01-9379.

96. Torres, Jorge, et al. "Fast Energy Storage Systems Comparison in Terms of Energy Efficiency for a Specific Application." *IEEE Access*, 2018, doi:10.1109/ACCESS.2018.2854915.

97. *Tour of HOMER Pro - YouTube*. https://www.youtube.com/watch?v=gTBwK8FCJ9o&t=1720s. Accessed 24 Nov. 2019.

98. *Project Profile_ High-Temperature Thermochemical Storage with Redox-Stable Perovskites for Concentrating Solar Power _ Department of Energy*.

https://www.energy.gov/eere/solar/project-profile-high-temperature-thermochemical-storage-redox-stable-perovskites.

99. US EPA, OAR. *Sources of Greenhouse Gas Emissions*. 2019.

100.   Wagner, Léonard. *Zinc-Carbon Battery - an Overview | ScienceDirect Topics*. 2014, https://www.sciencedirect.com/topics/engineering/zinc-carbon-battery.

101.   Zhang, Chunjiang, et al. "A Control Strategy for Battery-Ultracapacitor Hybrid Energy Storage System." *Diangong Jishu Xuebao/Transactions of China Electrotechnical Society*, vol. 29, no. 4, Chinese Machine Press, 2014, pp. 334–40, doi:10.1109/APEC.2009.4802757.

102.   Zhao, H., et al. "Optimal Siting and Sizing of Energy Storage System for Power Systems with Large-Scale Wind Power Integration." *Citation*, APA, 2015, doi:10.1109/PTC.2015.7232615.

Appendix

This appendix is designed as a quick reference for Hybrid Electric Vehicle (HEV) model and simulation, which contains screenshots from MATLAB-Simulink. It illustrates the inner blocks that are used in each sub-system.

Overview of the HEV modeling:

In this model, a hybrid electric vehicle with a series parallel architecture will be simulated by using MATLAB-SIMULINK (2019a) software. This model, which is shown in the next figure, consists of a control system, mechanical system, and an electrical system.
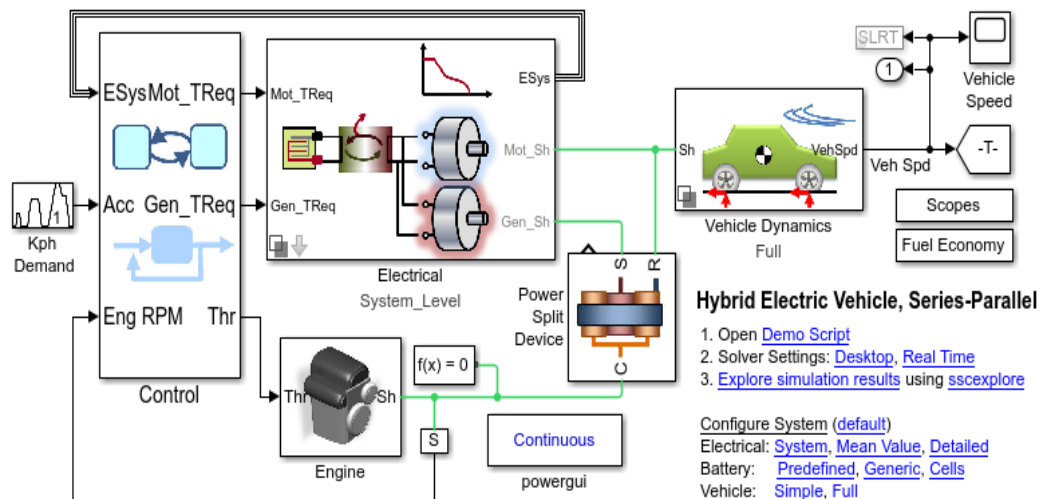
Overall System Requirements

The following requirements apply to the HEV model:

Dimensions:

1.	Curb Weight:	1325 kg
2.	Length	4450 mm
3.	Width	1725 mm
4.	Height	1490 mm

Performance

1.	Total Range	870 km
2.	Electric Range	18 km

Engine System Requirements

The following requirements apply to the functionality of this module.

ICE

3. Power   57 kW @5000 RPM
4. Min Speed   1000 rpm
5. Max Speed   4500 rpm
6. Torque   115 Nm @ 4200 RPM

Fuel Consumption

The following requirements apply to the fuel consumption:

Regular Gas

7. City   51 MPG
8. Highway   49 MPG
9. Combined   50 MPG

Elec + Gas
1. Combined   95 MPG - e

Speed Controller Module Requirements

The following requirements apply to the Speed Controller module.

2. The controller module will implement at a minimum proportional and
    integral control.

3. Upon a change of angle, the system must be within 5% of the final
    value within 0.1 seconds (Settling Time).

4. Upon a change of 10% the system must achieve 10% of the final value
    within 0.7 seconds.

Current Controller Module Requirements

The following requirements apply to the Current Controller module.

5. The current must remain within 1% of the command value.

6. The current may not exceed XXX amperes.

Electrical system:

The electrical system has a motor, generator, DC-DC converter, and a battery models as shown in the figure below.
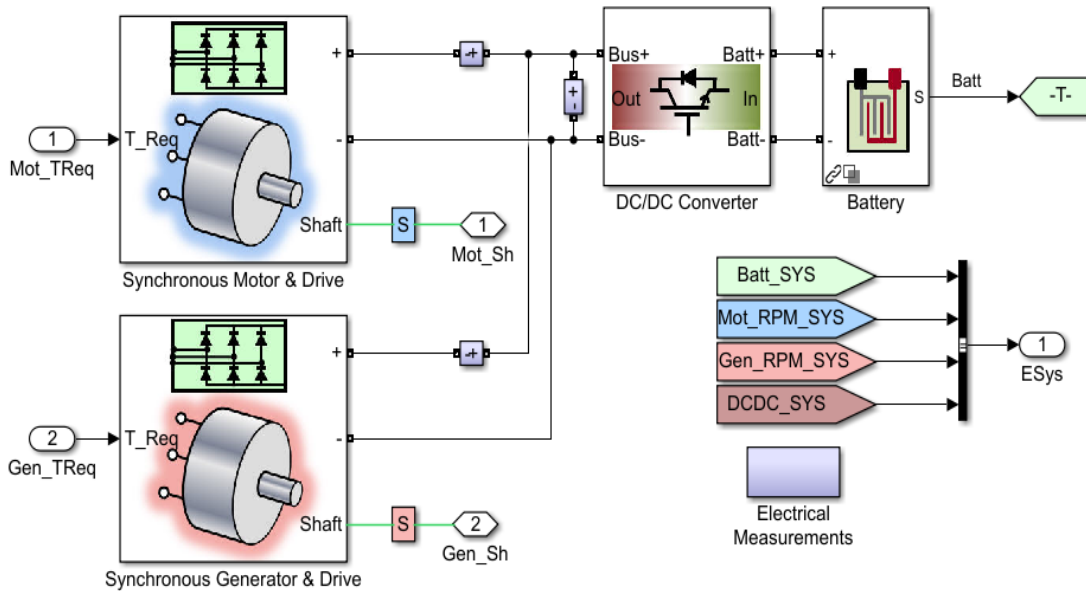
Battery model:

In the battery system block, you have the option of using predefined, generic, and custom models depending on which portion of the system you are focusing on. These battery models are shown bellow.
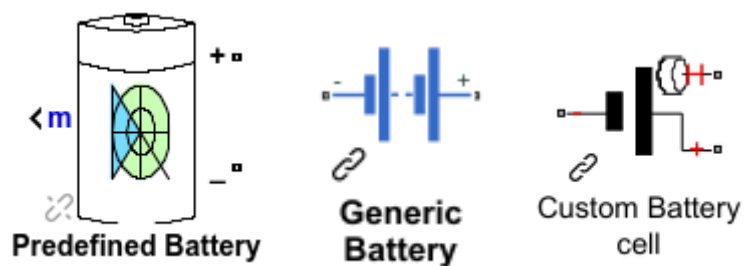
Predefined battery model:

The next figures show how the predefined battery block is used in our hybrid electric vehicle system model.
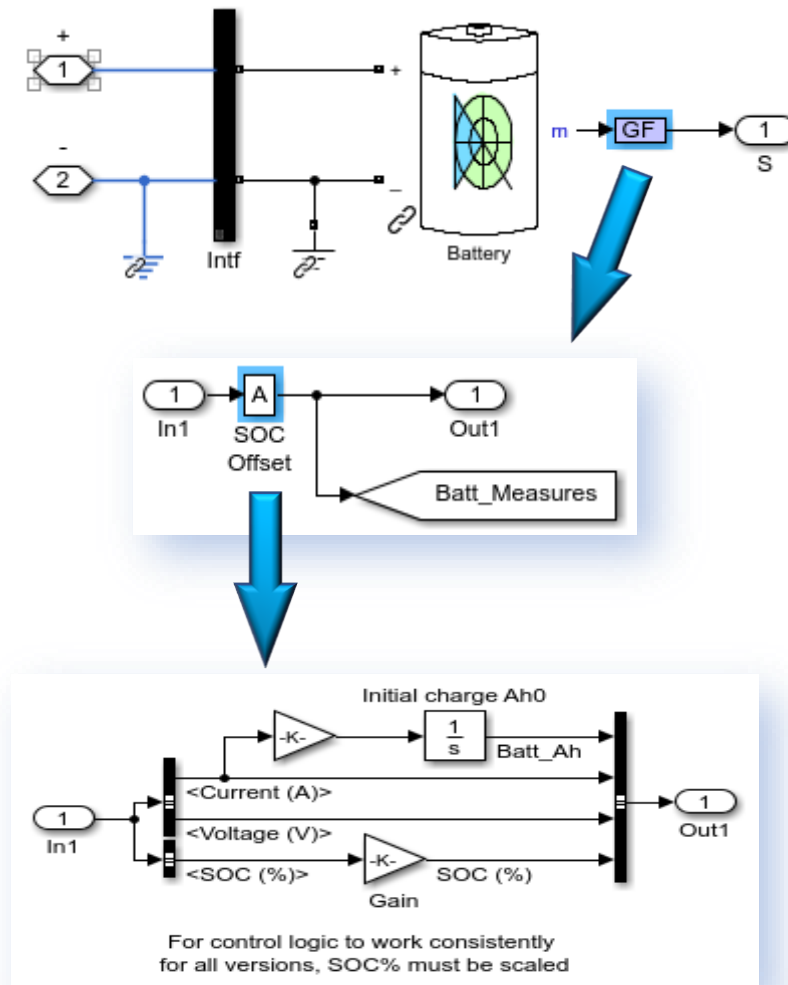
Predefined battery parameters:

Block Parameters: Battery

Temperature and aging (due to cycling) effects can be specified for Lithium-Ion battery type.

| Parameters | Discharge |

☑ Determined from the nominal parameters of the battery

Maximum capacity (Ah) 8.7231

Cut-off Voltage (V) 150

Fully charged voltage (V) 235.5932

Nominal discharge current (A) 1.62

Internal resistance (Ohms) 0.24691

Capacity (Ah) at nominal voltage 7.7885

Exponential zone [Voltage (V), Capacity (Ah)] [216.9492   1.62]

Display characteristics

Discharge current [i1, i2, i3,...] (A) [50 100]

Units Time ▾   Plot

OK   Cancel   Help   Apply

Nominal Current Discharge Characteristic at 0.2C (1.62A)

Legend: Discharge curve, Nominal area, Exponential area

E0 = 217.4484, R = 0.24691, K = 0.25936, A = 18.5448, B = 1.8519

Legend: 50 A, 100 A
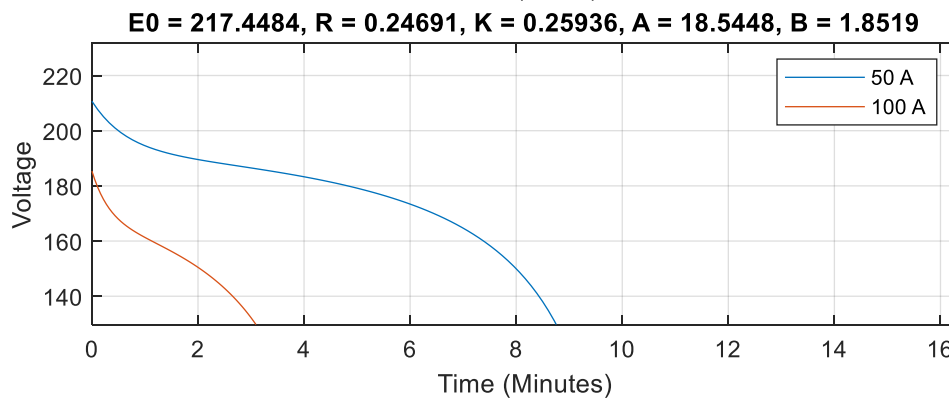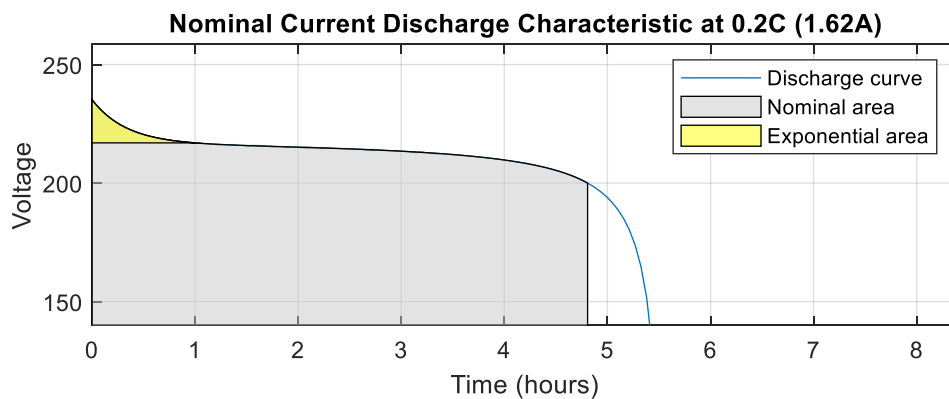
Generic battery model:

The next figure shows how the generic battery block is used in our hybrid electric vehicle system model.
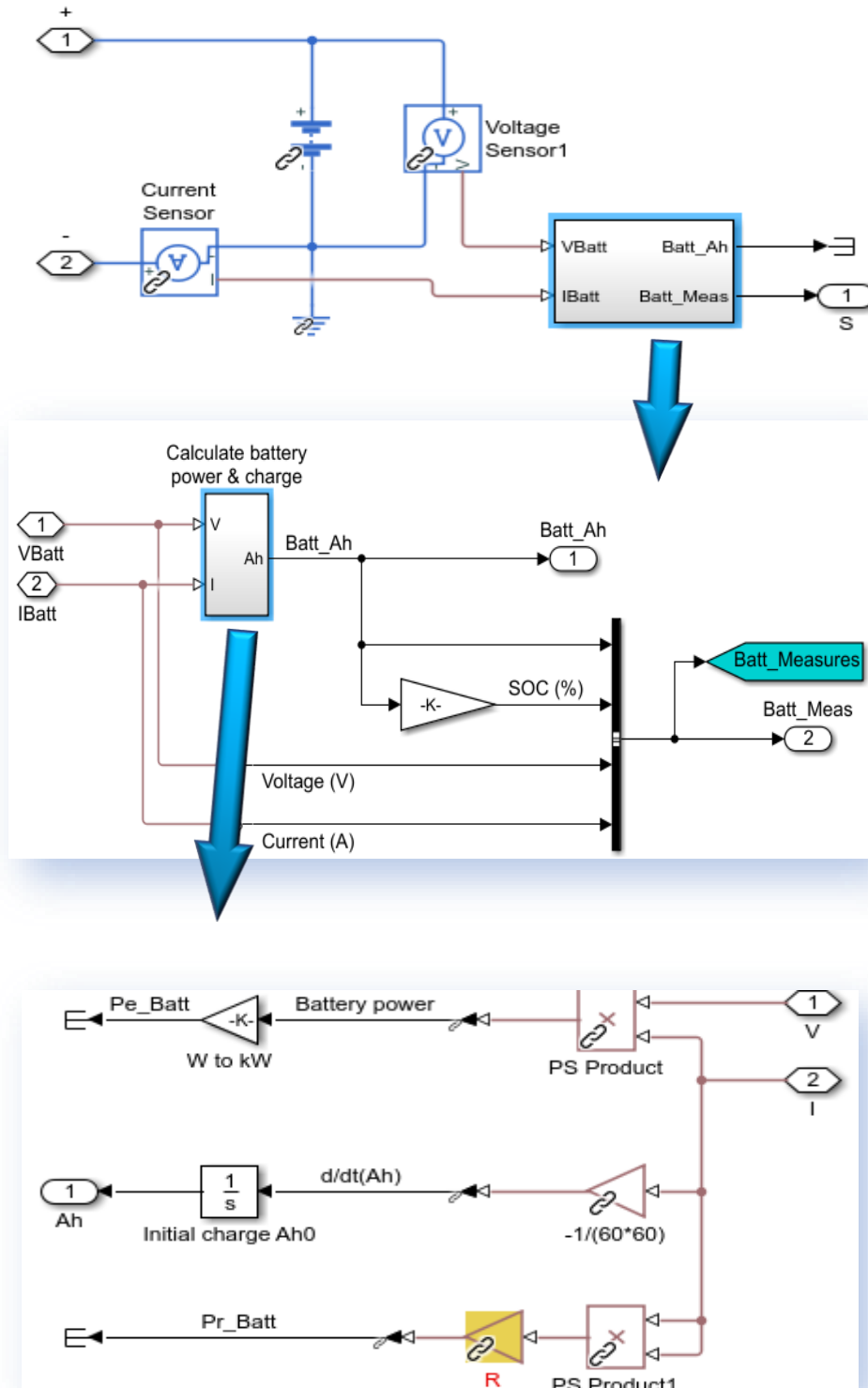
Generic Lossy Ultracapacitor (source code):

```
component LossyUltraCapacitor

% Lossy Ultracapacitor
% Models an ultracapacitor with resistive losses. The capacitance C
% self-discharge resistance is included in parallel with the capacitor,
% and an equivalent series resistance in series with the capacitor.
 0
% Copyright 2008-2017 The MathWorks, Inc.

  nodes
    p = foundation.electrical.electrical; % +:top
    n = foundation.electrical.electrical; % -:bottom
  end

  parameters
    C0 = { 1, 'F' };    % Nominal capacitance C0 at V=0
    Cv = { 0.2, 'F/V'}; % Rate of change of C with voltage V
    R = {2, 'Ohm' };    % Effective series resistance
    Rd = {500, 'Ohm' }; % Self-discharge resistance
  end

  variables
    i = { 0, 'A'   }; % Current
    vc = {value = { 0, 'V' }, priority = priority.high}; % Capacitor voltage
  end

  branches
    i : p.i -> n.i; % Through variable i from node p to node n
  end

  equations
    assert(C0 > 0)
    assert(R > 0)
    assert(Rd > 0)
    let
      v = p.v-n.v; % Across variable v from p to n
    in
      i == (C0 + Cv*vc)*vc.der + vc/Rd; % Equation 1
      v == vc + i*R;              % Equation 2
    end
  end

end
```

The capacitance C depends on the voltage V according to the following equations

$$C = C_0 + V \frac{dc}{dv}$$

$$V = V_c + i \times R$$

$$i = (C_0 + C_v \times v_c) \frac{dv_c}{dt} + \frac{v_c}{r_d}$$

Where:

C_0: *Nomoinal capacitance at* $V = 0$

C_v: *Rate of change of C with voltage V*

R: *Effictive series resistance*

r_d: *self* − *dischage resistance*

i: *current*

v_c: *capacitor voltae*

Battery DC-DC- converter model:
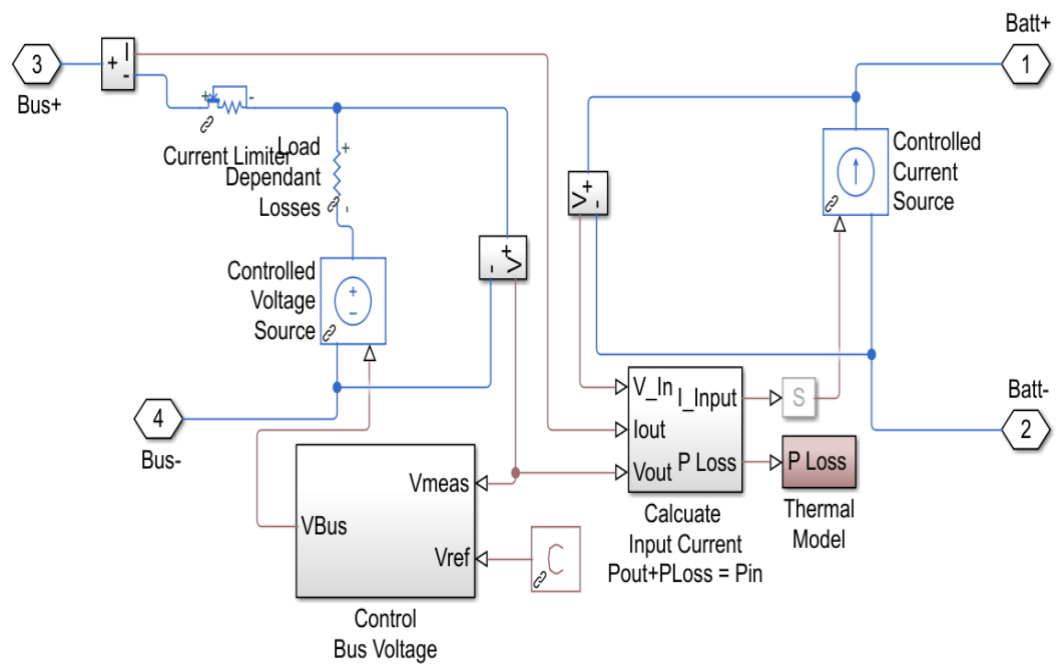
Motor model:
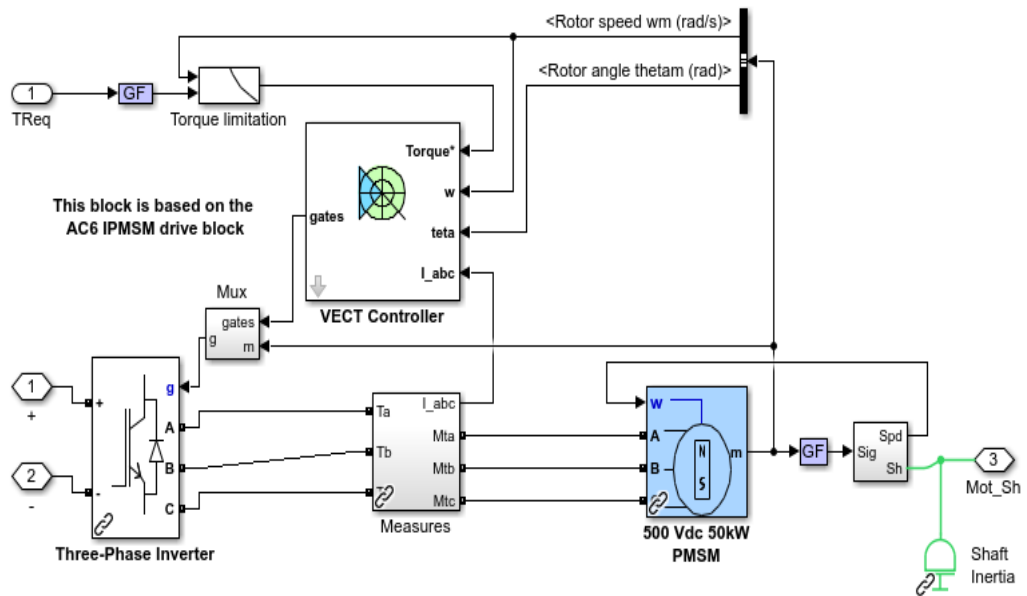
VECT Controller:
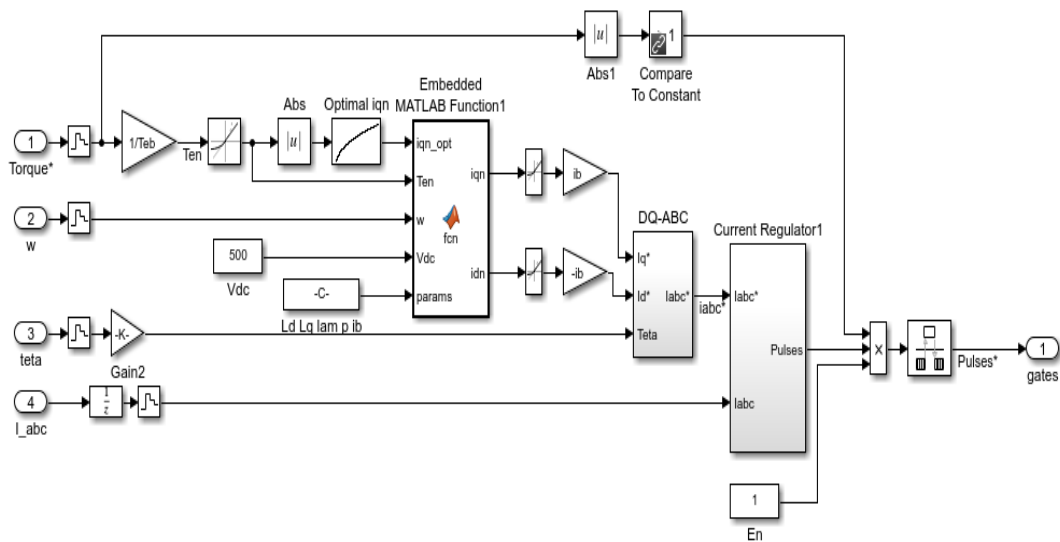
Three phase inverter parameters:

Block Parameters: Three-Phase Inverter ✕

Universal Bridge (mask) (link)

This block implement a bridge of selected power electronics devices. Series RC snubber circuits are connected in parallel with each switch device. Press Help for suggested snubber values when the model is discretized. For most applications the internal inductance Lon of diodes and thyristors should be set to zero

Parameters

Number of bridge arms: 3

Snubber resistance Rs (Ohms)

5000

Snubber capacitance Cs (F)

inf

Power Electronic device IGBT / Diodes

Ron (Ohms)

1e-3

Forward voltages [Device Vf(V) , Diode Vfd(V)]

[0 0]

Measurements None

OK   Cancel   Help   Apply

Drive cycles from ADVISOR software:
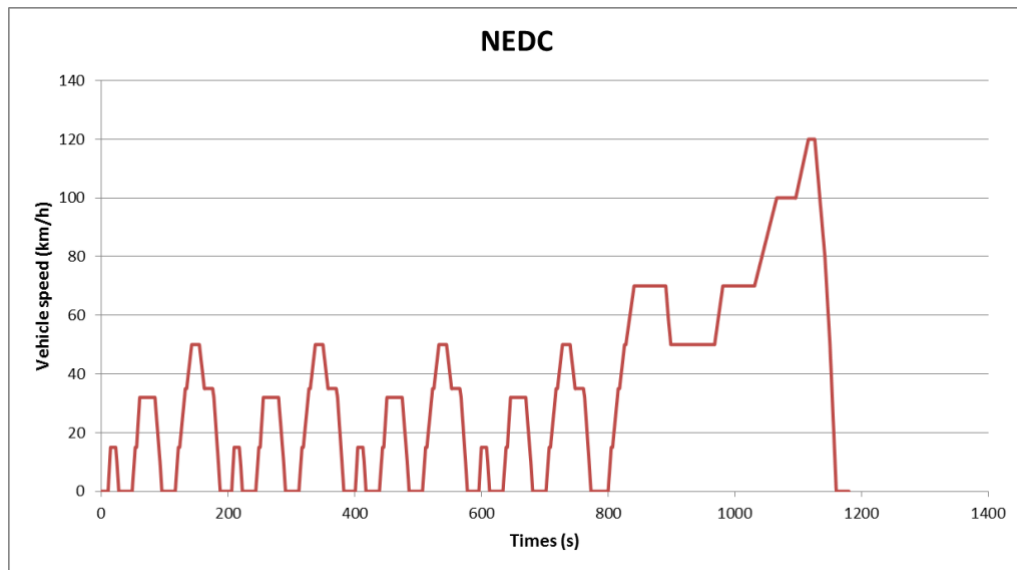
time:	1184	s
distance:	10.93	km
max speed:	120	km/h
avg speed:	33.21	km/h
max accel:	1.06	m/s^2
max decel:	-1.39	m/s^2
avg accel:	0.54	m/s^2
avg decel:	-0.79	m/s^2
idle time:	298	s
no. of stops:	13	
max up grade:	0	%
avg up grade:	0	%
max dn grade:	0	%
avg dn grade:	0	%

Figure (5.1) Statistics of NEDC
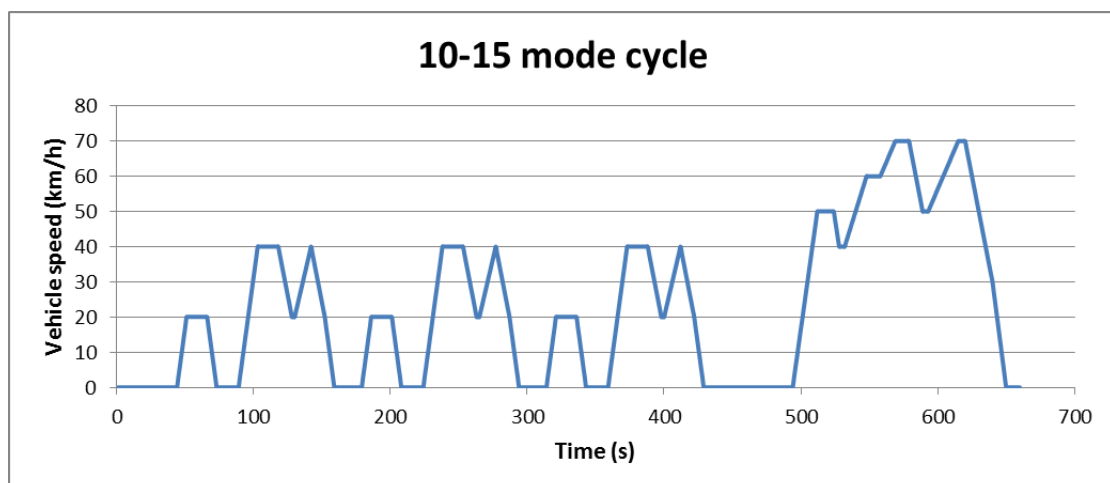
time:	660	s
distance:	4.16	km
max speed:	69.97	km/h
avg speed:	22.68	km/h
max accel:	0.79	m/s^2
max decel:	-0.83	m/s^2
avg accel:	0.57	m/s^2
avg decel:	-0.65	m/s^2
idle time:	215	s
no. of stops:	7	
max up grade:	0	%
avg up grade:	0	%
max dn grade:	0	%
avg dn grade:	0	%

Figure (5.2) Statistics of 10-15 cycle
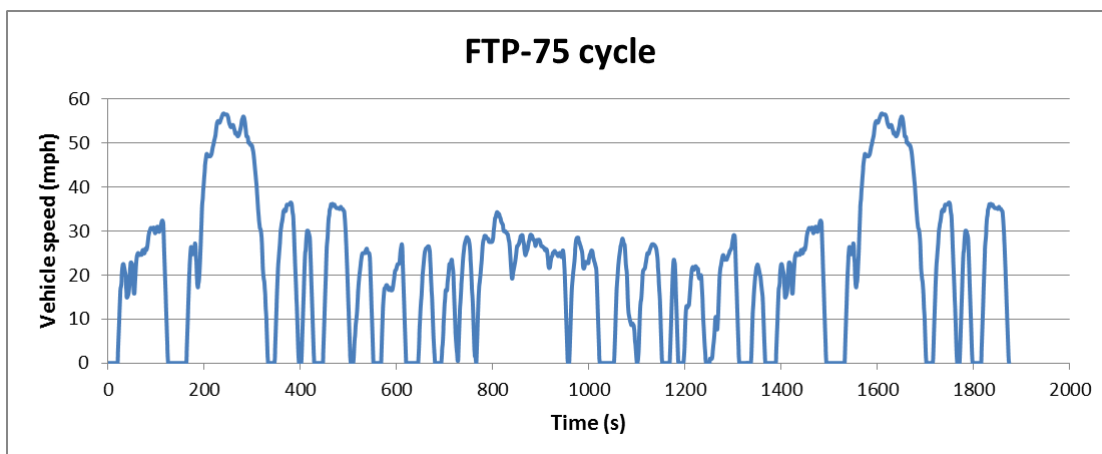
time:	2477	s
distance:	17.77	km
max speed:	91.25	km/h
avg speed:	25.82	km/h
max accel:	1.48	m/s^2
max decel:	-1.48	m/s^2
avg accel:	0.51	m/s^2
avg decel:	-0.58	m/s^2
idle time:	360	s
no. of stops:	22	
max up grade:	0	%
avg up grade:	0	%
max dn grade:	0	%
avg dn grade:	0	%

Figure (5.3) Statistics of FTP-75

Internal combustion engine (ICE) fuel consumption (rows values are speed vector 'RPM' and columns values are torque vector 'Nm')

Breakpoints	Column	(1)	(2)	(3)	(4)	(5)	(6)	(7)	(8)	(9)	(10)
Row		24.81	32.96333...	41.11666...	49.26999...	57.42333...	65.57666...	73.72999...	81.88333...	90.03666...	98.19
(1)	1209.7	0.320323170...	0.377757995...	0.445642539...	0.523976803...	0.612760786...	0.711994489...	0.821677911...	0.941811052...	1.072393913...	1.213426494...
(2)	1520.733...	0.359702601...	0.428590582...	0.507928282...	0.597715701...	0.697952840...	0.808639698...	0.929776275...	1.061362572...	1.203398589...	1.355884325...
(3)	1831.766...	0.407361765...	0.487702901...	0.578493756...	0.679734331...	0.791424625...	0.913564639...	1.046154372...	1.189193825...	1.342682996...	1.506621888...
(4)	2142.8	0.463300661...	0.555094952...	0.657338963...	0.770032693...	0.893176143...	1.026769312...	1.170812201...	1.325304809...	1.490247136...	1.665639183...
(5)	2453.833...	0.527519289...	0.630766736...	0.744463902...	0.868610788...	1.003207393...	1.148253718...	1.303749762...	1.469695525...	1.646091008...	1.832936210...
(6)	2764.866...	0.600017649...	0.714718251...	0.839868573...	0.975468614...	1.121518375...	1.278017855...	1.444967055...	1.622365974...	1.810214612...	2.008512970...
(7)	3075.900...	0.680795741...	0.806949499...	0.943552976...	1.090606173...	1.248109089...	1.416061725...	1.594464080...	1.783316154...	1.982617948...	2.192369461...
(8)	3386.933...	0.769853565...	0.907460479...	1.055517111...	1.214023464...	1.382979535...	1.562385326...	1.752240837...	1.952546067...	2.163301016...	2.384505685...
(9)	3697.966...	0.867191122...	1.016251190...	1.175760979...	1.345720487...	1.526129714...	1.716988660...	1.918297326...	2.130055712...	2.352263816...	2.584921641...
(10)	4009	0.972808410...	1.133321634...	1.304284578...	1.485697242...	1.677559624...	1.879871726...	2.092633548...	2.315845089...	2.549506349...	2.793617328...

The following table shows the overall hybrid electric vehicle model parameters.

1- Electrical System		
Predefined battery block		
Specs.	**Value**	**Unit**
Rated Capacity	8.1	Ah
Nominal Voltage	200	V
Initial State of Charge	75.75	%
Series Resistance	0.02	Ohm
Generic battery system		
Nominal Voltage	217	V
Internal Resistance	0.2469	Ohm
Rated Capacity	6.9	Ah
Initial Charge	6.9	Ah
Exponential Voltage	215.0342	V
Exponential Charge	2.3438	C
R1	1.8	Ohm
R2	0.3	Ohm
C1 (capacitance)	2500	F
C1 (initial voltage)	19	V

C1 (series resistance)	1×10^{-6}	Ohm
Max. capacity	6.9	F
Battery system current	12	A
Battery system voltage	100	V
Battery system power	21000	W
Ultracapacitor		
Nominal Capacitance	1000	F
Rate of change of nominal capacitance with voltage	0.2	F/V
Series resistance	10	Ohm
Self-discharge resistance	500	Ohm
Initial voltage	217	V
Permanent Magnet Synchronous Motor (IPMSM)		
Motor power	50	kW
DC voltage	500	V
Number of phases	3	phases
Pole pairs	4	poles
Back EMF waveform	Sinusoidal	-
Rotor type	Salient pole	-
Rotor flux position when theta=0	90 degrees behind phase A axis (modified park)	-
Mechanical input	speed	-
Flux linkage (flux induced by magnets)	0.17566614	Wb
Stator phase resistance	0.0910	Ohm
Damping	1×10^{-5}	Nm/(rad/s)
Torque control time constant	0.0267	Ses
Shaft inertia	0.2	$kg\ m^2$
Series resistance	0.01	Ohm

Inductances $[L_d, L_q]$	[0.0016, 0.0021]	H
Efficiency	91	%
Torque-speed LUT	[0 1200 2000 3000 4000 5000 6000 6500 10000]	RPM
	[400 400 225 150 100 80 70 0 0]	Nm
Motor Drive (Three-Phase Inverter)		
Number of bridge arms	3	-
Power electronics device	IGBT/Diodes	-
Snubber resistance (Rs)	5000	Ohm
R on	1×10^{-3}	Ohm
Motor Vector Controller		
Motor pairs of poles	4	Poles
Max. switching frequency	20	kHz
Sampling time	20×10^{-6}	Sec
Current hysteresis bandwidth	0.1	A
(PMSM) Generator		
Generator power	30	kW
DC voltage	500	V
Number of phases	3	Phases
Pole pairs	1	Poles
Back EMF waveform	Sinusoidal	-
Rotor type	Salient pole	-
Rotor flux position when theta=0	90 degrees behind phase A-axis (modified park)	-
Mechanical input	speed	-
Flux linkage	0.192	Wb
Stator phase resistance	0.0048	Ohm

Inductances $[L_d, L_q]$	$[0.635, 0.635]$	mH
Damping	1×10^{-5}	Nm/(rad/s)
Torque control time constant	0.04	Sec
Shaft inertia	0.2	$kg\ m^2$
Series resistance	0.01	Ohm
Torque independent electric loss	0	-
Shaft stiffness	1000	W
Shaft damping	100	W
Torque-speed LUT	[0 1200 2000 3000 4000 10000 15000]	RPM
	[400 400 250 150 110 0 0]	Nm
Generator Drive (Three-Phase Inverter)		
Number of bridge arms	3	-
Power electronics device	IGBT/Diodes	-
Snubber resistance (Rs)	5000	Ohm
R on	1×10^{-3}	Ohm
Generator Vector Controller		
Generator pairs of poles	1	Poles
Max. switching frequency	20	kHz
Sampling time	20×10^{-6}	Sec
Current hysteresis bandwidth	0.1	A
UC's DC-DC converter		
Output voltage	500	V
Resistance loss	0.6250	Ohm
Kp	0.0095	-
Ki	5	-
Min. input voltage	450	V
Battery's DC-DC converter		

Output voltage	500	V
Resistance loss	0.6250	Ohm
Kp	0.01	-
Ki	10	-
Min. input voltage	20	V
Current limit	41	A
Voltage drop when current starts to limit	5	V
Mean Boost Kp	1×10^{-3}	-
Mean Boost Ki	1	-
Electrical power to heat	0.1	-
Thermal Mass	1	kg
Specific heat	100	J/kg/K
Initial temperature	25	C
Air temperature	298	K
Convection area	20	cm^2
Convection heat transfer coefficient	100	W/m^2K
2- Control System		
Engine start RPM	800	RPM
Engine Stop RPM	790	RPM
ICE Kp	0.02	-
ICE Ki	0.01	-
Generator Kp	10	-
Generator Ki	3	-
Motor Kp	500	-
Motor Ki	300	-
Vehicle speed Kp	0.02	-
Vehicle speed Ki	0.04	-

3- Mechanical System		
Vehicle parameters		
Mass	1200	kg
Wheel inertia	0.1	$kg\ m^2$
Aero drag coefficient	0.26	-
Incline	0	-
Engine vehicle gear ratio	1.3	-
Distance from Center of Gravity (CG)to rear axel	1.35	m
Distance from Center of Gravity (CG)to front axel	1.35	m
Distance from Center of Gravity (CG)to ground	0.5	m
Frontal area	2.16	m^2
Air density	1.18	kg/m^3
Gravitational acceleration	9.81	m/s^2
Tire parameters		
Tire Radius	0.3	m
Tire inertia	1e-2	$kg.m^2$
Rated vertical load	3000	N
Rated peak long force	3500	N
Slip at peak force	6	%
Relaxation length	0.25	%
Transmission Parameters		
Inertia	0.5	$kg.m^2$
Friction	1e-04	$N.m.s/rad$
Power Split parameters		
Ratio of ring to sun	2.6	

Internal combustion engine (ICE) Parameters		
Shaft inertia	0.25	
Max. Power	57	kW
Speed at Max. Power	5000	RPM
Max. speed	6000	RPM
Min. speed	1000	RPM
Stall speed	500	RPM
Torque at 4200 rpm	115	Nm
Friction	0.2079	$N.m.s$ $/rad$
Sensor time constant	0.005	Sec
ICE fuel consumption per revolution	25	mg/rev
Gasoline density	750	kg/m^3